



ScuDo

Scuola di Dottorato ~ Doctoral School

WHAT YOU ARE, TAKES YOU FAR



Doctoral Dissertation  
Doctoral Program in Chemical Engineering (32<sup>th</sup> Cycle)

# **Aqueous phase reforming of biorefinery side-streams: challenges towards the industrial application**

**Giuseppe Pipitone**

\* \* \* \* \*

## **Supervisors**

Prof. Raffaele Pirone, Supervisor  
Prof. Samir Bensaid, Co-Supervisor

## **Doctoral Examination Committee:**

Prof. Claudio Ampelli, Referee, Università degli Studi di Messina  
Prof. Serena Esposito, Referee, Politecnico di Torino  
Prof. Gianluca Landi, Referee, Istituto di ricerca sulla combustione  
Prof. Nunzio Russo, Referee, Politecnico di Torino  
Prof. Onofrio Scialdone, Referee, Università degli Studi di Palermo

Politecnico di Torino  
November 15, 2019

This thesis is licensed under a Creative Commons License, Attribution - Noncommercial - NoDerivative Works 4.0 International: see [www.creativecommons.org](http://www.creativecommons.org). The text may be reproduced for non-commercial purposes, provided that credit is given to the original author.

I hereby declare that, the contents and organisation of this dissertation constitute my own original work and does not compromise in any way the rights of third parties, including those relating to the security of personal data.

.....  
Giuseppe Pipitone  
Turin, November 15, 2019

# Summary

The challenge for sustainable and renewable sources of energy passes through the use of biomass. The biorefineries aim to convert the conventional technologies of the fossil-based industry to the more complex exploitation of biomass. One of the key bottlenecks is the complete valorization of their organic content, often lost in the aqueous side streams. Aim of the present work was the investigation of the aqueous phase reforming process in order to convert carbon-laden water fractions into a gas mixture rich in hydrogen, looking at three different kind of starting materials.

Alginate was tested as representative of the sugar fraction derived from aquatic biomass. The influence of several operating conditions was investigated (catalyst and alginate loading, reaction time, reaction temperature, hydrogen partial pressure, pH) towards the hydrogen selectivity, hydrogen yield and carbon conversion to gas. Among the results, it was observed that more diluted solutions allowed the carbon conversion to be increased, while a maximum was observed for the hydrogen selectivity. The production of hydrogen reached a plateau, due to the formation of intermediate liquid products recalcitrant for hydrogen formation. Finally, the higher pH led to higher hydrogen yield, reducing the dehydration pathways responsible for the decrease of selectivity.

Seventeen compounds belonging to different classes of molecules (carboxylic and bicarboxylic acids, hydroxyacids, aromatics, alcohols and polyalcohols, ketones) have been selected to be representative of the carbon-laden aqueous streams derived from hydrothermal liquefaction of lignocellulosic biomass. The study focused initially on the influence of the reaction temperature on the performance. The investigation consented to define a scale of reactivity among the seventeen compounds. Glycolic acid, one of the most present compounds in the HTL-derived wastewater, reported one of the highest hydrogen yields, with the gas phase composed only by hydrogen and carbon dioxide. On the other hand, acetic acid, representative of carboxylic acids, catalytically decomposed into carbon dioxide and methane, with a negligible production of hydrogen. Binary and ternary synthetic mixtures have been tested, highlighting competitive adsorption issues. Tests performed at different reaction time suggested possible reaction pathways for glycolic acid, acetic acid and lactic acid. Moreover, the study of the ternary mixture pointed out the differences in reactivity because of

the adsorption, while the selectivity remained analogous to the single-compound tests. The aqueous phase derived from the hydrothermal liquefaction of a lignin-rich stream was subjected to APR. It was found that the reaction performance was linked with the aromatic content. For this reason, diethyl-ether was used to perform a liquid-liquid extraction, reducing the presence of aromatics and improving the hydrogen yield.

Finally, the sugar-laden aqueous phase derived from an industrial bioethanol plant was investigated, suggesting an alternative pathway of valorization for the hemicellulose fraction of lignocellulosic biomass. The influence of temperature and carbon concentration was studied initially on the model compounds (glucose, xylose, sorbitol and xylitol) and afterwards on the industrial hydrolysate, showing that the hydrogen yield increased with the reaction temperature and at more diluted concentrations. In this case, no adsorption issues were observed, being the experimental results obtained in the case of binary mixtures analogous to the ones from the linear combination of single-compounds tests. Given that the sugar alcohols are more prone to hydrogen production, a pretreatment of the sugar solution was performed to convert them selectively to the corresponding alcohols. A net hydrogen production was obtained at different carbon concentration.

The research performed allowed to look at the aqueous phase reforming as a possible process for the valorization of aqueous by-products in the biorefinery context. The main findings showed that it may be possible to reduce the waste production converting the organic content of by-products into a valuable gas, decreasing the external need of hydrogen of a biorefinery.

# Acknowledgment

Part of the research reported in this work has received funding from the European Union's Horizon 2020 research and innovation program under grant agreement N°764675.

Beta-Renewable S.p.A and RE-CORD (Renewable Energy Consortium for Research and Development) are deeply acknowledged for the supply of the real feedstocks.

# Contents

1. Summary.....	ii
2. Acknowledgment.....	iv
3. Contents.....	v
4. List of Tables.....	viii
5. List of Figures.....	x
6. Chapter 1 Introduction.....	1
1.1 Global warming at a glance.....	1
1.2 Renewable energy sources.....	2
1.2.1 Hydropower energy.....	3
1.2.2 Wind energy.....	3
1.2.3 Solar energy.....	3
1.2.4 Bio-based energy.....	4
1.3 The biorefinery concept.....	6
1.4 Aqueous phase reforming.....	9
1.4.1 Introduction to APR.....	9
1.4.2 Influence of reaction parameters.....	12
1.4.3 Towards the application of aqueous phase reforming.....	19
1.5 Aim and structure of the work.....	22
7. Chapter 2 Materials and Method.....	24
2.1 Materials.....	24
2.2 Catalytic tests.....	25
2.2.1 Aqueous phase reforming tests.....	25
2.2.2 Hydrogenation reactions.....	26
2.3 Characterization analysis.....	27
2.4 Description of performance's indicators.....	28
8. Chapter 3 Valorization of alginate.....	31
3.1 Introduction.....	31
3.2 Results and discussion.....	32
3.2.1 Effect of the catalyst amount.....	32

3.2.2	Effect of alginate concentration .....	34
3.2.3	Effect of the reaction temperature .....	36
3.2.4	Effect of the reaction time .....	37
3.2.5	Effect of the hydrogen pressure .....	39
3.2.6	Effect of the pH.....	41
3.2.7	Catalyst reutilization and characterization.....	42
3.3	Conclusions .....	45
9.	Chapter 4 Exploitation of sugar-based biorefinery streams.....	47
4.1	Introduction .....	47
4.2	Results and discussion.....	49
4.2.1	Characterization hydrolysate .....	49
4.2.2	Influence of the reaction temperature and carbon concentration....	50
4.2.3	Mixtures of model compounds .....	58
4.2.4	Hydrogenation-APR tests .....	61
4.2.5	Reuse of the catalyst .....	64
4.3	Conclusions .....	71
10.	Chapter 5 Hydrothermal liquefaction-derived aqueous streams.....	73
5.1	Introduction .....	73
5.2	Results and discussion.....	75
5.2.1	Influence of the reaction temperature .....	75
Carboxylic acids	.....	76
Hydroxyacids and bicarboxylic acids	.....	79
Mono-alcohols	.....	84
Polyalcohols.....	.....	87
Ketoacids, ketones and aromatics	.....	89
5.2.2	Study of binary and ternary mixtures .....	91
Binary mixtures.....	.....	93
5.2.3	Characterization and stability of the catalyst.....	96
5.3	Conclusions .....	100
11.	Chapter 6 Valorization of aqueous phase derived from lignin-rich hydrothermal liquefaction.....	101
6.1	Introduction .....	101
6.2	Results and discussion.....	102
6.2.1	Model compounds.....	102

6.2.2 HTL aqueous phase synthetic mixture.....	108
6.2.3 Case study: APR of the water fraction from HTL of lignin .....	110
6.3 Conclusion.....	122
12. Conclusions.....	123
13. References.....	125



# List of Tables

Table 1. List of compounds used for the investigation. ....	24
Table 2. Influence of the catalyst amount on the carbon conversion to gas, hydrogen yield, hydrogen selectivity and composition of the obtained gas phase. Reaction conditions: 1 wt.% alginate solution, T: 225 °C, reaction time: 6 h.....	33
Table 3. Influence of the alginate amount on the carbon conversion to gas, hydrogen yield, hydrogen selectivity and composition of the obtained gas phase at different amount of catalyst. Reaction conditions: T: 225 °C, reaction time: 6 h. ....	34
Table 4. Contribution to the total CO <sub>2</sub> production coming from the APR reaction (evaluated from the reaction stoichiometry, APR-CO <sub>2</sub> ) and from alternative pathways (Excess CO <sub>2</sub> ), with the influence of the catalyst on the production of Excess CO <sub>2</sub> (Catalytic excess). ....	36
Table 5. Influence of the reaction temperature with and without catalyst on the carbon conversion to gas, hydrogen yield, hydrogen selectivity and composition of the obtained gas phase. Reaction conditions: 1 wt.% alginate solution, reaction time: 6 hours. ....	36
Table 6. Influence of the time reaction on the carbon conversion to gas, hydrogen yield, hydrogen selectivity and composition of the obtained gas phase. Reaction conditions: 1 wt.% alginate solution, 0.8 g catalyst, T: 225 °C.....	38
Table 7. Influence of the hydrogen partial pressure on the carbon conversion to gas, hydrogen yield and selectivity. Reaction conditions: 1 wt.% alginate solution, T: 225 °C, 0.8 g Pt/C, 6h.....	40
Table 8. Influence of the pH on the carbon conversion to gas, hydrogen yield, hydrogen selectivity and composition of the obtained gas phase. Reaction conditions: 1 wt.% alginate solution, 0.8 g catalyst, T: 225 °C, time: 6 h.....	41
Table 9. Characterization of the wheat straw hydrolysate. ....	49
Table 10. Textural characteristic of the fresh and spent catalysts. All tested mixtures were at an overall 0.9wt.% of carbon, except for the last line that was at 0.6 wt.%. Reaction conditions: 270 °C, 2 h reaction time.....	68
Table 11. List of investigated model compounds. ....	76
Table 12. Influence of carbon concentration on APR of model compounds. Reaction conditions: 0.375 g 5% Pt/C, Liquid phase amount: 75 g, Temperature 270°C, Reaction time 120 min.....	105
Table 13. HTL-AP quantification of main compounds and ICP analysis.....	111

Table 14. Aqueous phase reforming of synthetic mixtures with and without DEE. Reaction conditions: 0.375 g 5% Pt/C, Liquid phase amount: 75 g, 0.9 wt.% C acids + 0.9 wt.% C DEE, 270 °C reaction temperature, 2 h reaction time. ....	118
Table 15. Textural characteristic of the fresh and spent catalysts.....	118

# List of Figures

Figure 1. Correlation between carbon dioxide concentration in the atmosphere and temperature change (modified from [3]).	1
Figure 2. General information on the different kind of feedstocks, processes, products and uses in the frame of bio-based economy (from [17]).	5
Figure 3. The biorefinery concept (from [18]).	7
Figure 4. Thermodynamic equilibrium for hydrogen production, modified from [39].	10
Figure 5. APR reaction pathways as proposed in [39].	11
Figure 6. Influence of chain length on APR performance [42].	12
Figure 7. Relative rates of the three main possible reactions under APR reaction conditions, as reported in [48].	14
Figure 8. Effect of Re addition on Pt/C [58].	16
Figure 9. Influence of reactor configuration on H <sub>2</sub> selectivity [64].	18
Figure 10. TOC content of kenaf and glucose before and after APR [73].	21
Figure 11. Parr top reactor component scheme.	25
Figure 12. Berghof reactor component scheme.	26
Figure 13. Carbon conversion to gas, hydrogen selectivity and hydrogen yield with catalyst after first, second and third use. Reaction conditions: 1 wt.% alginate solution, T: 225 °C, 0.8 g Pt/C, 6h.	42
Figure 14. Carbon conversion to gas and hydrogen selectivity obtained after the APR of the liquid effluent and comparison with the fresh one. Reaction conditions: 1 wt.% alginate solution, T: 225 °C, 0.8 g Pt/C, 6h.	43
Figure 15. XRD spectra of fresh and spent catalyst after APR of 1 wt.% alginate solution, T: 225 °C, 0.8 g Pt/C, 6h.	43
Figure 16. TGA spectra of the fresh and spent catalyst after APR of 1 wt.% alginate solution, T: 225 °C, 0.8 g Pt/C, 6h.	45
Figure 17. Block-flow diagram of a bioethanol plant with valorization of the C5 sugars via APR.	49
Figure 18. Influence of temperature on the APR performance of glucose (A), xylose (B), sorbitol (C) and xylitol (D). Reaction conditions: 0.375 g Pt/C catalyst, 2 hours reaction time, 0.9 wt.% carbon concentration.	53
Figure 19. Influence of the reaction temperature on the composition of the gas phase obtained after APR of glucose (a), xylose (b), sorbitol (c) and xylitol (d). APR reaction conditions: 2 h reaction time, 0.9 wt.% carbon.	53
Figure 20. Influence of reaction temperature on APR performance of wheat straw hydrolysate (A) and composition of the produced gas phase (B). Reaction conditions: 0.375 g Pt/C catalyst, 2 hours reaction time, 0.9 wt.% carbon concentration.	54

Figure 21. Influence of the carbon concentration on the APR performance of glucose (A), xylose (B), sorbitol (C) and xylitol (D). Reaction conditions: 0.375 g Pt/C catalyst, 2 hours reaction time, 270 °C reaction temperature. ....	56
Figure 22. Influence of the carbon concentration in wt.% on the composition of the gas phase obtained after APR of glucose (a), xylose (b), sorbitol (c) and xylitol (d). APR reaction conditions: 2 h reaction time, 270 °C.....	57
Figure 23. Influence of the carbon concentration on APR performance of wheat straw hydrolysate (left) and composition of the produced gas phase (right). Reaction conditions: 0.375 g Pt/C catalyst, 2 hours reaction time, 270 °C reaction temperature. ....	58
Figure 24. Influence of reaction temperature on the performance of APR of a glucose-xylose (A) and sorbitol-xylitol (B) mixture. The points jointed by a dotted line are referred to the linear combination of the singular components. Reaction conditions: 0.375 g Pt/C catalyst, 2 hours reaction time, 0.9 wt.% total carbon concentration.....	59
Figure 25. Influence of carbon concentration on the performance of APR of a glucose-xylose (A) and sorbitol-xylitol (B) mixture. The points jointed by a dotted line are referred to the linear combination of the singular components. Reaction conditions: 0.375 g Pt/C catalyst, 2 hours reaction time, 270 °C reaction temperature. ....	60
Figure 26. Influence of carbon concentration on gas phase composition and hydrogen production of a glucose-xylose (left) and sorbitol-xylitol (right) mixture. Reaction conditions: 0.375 g Pt/C catalyst, 2 hours reaction time, 270 °C reaction temperature. ....	61
Figure 27. Influence of carbon concentration on the hydrogenation of a glucose-xylose mixture (A) and on the APR of the hydrogenated feed (B). Hydrogenation reaction conditions: 0.188 g Ru/C catalyst, 1 h reaction time, 180 °C, 15 bar H <sub>2</sub> pressure. APR reaction conditions: 0.375 g Pt/C catalyst, 2 h reaction time, 270 °C. ....	63
Figure 28. Influence of carbon concentration on the hydrogenation of the hydrolysate (A) and on the APR of the hydrogenated feed (B). Hydrogenation reaction conditions: 0.188 g Ru/C catalyst, 1 h reaction time, 180 °C, 15 bar H <sub>2</sub> pressure. APR reaction conditions: 0.375 g Pt/C catalyst, 2 h reaction time, 270 °C. ....	63
Figure 29. Influence of the reaction temperature on the reusability of the catalyst with a glucose-xylose mixture. APR reaction conditions: 270 °C, 2 h reaction time, 0.9 wt.% C. ....	65
Figure 30. Influence of the reaction temperature on the reusability of the catalyst with the hydrolysate. APR reaction conditions: 270 °C, 2 h reaction time, 0.9 wt.% C. ....	66
Figure 31. Washing treatment of a spent catalyst after APR of hydrolysate 0.9 wt.% C at 270 °C. ....	66
Figure 32. APR performance of hydrolysate (left) and glucose-xylose mixture (right) with fresh catalyst, spent catalyst and regenerated (after ethanol washing)	

catalyst. APR reaction conditions: 0.9 wt.% C, 270 °C reaction temperature, 2h reaction time. ....	67
Figure 33. FESEM images of the fresh catalyst (A) and spent catalyst after the aqueous phase reforming of hydrolysate solution (B) and hydrogenated hydrolysate solution (C). APR reaction conditions: 270 °C, reaction time 2 h, 0.9 wt. % C. ....	68
Figure 34. ATR-IR spectra of fresh catalyst and spent catalyst after the aqueous phase reforming of a glucose-xylose hydrogenated solution, a glucose-xylose solution and a hydrolysate. APR reaction conditions: 270 °C, reaction time 2 h, 1.8 wt. % C. ....	69
Figure 35. Thermogravimetric analysis of fresh catalyst (black line) and spent catalyst after the aqueous phase reforming of a glucose-xylose hydrogenated solution (blue line), a glucose-xylose solution (red line) and a hydrolysate (purple line). APR reaction conditions: 270 °C, reaction time 2 h, 1.8 wt. % C. TGA temperature program: heat from 30 °C to 1000 °C @ 20 °C/min in nitrogen atmosphere with a purge rate of 20 mL/min. ....	70
Figure 36. IR analysis of evolving gas from fresh and spent catalysts reported in Figure 13; water (blue line), carbon dioxide (red line), carbon monoxide (black line), methane (purple line), carbonylic groups (green line). ....	71
Figure 37. Influence of the reaction temperature on the APR of carboxylic acids (A) and composition of the liquid phase of acetic acid (B-left) and propionic acid (B-right); the numbers in the figure close to the reagent peak refers to the conversion; *: unknown. Reaction conditions: 0.133 M feed, 0.375 g 5% Pt/Al <sub>2</sub> O <sub>3</sub> , reaction time 2 h. ....	78
Figure 38. Influence of the reaction temperature on the composition of the gas phase from APR of carboxylic acids. Reaction conditions: 0.133 M feed, 0.375 g 5% Pt/Al <sub>2</sub> O <sub>3</sub> , reaction time 2 h. ....	79
Figure 39. Hypothetic mechanism for the reforming of acetic acid (A) as suggested from [150] and propionic acid as proposed in this work (B). ....	79
Figure 40. Influence of the reaction temperature on APR of hydroxyacids and bicarboxylic acids. Reaction conditions: 0.133 M feed, 0.375 g 5% Pt/Al <sub>2</sub> O <sub>3</sub> , reaction time 2 h. ....	81
Figure 41. Influence of the reaction temperature on the composition of the gas phase from APR of hydroxyacids and bicarboxylic acids (1) and on the composition of the liquid phase from APR of glycolic acid (B-left) and lactic acid (B-right); the numbers in the figure close to the reagent peaks refer to the conversion; *: unknown. Reaction conditions: 0.133 M feed, 0.375 g 5% Pt/Al <sub>2</sub> O <sub>3</sub> , reaction time 2 h. ....	82
Figure 42. Suggested reaction mechanism for the APR of glycolic acid (A) and lactic acid (B). ....	83
Figure 43. Influence of the reaction temperature on APR of monoalcohols. Reaction conditions: 0.133 M feed, 0.375 g 5% Pt/Al <sub>2</sub> O <sub>3</sub> , reaction time 2 h. ....	84
Figure 44. Influence of the reaction temperature on the composition of the gas phase from APR of monoalcohols (A) and on the liquid phase of ethanol (7-B left) and butanol (7-B right); the numbers in the figure close to the reagent peak refers	

to the conversion; *: unknown compounds. Reaction conditions: 0.133 M feed, 0.375 g 5% Pt/Al <sub>2</sub> O <sub>3</sub> , reaction time 2 h. ....	85
Figure 45. Suggested reaction mechanisms for monoalcohols. ....	87
Figure 46. Influence of the reaction temperature on APR of polyalcohols. Reaction conditions: 0.133 M feed, 0.375 g 5% Pt/Al <sub>2</sub> O <sub>3</sub> , reaction time 2 h. ....	88
Figure 47. Influence of the reaction temperature on the composition of the gas phase from APR of polyalcohols. Reaction conditions: 0.133 M feed, 0.375 g 5% Pt/Al <sub>2</sub> O <sub>3</sub> , reaction time 2 h. ....	89
Figure 48. Influence of the reaction temperature on APR of levulinic acid, 4 methyl 2 pentanone and guaiacol. Reaction conditions: 0.133 M feed, 0.375 g 5% Pt/Al <sub>2</sub> O <sub>3</sub> , reaction time 2 h. ....	90
Figure 49. Influence of the reaction temperature on the composition of the gas phase from APR of levulinic acid, 4 methyl 2 pentanone and guaiacol. Reaction conditions: 0.133 M feed, 0.375 g 5% Pt/Al <sub>2</sub> O <sub>3</sub> , reaction time 2 h. ....	91
Figure 50. Influence of the concentration of feed on the performance of APR. Reaction conditions: 270 °C, 0.375 g 5% Pt/Al <sub>2</sub> O <sub>3</sub> , reaction time 2 h. ....	93
Figure 51. Results of four equimolar binary mixtures. Reaction conditions: 270 °C, 0.375 g 5% Pt/Al <sub>2</sub> O <sub>3</sub> , reaction time 2 h. ....	95
Figure 52. Results from ternary mixtures constituted by glycolic acid, acetic acid and lactic acid (left) and glycolic acid, acetic acid and ethanol (right). Reaction conditions: 270 °C, 0.375 g 5% Pt/Al <sub>2</sub> O <sub>3</sub> , reaction time 2 h. ....	96
Figure 53. Thermogravimetric analysis of the spent catalyst performed in nitrogen and air (left) and XRD analysis of the fresh and spent catalyst with cristobalite as internal standard (right). ....	97
Figure 54. FESEM images of the fresh (left) and spent catalyst (right) after APR of lactic acid at 230 °C. ....	98
Figure 55. ATR-IR spectra of spent catalysts after APR; the spectra of the fresh catalyst is added for comparison. ....	99
Figure 56. Influence of catalyst reuse on the performance of APR of a glycolic-acetic-lactic mixture. Reaction conditions: 0.133 M feed (0.044 M per acid), 270 °C, 0.375 g 5% Pt/Al <sub>2</sub> O <sub>3</sub> , reaction time 2 h. ....	100
Figure 57: Block flow diagram of a HTL-APR integrated plant. HTL: hydrothermal liquefaction; HT: hydrotreatment (upgrade block). ....	102
Figure 58. Amount-time profile for APR of acetic acid (A), glycolic acid (B), Lactic acid (C-D). Reaction conditions: 0.375 g 5% Pt/C, Liquid phase amount: 75 g, 0.9 wt.% C feed, Temperature 270°C. ....	107
Figure 59. Proposed reaction scheme for lactic acid APR. ....	107
Figure 60. Amount-time profile for APR of a synthetic ternary mixture. Reaction conditions: 0.375 g 5% Pt/C, Liquid phase amount: 75 g, total 0.9 wt.% C glycolic, acetic and lactic acid (0.3 wt.% C per component), 270 °C reaction temperature. ....	108
Figure 61. Influence of carbon concentration on the reaction parameters (A) and conversion (B) of APR of the synthetic mixture. Reaction conditions: 0.375 g 5% Pt/C, Liquid phase amount: 75 g, 270°C reaction temperature, 2 h reaction time. ....	109

Figure 62. Influence of reaction temperature on the reaction parameters of APR of the synthetic mixture. Reaction conditions: 0.375 g 5% Pt/C, Liquid phase amount: 75 g, 1.8 wt. % C, 2 h reaction time. ....	110
Figure 63. HPLC chromatograms of the HTL-AP (1: glycolic acid, 2: lactic acid, 3: glycerol, 4: acetic acid, 5: acetaldehyde, 6: methanol, 7: catechol, 8: phenol, 9: guaiacol).....	112
Figure 64. Influence of carbon concentration on reaction parameters of APR of the HTL-AP. Reaction conditions: 0.375 g 5% Pt/C, Liquid phase amount: 75 g, 270°C reaction temperature, 2 h reaction time. ....	113
Figure 65. HPLC chromatograms of the feed and product for the first test (left) and second test (right) of the HTL-AP sample. Reaction conditions: 0.375 g 5% Pt/C, wt.% C feed, 270°C reaction temperature, 2 reaction time (1: glycolic acid 2: lactic acid 3: glycerol 4: acetic acid 5: acetaldehyde 6: methanol 7: catechol 8: phenol 9: propionic acid).....	113
Figure 66. H <sub>2</sub> productivity (A) and H <sub>2</sub> production (B) for the APR of HTL-AP. Reaction conditions: 0.375 g 5% Pt/C, Liquid phase amount: 75 g, 270°C reaction temperature, 2 h reaction time. ....	114
Figure 67. APR of glycolic acid with different catalysts. Reaction conditions: 0.375 g 5% Pt/C, Liquid phase amount: 75 g, 0.9 wt.% C glycolic acid, reaction temperature 270°C, reaction time 2 h. ....	115
Figure 68. HPLC chromatograms of HTL-AP and treated HTL-AP feeds (1: glycolic acid 2: lactic acid 3: glycerol 4: acetic acid 5: acetaldehyde 6: methanol 7: catechol 8: phenol 9: guaiacol 10: DEE). ....	117
Figure 69. Influence of carbon concentration and DEE pretreatment on the H <sub>2</sub> production for APR of different batches. Reaction conditions: 0.375 g 5% Pt/C, Liquid phase amount: 75 g, 270 °C reaction temperature, 2 h reaction time. ....	117
Figure 70. TGA-IR of spent catalyst after APR 1 <sup>st</sup> test of HTL-AP. Reaction conditions: 0.375 g 5% Pt/C, 0.8 wt.% C, reaction temperature 270 °C, reaction time 2 h. Analysis conditions: heat from 30 °C to 1000 °C @ 20 °C/min in nitrogen atmosphere with a purge rate of 20 mL/min under nitrogen. A: TG results; B: IR-Absorption peak during TGA of water, CO <sub>2</sub> , CH <sub>4</sub> , aliphatic fragments and primary alcohols; C: Infrared spectra at 408°C. ....	119
Figure 71. TGA-IR of spent catalyst after APR 2 <sup>nd</sup> test of HTL-AP. Reaction conditions: 0.375 g 5% Pt/C, 0.8 wt.% C, reaction temperature 270 °C, reaction time 2 h. Analysis conditions: heat from 30 °C to 1000 °C @ 20 °C/min in nitrogen atmosphere with a purge rate of 20 mL/min under nitrogen. A: TG results; B: IR-Absorption peak during TGA; C: Infrared spectra at 198°C; D: Infrared spectra at 298 °C. ....	121
Figure 72. XPS spectra of fresh and spent catalysts after aqueous phase reforming. Reaction conditions: 0.375 g 5% Pt/C, 0.8 wt.% C feed (HTL-AP or treated HTL-AP 3), 270 °C reaction temperature, 2 h reaction time. ....	122

# Chapter 1 Introduction

## 1.1 Global warming at a glance

In 1896, Arrhenius published the first paper in which the concentration of CO<sub>2</sub> in the atmosphere was linked with the temperature on the planet [1]. Afterwards, in *Worlds in the Making*, he explored the role that the mankind has on the emissions, surprisingly (for our time) looking to the beneficial effects of the global warming, such as increasing crops yields and avoiding a new Ice Age.

The awareness on the effect of human activity has increased during the last decades constantly, due to several causes. The scientific community, thanks to the escalation of collected data, is almost entirely agreed on assuming that the increase in the level of temperature is due to human activities, and that the CO<sub>2</sub> emissions are considered as the main cause [2]. In the following Figure 1, the correlation between the level of CO<sub>2</sub> in the atmosphere (obtained by arctic measurements) and temperature change is reported [3].

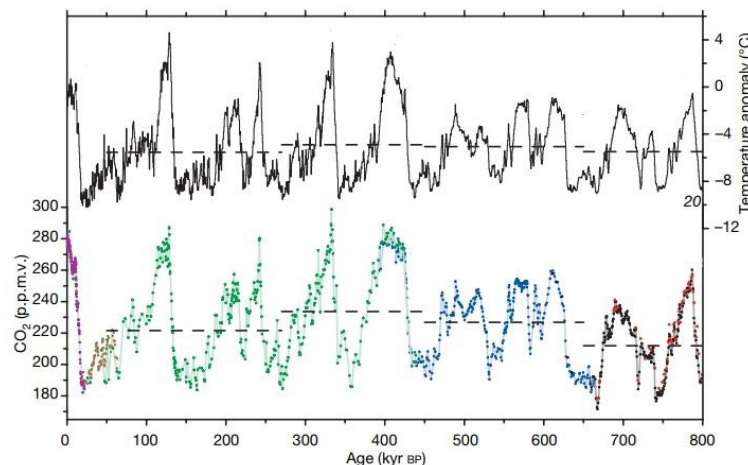


Figure 1. Correlation between carbon dioxide concentration in the atmosphere and temperature change (modified from [3]).

Burning of fuels (for the electricity/heat generation sector and for transportation) and deforestation are considered main drivers for the anthropogenic green-house effect [4]. 24 billion metric tons of carbon dioxide are emitted per year by stationary and mobile sources, and its concentration is 40% higher than before the industrial revolution [2]: reducing these numbers, despite the increase in population and the growth of modern economy, is one of the main challenges that human beings are facing in this era.

The Inter-governmental Panel on Climate Change (IPCC) declared that if the level of the emission remains with the modern rate, there will be an increase of 6



°C over the average [2]. While the scientists agree on the causes, the consequences of global warming are less clear. Anyway, some of the most plausible seem to be the sea level rise, impacts on the weather (heatwaves), flooding, biodiversity, diseases. Given that this scenario may lead to catastrophic consequences, the scientific community and policy makers try to go together towards finding a portfolio of solutions for this issue, working both in terms of climate change modification and adaptation.

The European Commission has developed in the last years several measures and proposed different strategies for the abatement of CO<sub>2</sub> emissions. In 2007, the European Union (EU) stated the 20/20/20 proposition, looking for a higher energy efficiency, reduction of greenhouse gas emissions and use of renewable energy sources. Overall, the experts suggest that the CO<sub>2</sub> concentration should not overcome 450 ppm to avoid 2°C in temperature rise by the end of the 21<sup>st</sup> century.

Bottom-line, the vicious circle of global warming should be stopped looking to several different strategies in order to decrease the green-house gas emissions, at the same time providing the energetic furniture that the society demands. No one has the magic wand to fix it with one simple solution; combined actions are necessary, like development of vehicle technologies, expansion of public transport, and including a greater awareness of society, modifying (adapting) our style of life.

Among the possible technologies, each one with different risk, cost and mitigation potential (i.e. nuclear energy, carbon capture and storage, etc.), a key role is played by the exploitation of renewable energy sources.

## **1.2 Renewable energy sources**

Renewable energy sources (RES) refer to rapidly and naturally replenishing resources of energy, not depleting on a human timescale. The use of renewable energy contributes to carry out the so-called sustainable development, that is satisfying the needs of the present generation, without compromising the future ones [5].

RES can provide electrical, thermal or mechanical energy. However, one of the characteristics of renewable energy is the oscillating nature of the output, leading to the need of storage.

In the last report, REN21 (an international policy networks of experts from governments, industry, academia etc.) estimated that 18.1% of the total energy consumption is renewable-based [6]. It is growing in the power sector, where renewable furnished 26% of the global electricity generation, while it remains low in the heating and cooling sector, as well as in the transport one, where it reached 3.3%. Here, electric vehicles interest is growing, while biofuels are the main drivers.

In the following, a short list of possible sources of renewable energy is reported.

### *1.2.1 Hydropower energy*

Hydropower exploits the potential energy of water from higher to lower elevations. Nowadays, this source is mainly dedicated to the production of electrical energy, being the main share of renewable energy in this sector. Hydropower is the most technically mature and reliable RES. In order to understand the importance of the technology, it is sufficient to think that the first reason for dams construction in Europe is power generation, only followed by irrigation and water supply.

It is estimated that hydropower will account for 16% of global electricity demand in 2023 [7]. Thanks to the possibility to be built at different scales, hydropower energy is a strategic key for the development of rural area, leading to small plants (< 10 MW) that are widely spread, with less capital costs and impact on the environment (two of the typical disadvantages of the technology) [8]. In this direction, some of the limitations that should be overcome are the capture of low-head resources, the deployment of fish-friendly turbines, together with no sediment build-up.

### *1.2.2 Wind energy*

If water is displaced by wind, here it comes the eolic technology, another well-developed electricity production route. Indeed, analogously to the hydropower energy, wind turbines convert the kinetic energy of wind into electrical energy thanks to the use of rotating blades. Wind energy is technologically mature, with good infrastructure and cost competitive [9]. In 2008 it accounted for 1.5% of global electricity production (about 121 GW, with only 1.1 GW installed offshore) [2], while in 2023 it will account for 6% of global electricity demand [7]. It has been estimated that the “economic-affordable” onshore productivity can overcome the human energy consumption. It can already be competitive with conventional fossil fuels in windy sites.

Wind energy is one of the best choices to provide electricity to remote areas thanks to the possibility to furnish small power. It has been simulated that large wind plants may increase the precipitation rate and the surface temperature [10]. For this reason, the development of small scales, with range from 1-20 kW and a diameter ranging from 3 to 10 m has been suggested.

However, there are still transmission capacity issues that need to be surpassed. For this and other reasons, it seems that the maximum fraction of electricity that can be obtained by eolic systems will be around 20%.

### *1.2.3 Solar energy*

Solar energy is widely considered as the real energy source of the future, given its abundancy and possibility to be exploited in great part of the planet,

without big discrepancy issues. The annual solar radiation is one order of magnitude greater than all the estimated fossil resources; 0.1% of the energy reaching the surface of the planet, converted with 10% efficiency, would surpass four times the world generating capacity. It is sufficient give these two data to understand how big the potential of solar energy is to solve our energetic issues [11].

It can be considered a source both as thermal and power outcome.

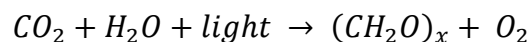
The thermal output can be exploited for cooking, water heating, crop drying [12]. For example, the use of solar water heater is beneficent for the environment, as it can mitigate about 1237 kg of CO<sub>2</sub> per year at half of its capacity [13].

On the other hand, the conversion to electric energy through the use of photovoltaic systems has been constantly growing through these years, thanks to the improvement in the economicity of the silicon technology, that decreased the price from 76.67 \$ in 1977 to 0.36 \$ in 2014 [12]. Solar energy, together with wind energy, have been seen by investors as dominant technologies for the future, receiving 47% of investments in 2016 [14].

#### *1.2.4 Bio-based energy*

Biomass is the only carbon-based renewable and sustainable source of energy. This is because the CO<sub>2</sub> emitted during the combustion is fixed by the plant during the growing stage, creating a greenhouse gas neutral circle [5]. Fossil sources (coal, crude oil, natural gas) have been produced by biomass decomposition through millions of years. This is the reason why biomass can be intended as a natural renewable substitution of conventional sources of energy and materials.

Biomass can be generally intended as all the matters on the plant of recent biological origin [2]. Thanks to the photosynthesis, it converts the carbon dioxide into a sugar molecule, releasing oxygen at the same time.



Sugar is present under the form of cellulose, hemicellulose and starch. Apart from sugar fraction, large aromatic compounds (defined as lignin) are present; finally, there can be the presence of triglycerides, alkaloids, resins etc.

Biomass is commonly divided into three generations.

First generation biomass refers to edible crops (sugarcane, corn, rapeseed), leading mainly to bioethanol and biodiesel. The high sugar or oil content and the simple conversion to the final product are the main advantages. However, because of the ethical issues raised by their exploitation (commonly known as food vs energy dilemma) and the high energetic input required for their cultivation, modern processes are being developed to avoid their use [15].

Second generation biomass is intended as lignocellulosic biomass, not edible, like dedicated crops or forestry residuals, that can give important advantages with respect to the first generation in terms of land use efficiency and environmental performance. Moreover, contrarily to the first generation, almost the whole plant can be used for energy production. It has been estimated that 476 million of tons of lignocellulosic biomass are necessary to satisfy the bio-products demand by 2030 [16]. The more complex internal structure compared to first generation leads to the necessity of pretreatment for their conversion into valuable products. Physical, chemical or biological processes are necessary to break the lignocellulosic skeleton and make all the components available for further reactions. Despite most of the processes based on second generation biomass are still at pre-commercial stage, the promised advantages in terms of competitive feedstocks and positive effects on the emissions, will lead to their development at full scale.

Finally, third generation is referred to aquatic biomass, like macro and microalgae. Macroalgae have high photosynthetic efficiency and rapid growth rate, without using fresh water or arable land [16]. Based on the composition of the biomass, different yields and energy conversion efficiencies can be obtained. For example, microalgae are richer in the lipid fraction, and for this reason most of the research have been focused on the production of biodiesel. In this scenario, the high cost of production seems to hinder this pathway. In the following Figure 2, a collection of processes and systems is depicted.

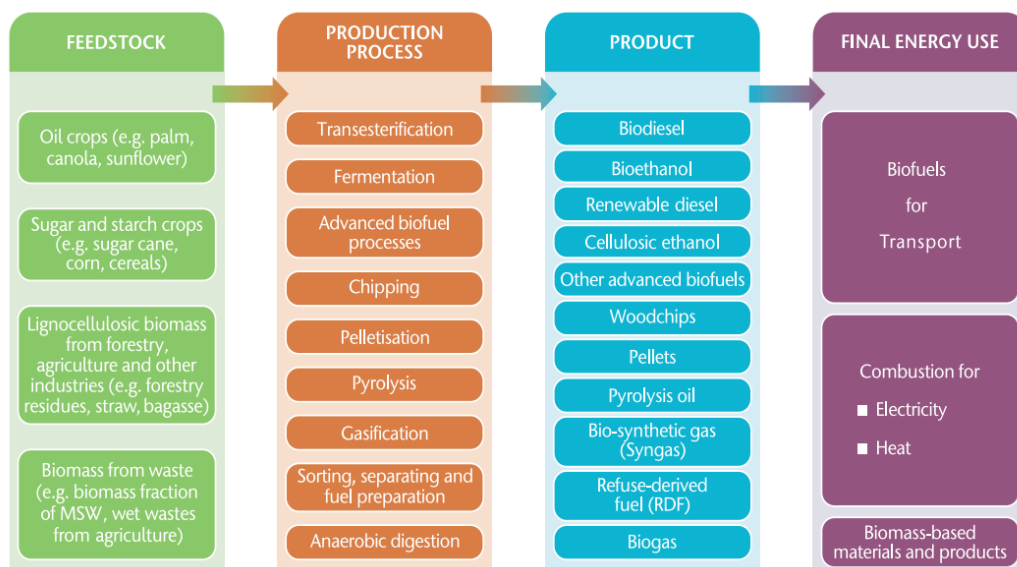


Figure 2. General information on the different kind of feedstocks, processes, products and uses in the frame of bio-based economy (from [17]).

In 2017, the exploitation of modern bioenergy (i.e. excluding the conventional use of biomass through burning) accounted for half of the renewable energy consumed, that is four times the contribution given by the summation of solar photovoltaic and eolic energy.

The price of the feed is often a key element when bio-based processes are analysed. Interestingly, it can range from negative prices (if waste biomass is used) to very high prices, when special crops are used.

The exploitation of biomass is based on different processes, commonly divided in thermochemical or biological processes. The conversion of biomass into products is carried out in a “new” place: the biorefinery. Its definition and peculiarities will be described in the following paragraph.

### 1.3 The biorefinery concept

Despite the apparent simplicity of the term and its closeness to the more familiar concept of the conventional refinery, the term biorefinery has three definitions [18]. For the sake of simplicity, let us consider the IEA definition: a biorefinery is the sustainable processing of biomass into a spectrum of marketable products [19].

The term biomass can refer to four different sectors: agriculture (with dedicated crops and with residue), forestry, industry and households, aquaculture [20]. In this sense, aim of the biorefinery should be the exploitation as much as possible the feed, at the same way as the refinery does with the oil barrel.

Sugar and starch based biorefineries aim to the production of bioethanol after a pretreatment, hydrolysis and fermentation (followed by distillation to increase the level of purity). Besides, lactic acid, 5-HMF, levulinic acid can be co-produced for financial viability and long-term sustainability [21]. The main by-products are CO<sub>2</sub> and unfermented grain residues or bagasse.

Lipid or triglyceride based biorefineries looks for fuels (biodiesel and hydrogenated vegetable oil) and oleochemicals (fatty acids and alcohols) production. Glycerol is an important by-product of biodiesel production (10 wt.%), from which many chemicals can be obtained like 1,2- and 1,3-propanediol, epichlorohydrin, acrylic acid.

Finally, a lignocellulosic biorefinery uses thermochemical conversions to produce fuels and chemicals starting from dry biomass, woody energy crops and waste biomasses (like the ones produced from starch based biorefineries). Biomass-to-liquid (BTL) technology, just to mention one example, looks to the productions of syngas by gasification of the biomass; afterwards, once that the gas stream is purified from contaminants, it can be used for heat and power production, or for liquid fuels thanks to Fischer-Tropsch reaction.

A biorefinery, thanks to different technologies, is able to produce not only energy (under the form of heat, liquid fuels, power), but also more valuable “refined” products, such as chemicals, fibers, biomaterials. Despite of that, currently the main goal for biorefineries is the production of biofuels. Each other by-product, should contribute to increase the economic and environmental benefits, towards the implementation of zero-waste production processes [19].

In the following Figure 3 the concept of biorefinery is reported.

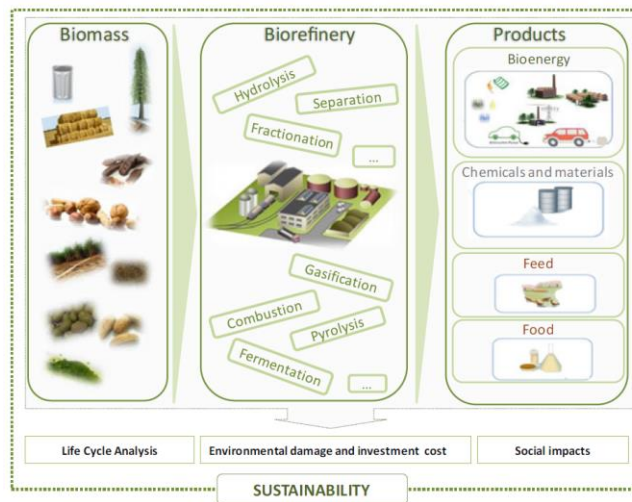


Figure 3. The biorefinery concept (from [18]).

Biorefineries should be designed also at small-medium sizes, helping to develop rural areas, reducing transportation costs (one of the drawback of bio-based industries) and preventing the dependence on imported energy sources [20]. For this goal, integrated systems should be developed, where the energetic and material interconnection will allow the complete use of the resource

Two different pathways are usually chosen for biomass valorization: biochemical and thermochemical conversion.

In the case of biochemical conversion of biomass, biological systems like enzymes are used for its valorization.

The enzymatic production of bioethanol is probably the most famous example of biochemical technology applied to biomass [22]. During this process, yeasts are able to convert the sugar monomers into ethanol, the most desired product, and other by-products (butanol, acetic acid, etc.) The technology of valorization of lignocellulosic biomass through fermentation is now at the large demonstration stage.

The second most known technology is the anaerobic digestion, where bacteria are able, slightly above the ambient temperature, to decompose organic matter into the so-called biogas, i.e. a mixture of methane and carbon dioxide [23]. The use of anaerobic digesters is nowadays a well-proven technology, widely used for the wastewater treatment. Indeed, it is able to convert a zero-value stream into a valuable gas, that can be upgraded and used as substituted natural gas.

Compared with biochemical processes, the thermochemical route is characterized by higher temperature and faster reaction rates. The thermochemical conversion can be carried out in dry or wet mode [24].

Dry route refers to three main reactions: combustion, gasification or pyrolysis. Combustion is referred to the production of energy as heat and power.

Gasification deals with the reaction of biomass at high temperature and with lower than stoichiometric oxygen, in order to produce commonly a

hydrogen/carbon monoxide mixture (syngas) to be used for petrochemical industry, or for energy production [25].

Pyrolysis allows the conversion of the feed into three different phases: a solid (char), constituted by inorganics and unconverted carbonaceous residues; a gas phase, constituted by low molecular weight gases; a liquid organic phase, constituted by a mixture of chemicals, and that can be used as a fuel after proper deoxygenation steps [26].

As dry processes may be expensive due to the necessity of a drying pretreatment, wet routes (i.e. hydrothermal) have been developed and are increasingly gaining attention [27].

Hydrothermal carbonization (160-250 °C) allows the production of a solid fuel with 35-60 % mass yields, depending on reaction parameters like the nature and loading of the feedstock, the reaction time, the temperature [28].

Hydrothermal liquefaction (300-350 °C) leads to the production of a biocrude (organic phase) as main product, similar to the oil derived from pyrolysis, that can be used as a fuel after suitable upgrade [29].

Finally, hydrothermal gasification (350-400 °C or 600-700 °C if carried out in near-critical or super-critical conditions, respectively) produces a gas mixture with different gas composition according to the level of temperature: hydrogen will be the main component at higher temperatures, while it will be methane at lower temperatures [30].

Each of these processes, beside the desired product, generates an aqueous side-stream with a consistent fraction of the inlet carbon. Indeed, the dissolved organics in the aqueous phase can account for 20 up to 50% of the initial loading [31]. Moreover, it has been estimated that the waste disposal cost is the second most important voice in the variable costs (33% at the actual state of technology), right after the feedstock costs, in the case of HTL of woody biomass [32].

While most of the literature has focused on the optimization of the reaction conditions for having the highest yield for a biocrude with the highest quality (i.e. mainly lowest oxygen concentration), there is a lack of knowledge on the characterization and valorization of the aqueous fractions derived from hydrothermal processes. On the other hand, the entire biomass should be exploited if the economic sustainability of the process must be reached. This means that also this fraction of the biomass should be recovered or converted into useful and valuable products.

The high-value added compounds present in the water fraction (phenols, carboxylic acids etc.) may be recovered thanks to the use of chromatographic or membrane separations. However, these techniques are very expensive and the composition of the aqueous phase very complex to allow the separation of a pure component. For this reason, processes able to valorize the by-products “as bulk” have been considered.

Anaerobic digestion has been applied for the production of biogas, but some of the dissolved organics may be toxic for the microorganisms present in the broth [33]. For this reason, pretreatments may be necessary to improve the

biodegradability of the molecules present in the aqueous phase (like adsorption on zeolites or activated carbon).

The wastewater can be used for algae cultivation, as the aquatic biomass is able to exploit its loading of organic and inorganic nutrients [34]. Even in this case, there is the risk that some compounds can be toxic for the growth of algae, such as ammonia compounds, or aromatic compounds (phenol, toluene, benzene) [35].

The catalytic hydrothermal gasification is another option to valorize the water fraction to produce a fuel gas [36]. Despite its effectiveness, it is energetically demanding due to its high temperatures (>600 °C).

The present work aimed to investigate a new candidate process for the valorization of wastewater derived from biomass processing: the aqueous phase reforming.

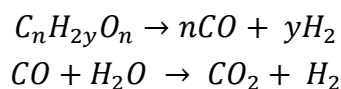
## 1.4 Aqueous phase reforming

Dumesic and coworkers published in 2002 a milestone paper in which biomass-derived molecules (glucose, sorbitol, glycerol) were catalytically converted into a gas phase where hydrogen constituted almost 50% of the products [37]. Starting from these first results, the aqueous phase reforming (APR) has been proposed as a valuable process to valorize carbohydrates and waste streams derived from biomass, in order to renewably produce hydrogen. Afterwards, it can be used to feed a fuel, cell, to perform hydrogenation processes etc.

In the next paragraphs, the main features of APR will be reported, together with its challenges and perspectives.

### 1.4.1 Introduction to APR

Starting from carbohydrates (C:O ratio of 1:1), hydrogen can be produced thanks to the following reactions



The first one represents the decomposition of the molecule into carbon monoxide and hydrogen, while the second equation refers to the water gas shift (WGS) reaction, where carbon monoxide reacts with water, leading to carbon dioxide and hydrogen.

As reported in the Figure 4, the reforming of alcohols and polyalcohols (methanol, ethylene glycol, glycerol etc.) is thermodynamically more favourable at lower temperature compared to alkanes. This outcome leads to several advantages. First of all, there is a reduction of required energy, carrying out the reaction at 230-270 °C, contrarily to the conventional steam reforming of alkanes,



whose working temperature is typically about 800 °C. Moreover, as the pressure is increased to maintain water in liquid phase, the energy for the vaporization is saved. The second benefit is that WGS is favourable in the same range of temperature. This means that, in the same reactor, the hydrogen production is pushed while the concentration of carbon monoxide is minimized. This is an important outcome if the stream is injected in a proton exchange membrane fuel cell (PEMFC), where CO can act as a poison for the anode [38]. Globally, APR would allow to produce a pressurized hydrogen-rich gas mixture in a single-reactor system, working at low temperature.

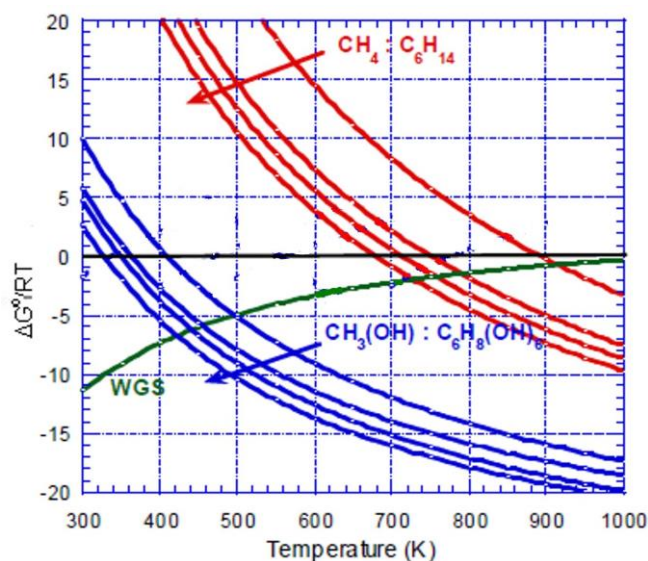


Figure 4. Thermodynamic equilibrium for hydrogen production, modified from [39].

Besides thermodynamic considerations, important kinetic (and selectivity) issues must be highlighted. In the Figure 5 the reaction mechanism suggested for APR shows the possible pathways. In the first step, the molecule adsorbs on the active sites of the catalyst, leaving a hydrogen molecule. The type of adsorption (site-carbon or site-oxygen) depends on the nature of the active site and is ruled by energetic considerations. For example, in the case of platinum catalyst, the adsorption with a carbon atom is favoured compared to the adsorption with oxygen [40]. After the adsorption, three main pathways can be followed. The first one, i.e. the desired one, contemplates the breaking of the C-C bond, with production of hydrogen and carbon monoxide. At this point, the latter should react with water through the WGS reaction, producing one more molecule of hydrogen and carbon dioxide. This is a key step in the whole reaction mechanism. One of the risk is that the catalyst is not able to activate effectively the WGS, favouring methanation reactions, that would reduce the hydrogen selectivity by CO reaction; or, the activity for methanation is high enough to activate the formed carbon dioxide, causing anyway the loss of one hydrogen molecule (series-selectivity). The consequence of these possible reaction pathways is that the choose of the

catalytic system must be selective towards WGS reaction much more than for methanation.

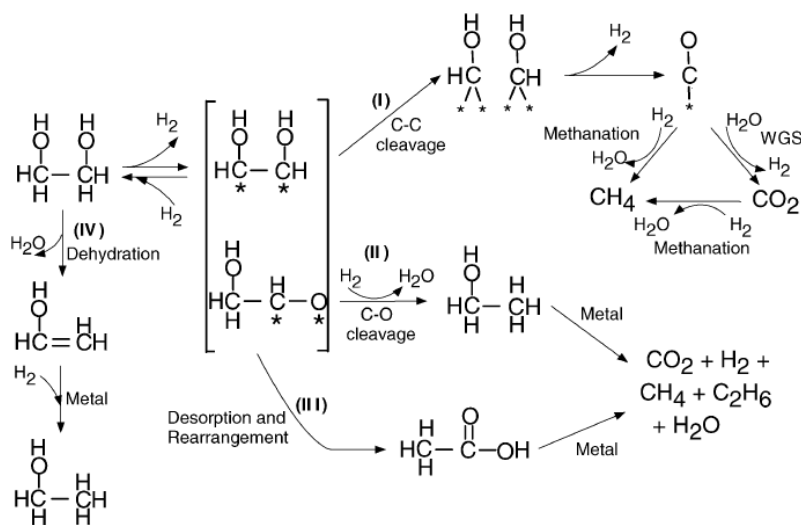


Figure 5. APR reaction pathways as proposed in [39].

One parallel-selectivity challenge involves the possibility that the adsorbed molecule undergoes to a C-O cleavage step. This reaction would involve hydrogen as reactant, and leads to an alcohol molecule, that can further react to produce hydrogen, but also alkanes, globally reducing the fraction of hydrogen in the feed that is converted into molecular  $H_2$ . Another parallel pathway refers to the desorption of the molecule and its rearrangement in the aqueous phase, leading to an organic acid and, by subsequent interaction with the catalyst, to hydrogen and alkanes. Finally, it is worthy to cite the possibility of a first homogeneous step, mainly influenced by the acidity/basicity properties of the support, that dehydrates the molecule, and afterwards produces an alcohol, by hydrogenation [39].

It is important to highlight here that two aspects arise from the undesired pathways. First point is the consumption of hydrogen, that, being the desired product, the decrease of its yield should be avoided. Second point is the deoxygenation of the molecule (as in the path II). Indeed, a key point in APR is the production of a CO molecule. If it is not the case, the formation of alkanes is favoured, and they cannot be further activated at these temperatures to produce hydrogen. This is also the reason why, conventionally, molecules with C:O ratio equals to 1 have been investigated.

Vlachos and coworkers used microkinetic modelling to evaluate the influence of the aqueous phase on the kinetic of APR [41]. In aqueous phase, the initial C-H scission is favoured as it has lower barrier energy than O-H scission. Moreover, the water solvation of the catalyst surface promotes the water gas shift, minimizing at the same time the poisoning effect due to the coverage of CO.

Once that the basis for APR have been reported, showing thermodynamic and kinetics considerations, in the following paragraph the parameters that influence the hydrogen yield and the carbon conversion will be reported.

### 1.4.2 Influence of reaction parameters

Because of the complexity of the reaction network, several parameters can be modified to tune the product distribution. In the following, the influence of the nature and concentration of the feed, temperature and pressure, catalyst, and reactor configuration will be reported.

As reported previously, the APR has been proposed to valorize biorefinery water fractions derived from biomass processing. For this reason, typically model compounds such as alcohols and polyalcohols, sugars and sugar alcohols have been studied [42]. For instance, glycerol has been extensively studied because it is a by-product of the biodiesel industry and finding a path for its valorization would be strategic for the entire process. Another important model compound is glucose, a highly present molecule in biomass as it acts for energy reserve. On the other hand, few works have been addressed to the study of more complex feeds, like cellulose, wastepaper or aqueous phase derived from other processes (pyrolysis, hydrothermal liquefaction etc.).

Starting from the first work on APR, it has been reported that the hydrogen yield is affected by the chain length, and it increases when the molecule is smaller (Figure 6) [37]. Indeed, it has been proposed that when a high molecular weight compound is used as feed, the reaction conditions can be tailored to produce heavier alkanes (butane, pentane, hexane). For example, hydrogen selectivity decreased from 99% to 36% moving from methanol to glucose, over 3% Pt/Al<sub>2</sub>O<sub>3</sub> at 265 °C, while the alkane selectivity increased from 3% to 33% [37].

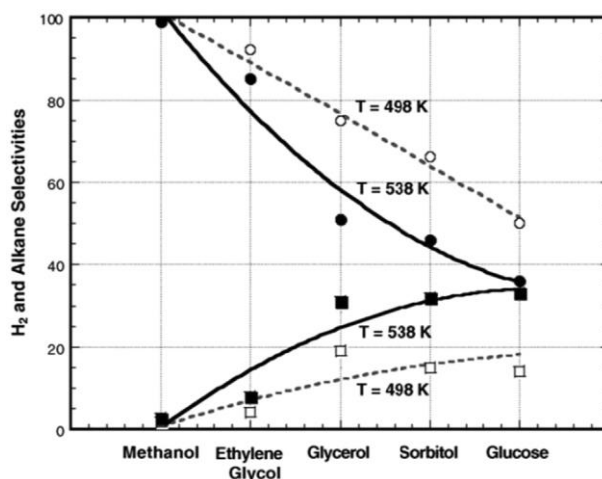


Figure 6. Influence of chain length on APR performance [42].

The typical range concentration for wastewater streams is 1-10 wt.% of organics. It has been observed that polyols are insensitive to the feed concentration [39]; on the other hand, glucose was found extremely recalcitrant towards hydrogen production in the case of concentrated solutions. It has been explained by the different reaction orders involved in the whole reaction network. Indeed, reforming reactions are fractional order for hydrogen production, despite the exact number depends on the feed (for example it is 0.8 for methanol and 0.3-

0.5 for ethylene glycol, because of the weaker adsorption of the former on the Pt surfaces) [43]. Conversely, glucose can undergo to homogeneous first order reactions [44], that are by consequence more favoured compared to reforming reactions the more concentrated is the starting solution. This challenge should be overcome if one wants to exploit a cheap and easily available molecule as glucose is. Modification of operating conditions such as lower reaction temperature, increase of active sites to favour surface reactions, change of the pH of the solution has been proposed. Moreover, another possibility consists on the pre-hydrogenation of the sugar to the corresponding sugar-alcohols, as sorbitol does not suffer from homogeneous decomposition.

The typical reaction temperature and pressure is in the 200-270 °C and 20-50 bar range. These conditions favour not only the desired reactions (reforming and WGS), but also methanation, Fischer-Tropsch etc. It has been reported that the increase in the reaction temperature led to an increase in the conversion of the feed, and in particular in the transformation to gaseous products [45]. This is due to the more favourable bond breaking reactions. At the same time, the hydrogen selectivity decreases, whereas carbon dioxide, carbon monoxide and methane selectivity increases [46]. The pressure of the system should be high enough to maintain the water in the liquid phase. It has been showed that the level of pressure has important kinetic consequences: higher pressure can reduce the rate of hydrogen production because it hinders the desorption of the products from the active sites, making them available for new reactions. Actually, it has been suggested that, for a selectivity point of view, the bubble-point conditions should be optimal for aqueous phase reforming [47].

Being a catalytically activated reaction, the catalytic system plays a fundamental role to convert the feedstock and produce selectively hydrogen, without being deactivated. Indeed, most of the published works dealing with aqueous phase reforming looked at optimizing these features.

Looking to the reaction network reported in the Figure 5, it is suggested that the optimal catalyst should maximize the C-C bond breaking and water gas shift activity, while the C-O bond breaking, methanation and Fischer-Tropsch activity should be hindered; moreover, the support should not allow dehydration reactions. Davda et al. reported a ranking among several VIII group metal catalysts supported on silica for the APR of ethylene glycol [48]. The choose of this group of the periodic table refers indeed to their known ability to carry out C-C cleavage reactions. They showed that Pt has similar activity to Ni, followed by Ru, Rh (similar to Pd) and finally Ir. Apart from activity (defined as the rate of CO<sub>2</sub> production), the selectivity to hydrogen was also measured. In this regard, Ru, Rh and Ni showed low selectivity (the latter reported also deactivation during the time on stream), with only Pt and Pd showing also high selectivity. This is because, as said before, not only the C-C bond breaking capacity is involved, but the catalyst should also be able to activate the water gas shift and minimize side reactions. In the Figure 7, a screening of the catalyst is reported looking at the comparison for the three main reactions: C-C cleaving (white bar), water gas shift (grey bar), methanation (black bar).

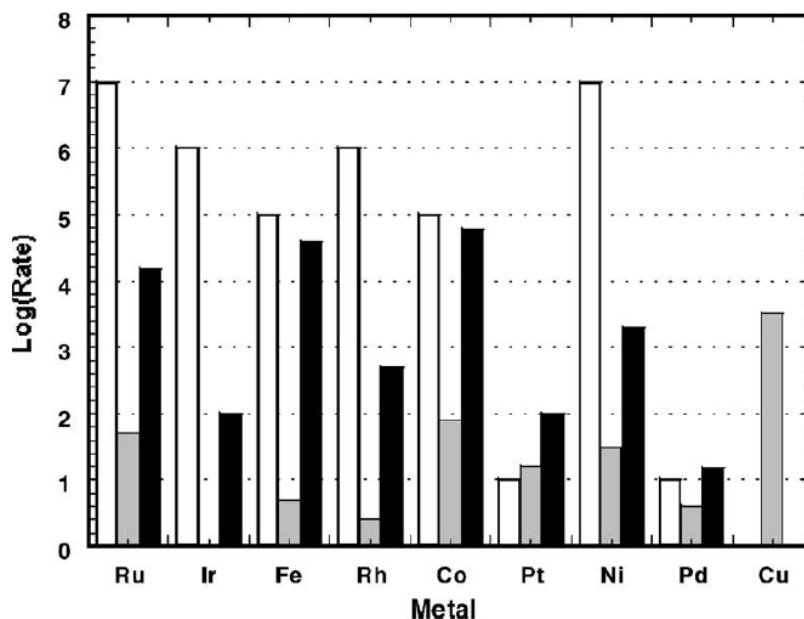


Figure 7. Relative rates of the three main possible reactions under APR reaction conditions, as reported in [48].

Being Pt the most promising active site, combining high activity and selectivity, it was chosen for the study of the effect of the support [49]. Even in this case, scope of the work was to evaluate a ranking in terms of activity and selectivity. First of all, silica and ceria supports showed deactivation (decrease of the activity >20%) during 24 h tests. Titania reported the highest hydrogen turnover frequency, followed by unsupported Pt-black, activated carbon and alumina. Lower TOFs were showed by silica-alumina support and zirconia. Moreover, Pt/C showed high carbon TOF, i.e. production of gaseous alkanes or liquid by-products. Alkanes may derive also from the reaction of the molecule with Bronsted acid sites on the support, that can favour acid-catalyzed dehydration reactions. In this case, ethylene glycol may be dehydrated to acetaldehyde, afterwards being hydrogenated on the Pt site to ethanol, that is an alkane precursor. Apart from ceria, the other supports seem not to influence the water gas shift. Moreover, a sintered version of the Pt/Al<sub>2</sub>O<sub>3</sub> catalyst reported small change compared to the original one, suggesting that the dispersion may play a small role for hydrogen production, compared to the effect of the support.

Wen et al. reported a study on the influence of the active component and the support for the APR of glycerol [50]. They observed the highest rate of hydrogen production for Pt catalyst supported on alumina; Cu showed also relatively high rate: however, it can be ascribed to dehydrogenation activity of the metal, and not to reforming one. At the same time, Co and Ni showed lower hydrogen production, together with deactivation phenomena because of loss of exposed metal sites, because of sintering (evaluated by H<sub>2</sub> chemisorption of the spent catalysts), oxidation of the active sites and carbon deposition. Afterwards, the

effect of the acidity of the support was measured using a basic support like MgO, neutral supports like Al<sub>2</sub>O<sub>3</sub>, SiO<sub>2</sub> and active carbon, a weak acidic support like SAPO-11, and an acidic support like HUSY. Neutral alumina exhibited the highest rate for hydrogen production, followed by basic MgO. Alumina showed crystallization phenomena during the time on stream, with formation of new boehmite phases. The particular results obtained by MgO are due to the alkali enhancement by absorption of carbon dioxide into the support [51]. Finally, acidic supports led mainly to alkane formation, through dehydration followed by hydrogenation. Moreover, in agreement with the previously cited work, the observed sintering of Pt did not play a role as deactivation was not observed.

Wawrzetz et al. investigated the effect of Pt particle size on glycerol APR and observed that the increase in the dimension caused a decrease in the formation of hydrogen and carbon dioxide, while the hydrodeoxygenation products increased [52]. So, it is possible that the reforming reactions are sensitive to the concentration of active sites at the support-metal boundary. The use of ATR-IR spectroscopy allowed to follow the reaction intermediates, looking in particular to glyceraldehyde and hydroxyacetone that were detected in the liquid phase only in small amounts.

In situ ATR-IR was used recently also by Sievers and coworkers for the APR of glycerol, sorbitol and glucose over Pt/Al<sub>2</sub>O<sub>3</sub> [53]. Contrarily to Wawrzetz they did not observe glyceraldehyde or hydroxyacetone peaks, while linear and bridged CO was recognized as dominant surface species, together with H atoms. The presence of dehydrogenated species has been suggested not by direct spectroscopic analysis. The size of the Pt particles affects the mode of adsorption of CO. For example, bridge adsorption requires a minimum size, so it is favoured on terrace, while decarbonylation occurs at edge and kink sites, from where the CO migrates to the terrace. In this case, having always the same size, the different ratio between bridge and linear was ascribed to the nature of the feed, and, therefore, to the competitive adsorption with the intermediates. Looking to the linear adsorption mode, it decreased from glycerol to glucose, so it was replaced by other surface species. Bridged CO is also more active toward water gas shift.

Platinum has been used also in combination with other metals to increase its effectiveness through synergic behaviour. Huber et al. screened more than 130 Pt and Pd bimetallic catalysts using a high-throughput reactor [54]. Reducible oxides, noble and base metals were used as second component in the bimetallic configuration. Ni, Co and Fe, at different atomic fractions compared to Pt, reported higher hydrogen production with respect to the monometallic catalyst. Ni and Co led to 1.5-2.8 times higher H<sub>2</sub> turnover frequencies, while the increase was lower for Fe. The reason for this behaviour can be ascribed to the lower heat of adsorption for H<sub>2</sub> and CO dissociation on the sites compared to Pt alone. The decrease in the d-band caused a decrease in the binding energy of hydrogen and carbon monoxide, leading to a decrease of the surface coverage caused by these molecules, and therefore higher availability for new ethylene glycol molecules to start the catalytic cycle.

Kim et al. studied the influence of addition of a second component at 1:1 molar ration on Pt-based CMK-3 supported catalysts [55]. Pt-Mn bimetallic catalysts showed the highest hydrogen production rate, while Pt-Re reported the highest conversion of ethylene glycol. Apparently, Mn did not participate in improving the C-C cleavage, but it helped to increase the selectivity towards hydrogen production, thanks to its effectiveness as promoter for water gas shift. Moreover, it hindered C-O bond breaking and dehydration reactions, as the reforming ratio based on the reaction stoichiometry (hydrogen/carbon dioxide ratio) was closer to the theoretical one in the case of the bimetallic catalyst.

King et al. reported the effect of Re addition on a Pt/C catalyst for the APR of glycerol (Figure 8) [56]. They observed that the addition of Re increased dramatically the conversion of glycerol and the hydrogen turnover frequency, despite the alkane selectivity increased as well. The authors highlighted that Re works as a promoter, because a test performed with a monometallic Re catalyst was not active. The reason was due to the beneficial influence of Re on the water gas shift step, working in a double way. On one side, the formation of Pt-Re alloys increase the rate of dehydrogenation; at the same time, the presence of ReOx species can give an alternative pathway for the production of CO<sub>2</sub> and H<sub>2</sub>, because CO can be oxidized by ReOx, while the latter can be re-oxidized by water, giving hydrogen. Ciftci et al. suggested that Re decreased the strength of adsorption of CO on Pt sites, decreasing its coverage at the steady state [57]. At the same time, the acidic character of the ReOx species, favour dehydration reactions, explaining the higher production of alkanes.

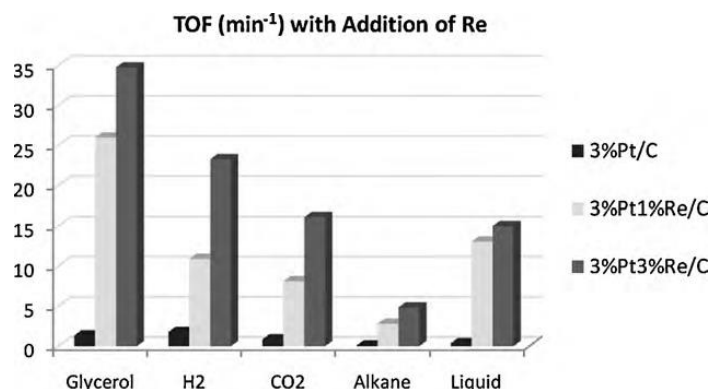


Figure 8. Effect of Re addition on Pt/C [58].

Tanksale et al. studied Pt-Ni bimetallic catalysts looking at the metal-support interaction aspects [59], studying the effect of impregnation sequences on alumina nanofibers, mesoporous zirconia and mixed oxide of ceria-zirconia-silica, which can affect the reducibility and activity of transition metal catalysts. While the two latter supports did not report effects by the preparation method, alumina nanofibers showed to be influenced by the impregnation sequence, and the strong metal-support interactions in the case of sequential impregnation likely caused the absence of alloy formation, worsening the performance of the catalytic system; on the other hand, the co-impregnated catalyst showed the highest hydrogen formation. This is because the formation of the alloy reduced the number of strong

CO-binding active sites (measured by microcalorimetry experiments), despite the Pt concentration is much lower than Ni concentration (1:33) [60]. The promoting effect of Pt allowed to increase the hydrogen production up to five times compared to the monometallic Ni.

Palladium catalysts have been tested for the APR of ethylene glycol, looking in particular to its interaction with  $\text{Fe}_3\text{O}_4$  support [61]. The performance of the catalyst synthesized by different methods (impregnation and co-precipitation) were analysed, with the latter allowing to obtain higher  $\text{H}_2$  TOF thanks to the synergism between the small Pd nanoparticles and the magnetite support. Indeed, this strong interaction increases the water gas shift rate, that is believed as the rate determining step for ethylene glycol on Pd catalysts. The co-precipitation method allowed also to have a catalyst with higher stability.

Despite platinum is the most used catalyst for aqueous phase reforming given its high performance, the development of alternative cheaper catalysts is important for the success and utilization of this process at industrial scale. Among the others, Nickel-based catalysts have been explored for their potential.

Shabaker et al. performed the APR of several polyols using monometallic Ni on different supports, and bimetallic Ni-based catalysts, together with Raney Ni and Raney Ni-Sn [62]. They observed that Ni/ $\text{TiO}_2$  supported catalyst was the most active and selective for hydrogen production. The addition of Sn allowed to increase the performance of the catalyst, despite it negatively affected its stability (leaching). The increase in selectivity may be due to the presence of Sn at Ni defect sites, or to the formation of alloy, that suppress the C-O bond breaking and methanation activity, as the latter in particular is favoured by the presence of defect sites. In order to overcome deactivation issues, the authors developed a method for adding Sn to Raney Ni catalyst, showing comparable results with Pt/ $\text{Al}_2\text{O}_3$  catalysts.

Wen et al. tested Ni-based catalysts for the aqueous phase reforming of cellulose [63]. In particular, the authors added Ce to Raney Ni catalysts at different molar ratios (Ce:Ni from 0.005 to 0.099), observing an increase in the hydrogen yield and selectivity at the optimal ratio (0.054). The addition of Ce caused an increase in the number of defects, however, being the methanation reactions structure-sensitive, only a fraction of them contributed to promote it. Analogously to Sn, Ce likely blocked the Ni sites for CO adsorption, suppressing methanation; at the same time, it contributed to the increase of water gas shift activity, thanks to the formation of reducible  $\text{CeO}_2$ . CO should be oxidized by the oxygen coming from ceria on metal particles; afterwards water caps the oxygen vacancy on the oxide.

Most of the works available in literature refers to the use of fixed bed reactors. However, being a gas-evolving reaction, the transport of products away from the active sites may play a fundamental role to increase the hydrogen productivity. It has been highlighted that the hydrogen partial pressure has a negative impact on the performance of the process, because it can block the active sites and create a series-selectivity issues, thanks to the high reactivity of hydrogen, in particular with platinum-based catalysts. For this reason, few works started to evaluate the



effect of reactor configuration or gas addition to promote the transport phenomena of the products.

Neira D'Angelo et al. evaluated the selectivity to hydrogen during sorbitol APR using a microchannel reactor, and compare it to the performance obtained using a fixed bed reactor [64] (Figure 9). The authors report that the conversion was not affected by the type of reactor, while the hydrogen selectivity was higher in the microchannel type in the whole range of conversion studied. The reason for these results can be ascribed to the more effective mass transport in the case of the microchannel with respect to the fixed bed. Once formed, hydrogen can be transferred to the gas phase, where it cannot further react, avoiding its consumption in hydrogenation/hydrogenolysis reactions.

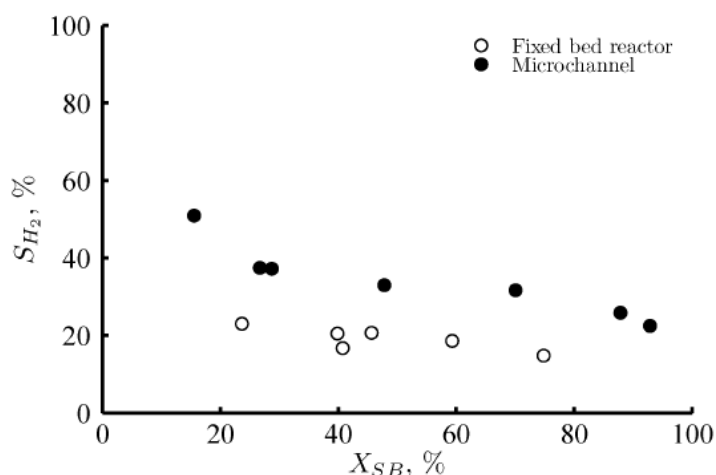


Figure 9. Influence of reactor configuration on  $H_2$  selectivity [64].

Moreover, they evaluated the effect of the hydrogen partial pressure co-feeding mixtures of nitrogen and hydrogen at different ratios. They observed a decrease of the sorbitol conversion and hydrogen selectivity when the hydrogen partial pressure increased, likely due to the strong adsorption of hydrogen on the active sites, reducing their availability. Finally, the increase of hydrogen production observed with the addition of a nitrogen flow, was coherent with the hypothesis that the local concentration of hydrogen is fundamental to avoid side-reactions. Adding an inert flow contributed to decrease its partial pressure and, as a consequence, the hydrogenation/hydrogenolysis kinetics. The same reactor configuration was used to investigate its advantages in the case of a more active catalyst (Pt-Ru), using again sorbitol as model compound [65]. While without a gas co-feeding the Pt-Ru catalyst was more active but less selective than the monometallic Pt, the use of hydrogen stripping allowed to increase the hydrogen selectivity in the case of the bimetallic, without affecting the activity. The authors found beneficent effects both on the sorbitol conversion and hydrogen selectivity up to  $1 \text{ m}^3_{\text{gas}}/\text{m}^3_{\text{liq}}$ , while a further increase did not cause any modification on the performance.

The same research group investigated a carbon on alumina membrane reactor for the APR of sorbitol [66]. The use of carbon decreased the interaction with water molecules thanks to its hydrophobicity, allowing the use of this membrane in wet conditions and also with a porous structure (2-50 nm) without risk of water loss. The membrane did not affect the level of conversion, since the partial pressure of hydrogen does not change (being the permeation unselective among the produced gas). However, the hydrogen selectivity was 2.5 times higher than the case without membrane, because the permeation prevented hydrogen-consuming side reactions.

Structured catalysts in microreactors were investigated by Entezary et al. for the APR of ethylene glycol and glycerol over Pt/Al<sub>2</sub>O<sub>3</sub> and Pt/CeO<sub>2</sub>-Al<sub>2</sub>O<sub>3</sub> catalysts [67]. The use of structured catalysts allows to reduce the risk of bypassing, leading to a stricter control on residence time of the feed. The use of the microreactors allowed higher hydrogen yield with the respect to fixed bed reactor (used as reference). The authors highlighted the importance of coupling to an active catalyst also an effective reaction configuration.

The influence of mass transport in the performance of the process has been studied considering the effect that the formation of bubbles can have on the microfluidic. Ripken et al. studied the influence of bubble on the momentum, heat and mass transport close to a catalytic surface [68]. The bubbles decreased the conversion in particular at high catalytic surface coverage, as they partially block the catalytic surface.

### *1.4.3 Towards the application of aqueous phase reforming*

As it was reported, most of the works has been referred to the development of effective catalytic systems able to produce hydrogen starting from model compounds. However, it is crucial to understand if the aqueous phase reforming can be adapted also to the use of more complex biomass, readily available and, therefore, cheap, to be economically competitive. In the last years, while this work was ongoing, some works started to be published looking to possible application of the aqueous phase reforming in an industrial reality.

In 2006 Valenzuela et al. published the first work in which real (woody) biomass was subjected to APR [69]. Pine saw dust was chosen as reference biomass. The use of a platinum-based catalysts allowed to increase the gas production compared to the case in which only a homogenous acid catalyst was used (5% H<sub>2</sub>SO<sub>4</sub>). Moreover, the gas composition significantly changed, with the increase of hydrogen concentration and the decrease of carbon monoxide and carbon dioxide. This is likely due to the water gas shift reaction that has been activated by platinum addition. Studying the reasons for the deactivation of the catalyst, the authors excluded the leaching, while suggested sulphur poisoning due to the presence of sulfuric acid in the reaction environment.

In 2008 Xiaonian and coworkers used APR as technique of degradation of organics in waste streams, like phenol, aniline, nitrobenzene etc. [70]. Raney Ni, Sn-modified Raney Ni and Pd/C were used as catalysts. The authors observed that

under optimal reaction conditions, the organics can be fully degraded, while the hydrogen selectivity changed according to the chemical structure of the feed. Sometimes, the recycle of the stream was necessary to reach the complete conversion. They observed that adding the Sn on the Raney Ni catalyst did not affect the conversion, but increased the hydrogen selectivity, as the methanation reaction was suppressed. The presence of nitrogen in the molecule complicates the reaction mechanism, where in this case also the C-N bond breaking was involved (for example in the case of aniline), and nitrogen-containing gas ( $\text{NH}_3$ ) can be produced as well.

In 2009 Vispute et al. studied the exploitation of the aqueous phase derived from pyrolysis oil production [71]. Bio-oil is a fuel that can be obtained from lignocellulosic biomass with a rapid heating at intermediate temperature in an inert environment. The water-soluble compounds were extracted using deionized water; afterwards the aqueous solution was subjected to hydrogenation, followed by APR. The pre-hydrogenation was carried out to stabilize the compounds (glucose, levoglucosan) that, otherwise, would cause coke production during the reforming step. Due to the poor performance in the APR step, the hydrogen consumption during the pretreatment was higher than the production during the reforming.

In 2010 Wen et al. performed the direct APR of cellulose over a Pt/C catalyst [72]. Despite the more complex conditions compared to the already studied of glucose APR, the hydrogen production was higher than the cited case. This is because the slow hydrolysis allowed no to increase locally the glucose concentration, favouring in this way the surface-catalyzed reaction (leading to hydrogen) with respect to homogenous reactions, leading to carbonaceous deposits and deactivating the catalyst. This explanation is linked with the observation that higher hydrogen yield was obtained with materials having higher degree of crystallinity, and therefore, slower hydrolysis and glucose production.

Irmak et al. published a work dealing with the APR of kenaf, a lignocellulosic biomass with fast growth rate and large production, up to 30 T/hectare [73]. The authors initially performed the hydrolysis of the biomass at water subcritical conditions, depolymerizing cellulose and hemicellulose; in the following, the obtained hydrolysate was subjected to APR over a 5% Pt/activated carbon catalyst. As comparison, also the solid biomass as such was tested, without any pretreatment. In the latter case, the gas produced was mainly constituted by carbon dioxide (46%), and also up to 16% of carbon monoxide; this result was ascribed to the presence of solid deposits that block the active sites preventing the water gas shift reaction. When the APR of the hydrolysate was performed, the gas was mainly constituted by hydrogen (60%) and no CO was detected. The comparison with glucose as model compound is reported in Figure 10.

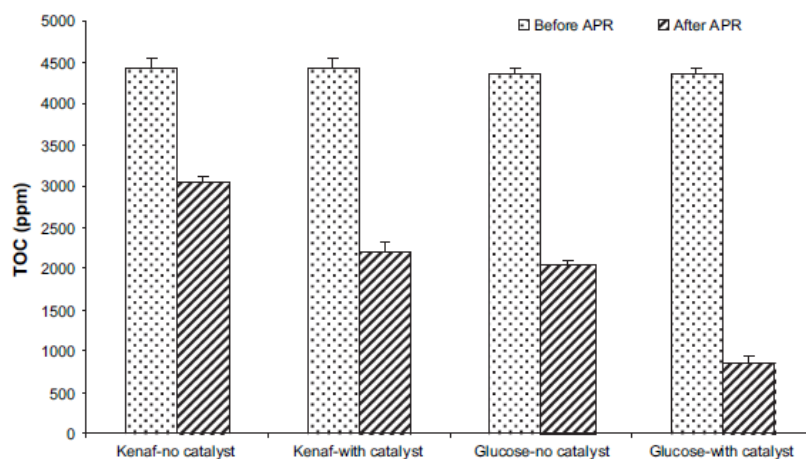


Figure 10. TOC content of kenaf and glucose before and after APR [73].

In 2018 Oliveira et al. studied the aqueous phase reforming of fish-canning industry effluents as a process for waste water treatment [74]. This is because the levels of salinity contained in the water, together with the variable organic loads, prevent the conventional disposal via biological treatment. The authors choose tuna-cooking effluents, with a pH equals to 6, TOC about 1900 mg C/L and COD about 5000 mg/L. They observed that the support was able to decrease the TOC and COD in a greater extent compared to the catalyst (Pt/C), because of the physical adsorption of the compounds into the support itself (55-75% vs 45-60%), confirmed by TGA analysis. The Pt catalyst supported on carbon black gave the highest gas yield, with CO<sub>2</sub> being the main component (about 82 mol.%), maybe because of its basicity, that favours reforming reactions. Three successive applications of the catalysts showed a deactivation in the case of Pt/carbon black (with decrease of gas production from 268 to 190 μmol), while it was stable in the case of the other supports. On the other hand, the hydrogen concentration increased, ascribed to the sintering phenomena that, reducing the low-coordination Pt sites, hindered the methanation reactions. Moreover, the specific surface area of the catalysts decreased after three cycles. The presence of inorganics, like chloride ions, may also have contributed to the stability of the catalyst.

In 2019 the same research group extended its investigation on the production of hydrogen from brewery wastewater [75], starting from information on the composition of real effluents. The different supports did not affect the decrease of TOC and COD, despite their different textural properties. Chloride, phosphate and sulphate anions concentrations were not affected by APR, while glycolate, acetate and formate were recognized as main anions after the reaction. The hydrogen yield reached about 290 mL H<sub>2</sub>/g COD, that is significantly higher than the yield obtained by anaerobic digestion with similar COD starting conditions (150 mL H<sub>2</sub>/g COD). The presence of carbonaceous deposits was considered responsible for the deactivation observed along 5 successive cycles.

Further improvements in APR development can derive from its coupling with other processes [76]. For example, it can be coupled with chemical looping combustion, co-producing heat and power, allowing at the same time the carbon dioxide separation. Another option derives from the coupling with a biological process, like carbohydrate fermentation for ethanol production, where the APR reactor can produce hydrogen from the ethanolic solution [77]. Indeed, the possibility to carry out the reforming in diluted conditions (contrarily to the case of ethanol steam reforming) prevents the energetic expenditure devoted to evaporation and concentration of the solution. Methane, a by-product of ethanol APR, can also be used as a fuel. In their work, the authors observed deactivation phenomena that have been ascribed to the presence of large biomolecules, and the stability of the catalyst was improved performing a nanofiltration as pretreatment. The fermentation-APR process allowed to obtain an energetic efficiency close to 60%, higher compared to the value obtained with the fermentation only (53%).

Aqueous phase reforming for hydrogen production is not applied at the industrial level yet, but preliminary analysis showed its potential for application. Murzin and coworkers recently published a techno-economic analysis about the APR of sorbitol [78], using Aspen HYSIS for process simulation, to produce 500 kg/h of hydrogen. This would be the amount necessary for the annual production of 100000 T of green diesel from tall oil. The costs for hydrogen production considered both capital investments and operational costs, and referred to the APR reactor, hydrogen purification section and consumption of utilities. The analysis showed that 91% of the cost of hydrogen is due to the feedstock price, therefore suggesting that sorbitol production should derive from lignocellulosic biomass in order to be economical attractive.

## **1.5 Aim and structure of the work**

Summarizing what has been reported so far, it is important to highlight that one of the limitations of biorefineries is the low exploitation for the carbon content of the biomass, that in turn leads to the formation of large amount of waste streams, commonly diluted carbon-laden aqueous solutions. As previously reported, the water fraction in the biorefineries need to be valorized for economic and environmental reasons. Together with other proposed solutions, aqueous phase reforming may be a competitive option because of its advantages such as the energetic efficiency, the low capital costs, the possibility to convert diluted solutions into a valuable gas phase. Despite the effort of the scientific community in this field, APR has been poorly investigated with truly representative biorefinery aqueous streams, while most of the studies looked at the development of effective catalysts with simple model compounds.

Aim of this work is looking at representative conditions for the application of APR in the biorefinery context. For this reason, the water fraction coming from three types of feedstocks and primary processes have been analysed, in order to challenge the APR process in different conditions.

At first, it was hypothesized to exploit the sugar fraction derived from the oil extraction process of algae for biofuel production. This is because typically only the fat fraction of algae is exploited. However, as explained previously, it is important that the entire organic content of biomass is valorized to have an economically competitive process. This experimental campaign has been described in the Chapter 3, where the aqueous phase reforming of alginate, a model compound representative of the algae carbohydrate fraction will be depicted.

In the Chapter 4 the typical biorefinery streams present in a bioethanol plant has been focused. Glucose, xylose and corresponding sugar alcohols have been subjected to APR, both alone and in mixtures. This is because the hemicellulose fraction of lignocellulosic biomass is poorly exploited with using conventional yeasts. A process configuration in which a hydrogenation reaction was performed before APR has been studied, going towards the use of more concentrated sugar solution. A real phase coming from the hydrolysis of wheat straw obtained from a demo-scale plant has been investigated as well.

In the Chapter 5 a thorough screening for the valorization of organics dissolved in the aqueous phase post hydrothermal liquefaction (HTL) has been reported. HTL is a promising process for alternative and renewable fuels, but the carbon recovery must be maximized also looking to the compounds dissolved in the aqueous phase. The influence of several reaction conditions (temperature, time, catalyst support) will be highlighted. Moreover, synthetic mixtures have been tested. Finally, an actual water phase derived from lignin-rich HTL from a laboratory-scale experimental campaign has been subjected to APR (Chapter 6).

Each of this study has been devoted to assess the potential of aqueous phase reforming for the production of hydrogen to be used in the biorefinery itself. In this way, a double advantage is proposed: from one side, the costs for waste disposal are reduced; on the other side, a valuable product is obtained, in a renewable way, reducing the dependence of the biorefinery from external fossil-based hydrogen. Indeed, dealing with the production of biofuel, one of the main drawbacks is the elevated oxygen content, typically reduced by hydrogenation. Because the use of non-renewable sources of energy during biorefinery processing should be minimized, aqueous phase reforming may therefore decrease the impact on greenhouse emissions, going towards a sustainable future.

# Chapter 2 Materials and Method

## 2.1 Materials

Several compounds representatives of molecules present in waste biorefinery streams were used. In the following Table 1 the complete list is reported.

Table 1. List of compounds used for the investigation.

<b>Carboxylic acids</b>	Formic acid
	Acetic acid
	Propionic acid
<b>Hydroxyacids</b>	Glycolic acid
	Lactic acid
<b>Bicarboxylic acids</b>	Succinic acid
	Glutaric acid
<b>Alcohols</b>	Methanol
	Ethanol
	1-Propanol
	2-Propanol
<b>Poly-alcohols</b>	Ethylene glycol
	Propylene glycol
	Glycerol
	Xylitol
	Sorbitol
<b>Sugars</b>	Glucose
	Xylose
	Sodium alginate
<b>Ketoacids</b>	Levulinic acid
<b>Ketones</b>	4 methyl 2 pentanone
	Cyclopentanone
<b>Aromatics</b>	Guaiacol

Apart from single compounds, actual biorefinery streams were used to get information of the influence of complex mixtures on the performance of the reforming.

A water fraction derived from lignin-rich hydrothermal liquefaction was kindly furnished by RE-CORD (Renewable Energy Consortium for Research and Development), Florence, Italy.

The aqueous phase derived from wheat straw hydrolysis was kindly furnished by Beta-Renewable S.p.A, Crescentino, Italy.

Commercial catalysts were used for the catalytic test. 3% Pt/C, 5% Pt/Al<sub>2</sub>O<sub>3</sub> and 5% Ru/C were purchased from Sigma Aldrich. Developmental 5% Pt/C was furnished by Johnson Matthey. The catalysts were used as received, without any

pretreatment, since tests performed with pre-reduced samples led to the same results.

## 2.2 Catalytic tests

### 2.2.1 Aqueous phase reforming tests

The APR catalytic tests were carried out in a 300 mL 4560 series mini bench top reactor (Parr), equipped with a 4848-model reactor controller (Parr). The reactor is manufactured in AISI 316L, able to resist to the corrosive environment of the hydrothermal conditions and in the case of the use of a hydrogen atmosphere. In the Figure 11, the top part of the reactor is depicted, together with the fittings associated with the systems. Two modifications to the reported descriptions are highlighted. First, the liquid sampling valve is not present; second, a digital pressure transducer is added to the system, allowing a more precise measure of the pressure at the end of the reaction. Indeed, an accurate recording of this value is fundamental to quantify the production of hydrogen, the desired product. The magnetic drive allows the stirring of the pressurized system, whereas the cooling coil consents a fast decrease of the temperature, quenching the reaction.

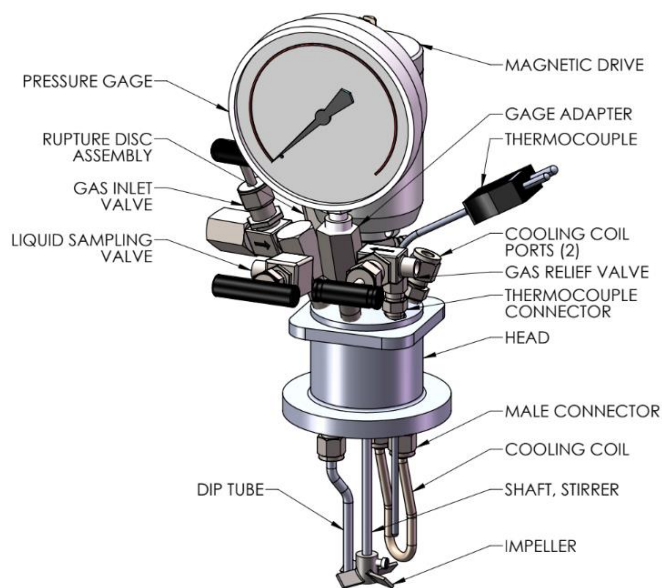


Figure 11. Parr top reactor component scheme.

A glass liner was used in the reactor to favour a simple recovery of the reaction products and catalyst. 75 grams of aqueous solution were used in the typical run. The desired amount of feed (model compound or actual biomass) was added to the deionized water. Random checks were performed to control the reliability of the weight procedure by HPLC analysis. Afterwards, the catalyst in powder form was added. The reactor was fastened thanks to six compression bolts, while the sealing was ensured by a flat-type PTFE gasket, able to resist up



to 300 °C. The air in the head atmosphere was removed thanks to five washing steps performed with nitrogen, in which the reactor was pressurized up to 7 barg. During the last step, 2 barg of nitrogen were added. The stirring rate was fixed at 500 rpm to prevent external mass transfer limitations. Subsequently, the reactor was heated up to the desired temperature thanks to an electric oven. The heating time necessary for reaching the set temperature was in the range of 45-60 minutes, and the reaction time was considered beginning when the desired temperature was reached. The reaction was stopped thanks to an internal cooling loop and an external cold-water bath. When the room temperature was approached, the value of the pressure obtained by the digital transducer was recorded ( $\pm 0.1$  bar precision). The gas in the headspace was collected in a sample syringe and further analysed by micro-GC. The reactor was opened, and the solution filtered by gravity using a paper filter. At this point, the filter containing the spent catalyst was dried overnight at 105 °C, while the liquid solution was collected to perform total carbon (TC) and HPLC analysis.

### 2.2.2 Hydrogenation reactions

The hydrogenation reactions have been performed in a 300 mL Berghof reactor, equipped with a BTC-3000 temperature controller. The internal part of the reactor is manufactured in PTFE, limiting the working temperature up to 230 °C. The component scheme of the reactor is reported in the following Figure 12. The use of a gas-induced stirrer consented to easily dissolve the hydrogen present in the head space directly into the liquid solutions, reducing possible mass transfer limitations at the gas-liquid interface.

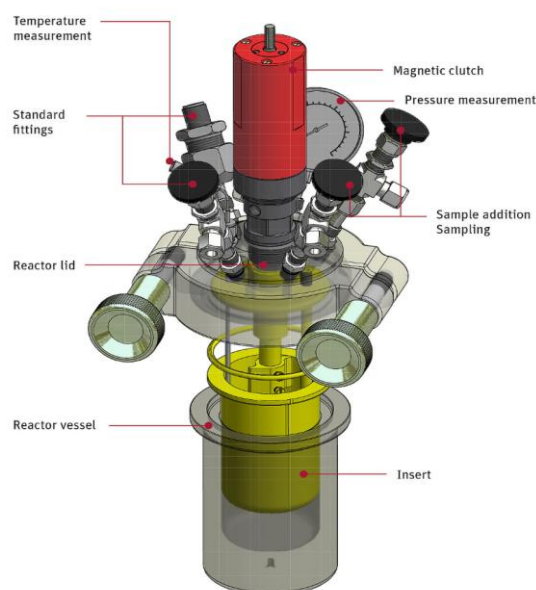


Figure 12. Berghof reactor component scheme.

The hydrogenation tests were prepared following the same methodology used for APR. In brief, the solution was prepared in a PTFE liner and the catalyst (5% Ru/C - powder form) was added. Once inserted in the reactor, it was fastened and washed from the atmospheric air by nitrogen. In the last step, 1 bar of nitrogen was maintained, to be used as internal standard for gas phase analysis. The stirring rate was fixed at 600 rpm. The reactor was heated up to the desired temperature (heating time approximately 1 h) and, at the end of the reaction, it was stopped thanks to an external cold-water bath. The gas phase was collected in a sample syringe, while the liquid solution was filtered and, afterwards, analysed by TC and HPLC. The spent catalyst was dried overnight at 105 °C in an oven.

## 2.3 Characterization analysis

The composition of the gas phase was analysed by a SRA Micro-GC, equipped with two columns. The Molsieve 5A column was used for the analysis of permanent gas, i.e. hydrogen, oxygen, nitrogen, methane and carbon monoxide; Argon was used as carrier, while the temperature of the column was set at 100 °C. The PoraPLOT U column was used for the analysis of carbon dioxide, ethane, ethylene and propane; Helium was used as carrier, while the temperature of the column was fixed at 85 °C. The injection temperature was set at 100 °C and the pressure at 2.1 bar. The quantification of the species in the gas mixture have been performed thanks to the equipped TCD detector, using external calibration. A double check on the quantification was done looking at the concentration of nitrogen, used as an internal standard.

The composition of the liquid phase was obtained by a Shimadzu Prominence HPLC. The system is equipped with a Rezex ROA-Organic acid H<sup>+</sup> (8%) column (300 mm \* 7.8 mm). A 5 mM H<sub>2</sub>SO<sub>4</sub> aqueous solution was used as mobile phase. The flow rate was fixed at 0.7 mL/min and the temperature of the column at 50 °C. The volume of sample injected was set at 10 µL. Two detectors in series were used: a refractive index detector (RID) and a photodiode array detector (PDA), with the latter working in the 190 – 380 nm range. The quantification was performed by external calibration.

The carbon content in the liquid phase was analysed by a Shimadzu TOC-V<sub>CSH</sub> analyser, equipped with a nondispersive infrared detector.

The fresh catalyst and some selected spent catalysts were characterized by several techniques.

A Micromeritics Tristar 3020 instrument was used for N<sub>2</sub> adsorption/desorption isotherm analysis at 77 K. About 0.1 g of sample was first degassed at 200 °C under nitrogen flow for 2 h, using a Micromeritics Flow Prep 060 system. The Brunauer-Emmett-Teller equation (BET) was used for the calculation of specific surface area, whereas the Barrett-Joyner-Halenda method (BJH) was used for the determination of the pore volume and pore size distribution.

A FESEM Zeiss Merlin, Gemini-II column was used for morphological and EDX analysis.

A Pananalytical X'Pert Pro diffractometer (Cu Ka radiation,  $2\Theta$  range 10-70, step 0.01, time per step 240 s) was used for structural characterization of the catalysts, via X-ray diffraction.

A Thermo Scientific iCAP Q ICP-MS analysis was performed to assess possible leaching of the active sites into the solution. Thanks to this analysis, the evaluation of the inorganics in the actual biomass feed was also performed. Thermal gravimetric analysis (TGA) was used to evaluate the presence of deposits on the surface of the catalyst using a TG 209 F1 Libra® (NETZSCH GmbH). About 0.01 g of sample was used per analysis, the heating rate was set at 10 °C/min, working in the 25-800 °C range, using a nitrogen or air flow at 60 mL/min. Fourier Transformed Infrared Spectroscopy (FT-IR) was performed by a Nicolet 5700 FTIR Spectrometer (ThermoFischer). 1 mg of sample was mixed with 200 mg of KBr, finely ground and pressed at 74 MPa for 2 minutes. 16 scans were signal-averaged at a 2  $\text{cm}^{-1}$  resolution in the 4000 – 400  $\text{cm}^{-1}$  range.

X-ray photoelectron spectroscopy (XPS) was performed using a PHI Model 5000 electron spectrometer, equipped with an aluminium anode (1468 eV) monochromatic source, 25 W power, high-resolution scan with 11.75 eV pass energy. C1s = 284.6 eV was used as reference.

## 2.4 Description of performance's indicators

The results obtained after the reaction were evaluated using several indicators. These indexes consent to estimate many features of the reaction, such as quantifying the production of hydrogen (the desired product), the conversion of the feed into carbon-containing gaseous species, the selectivity to desired and undesired products and so on. In the following, the equations used to calculate the indicator are reported.

The carbon to gas conversion is defined as the ratio between the moles of carbon present in final gaseous mixtures  $\text{mol}_{\text{fin}} C_{\text{gas}}$  and the moles of carbon present in the feed  $\text{mol}_{\text{in}} C_{\text{feedstock}}$

$$\text{Carbon to gas (\%)} = 100 * \frac{\text{mol}_{\text{fin}} C_{\text{gas}}}{\text{mol}_{\text{in}} C_{\text{feedstock}}}$$

The APR hydrogen yield  $\text{APR} - Y_{\text{H}_2}$  is defined as the ratio between the moles of hydrogen obtained at the end in the gaseous products  $\text{mol}_{\text{fin}} \text{H}_2$  and the initial moles of feed  $\text{mol}_{\text{in}} \text{feedstock}$ , divided by the (y+n) parameters present in the reaction stoichiometry to reach a maximum 100% yield

$$\text{APR} - \text{H}_2 \text{ yield (\%)} = 100 * \frac{\text{mol}_{\text{fin}} \text{H}_2}{(y + n) * \text{mol}_{\text{in}} \text{feedstock}}$$

The hydrogen gas distribution is defined as the ratio between the moles of hydrogen obtained at the end in the gaseous products under the form of molecular hydrogen and the total moles of hydrogen present in the final gaseous mixture, i.e. present also under the form of alkanes

$$\text{H}_2 \text{ gas distribution (\%)} = \frac{\text{mol}_{\text{fin}} \text{H}_2}{\text{mol}_{\text{fin}}(\text{H}_2 + 2 * \text{CH}_4 + 3 * \text{C}_2\text{H}_6 + 4 * \text{C}_3\text{H}_8)}$$

The APR H<sub>2</sub> selectivity APR – S<sub>H<sub>2</sub></sub> is defined as the ratio between the moles of hydrogen and carbon dioxide in the gaseous products and the ideal ratio derived from the reforming reaction stoichiometry

$$\text{APR H}_2 \text{ selectivity(\%)} = 100 * \frac{\text{mol}_{\text{fin}}(\text{H}_2/\text{CO}_2)}{(\text{H}_2/\text{CO}_2)_{\text{teo}}}$$

The hydrogen productivity is defined as the ratio between the mmoles of hydrogen in the gas phase and the moles of carbon in the feed. This indicator was used mainly in the case of complex mixtures, such as when actual biomass streams were used: this is because it was not possible to define the other indicators not having a simple reaction stoichiometry

$$\text{H}_2 \text{ productivity} = \frac{\text{mmol}_{\text{fin}} \text{H}_2}{\text{mol}_{\text{in}} \text{C}_{\text{feedstock}}}$$

The results obtained with the mixtures were compared with the linear combination of the results obtained in the mono-compound solution. As an example, the linear combination referring to the carbon to gas conversion has been calculated according to the following equations

$$\text{CtoG}_{133 \text{ mM}} = 1/2 * (\text{CtoG}_{\text{glycolic } 133 \text{ mM}} + \text{CtoG}_{\text{acetic } 133 \text{ mM}})$$

$$\text{CtoG}_{67 \text{ mM}} = 1/2 * (\text{CtoG}_{\text{glycolic } 67 \text{ mM}} + \text{CtoG}_{\text{acetic } 67 \text{ mM}})$$

Regarding the hydrogenation reactions, we defined the conversion of the feed (glucose and xylose) as the ratio between the reacted and the starting moles

$$\text{Conversion}_{\text{glucose}}(\%) = 100 * \frac{\text{mol}_{\text{in}}\text{glucose} - \text{mol}_{\text{fin}}\text{glucose}}{\text{mol}_{\text{in}}\text{glucose}}$$

While the yield was defined as the ratio between the moles of product and the starting moles of the feed

$$\text{Yield}_{\text{sorbitol}}(\%) = 100 * \frac{\text{mol}_{\text{fin}}\text{sorbitol}}{\text{mol}_{\text{in}}\text{glucose} + \text{mol}_{\text{in}}\text{xylose}}$$

# Chapter 3 Valorization of alginate

## 3.1 Introduction

As reported in the chapter 1, biomass is classified according to three generations. First generation refers mainly to edible crops, second generation to lignocellulosic materials, while third generation mainly consists of micro- and macroalgae. Algae-deriving biomass permits to overcome the “food vs fuel” debate raised by first generation, reducing at the same time the space required for cultivation, that is a major limitation of second generation. Macroalgae are widely distributed on the planet and are classified as brown, red or green algae. Unlike second generation, macroalgae are not constituted by lignin, making easier their processing. On the other hand, they do have a high content of carbohydrates, suggesting the production of bioethanol as possible pathway for their conversion into biofuel [79].

Alginate is one of the most present carbohydrates in the external wall cell of brown macroalgae [80]. Two different units (mannuronic and guluronic acid), linked by  $\beta$ -1,4- glycosidic bonds constitute alginate. It can be used as food additive, drug delivery system, or for textile printing. Moreover, apart from its conversion into a biofuel, it can be seen as a source of value-added compounds.

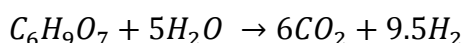
Aida et al. investigated the hydrothermal treatment of sodium alginate into valuable compounds such as lactic acid, malic acid or succinic acid from 150 to 400 °C [81]. They observed that increasing the reaction temperature allowed the conversion of alginate to be higher into smaller organic acids, whereas at lower temperatures, mainly high molecular weight compounds were detected. The authors concluded that the alginate-containing seaweeds could be an interesting feedstock for biomass refinery processes to obtain liquid products.

Jeon et al. investigated the influence of some reaction conditions (pH, temperature) on the products distribution [82]. Furfural and glycolic acid were produced at acidic conditions, while lactic, fumaric and malic acid were obtained at basic conditions. On the other hand, the reaction temperature mainly affected the molecular weight distribution of the final products. The authors suggested that alginate could be an alternative to cellulose for the production of furfural and value-added organic acids.

Ban et al. studied the selective conversion of alginate into mannuronic and guluronic acid (i.e. its two monomers) using a sulfonated glucose-derived carbon catalyst [83]. However, they observed a consecutive degradation, leading to the formation of humins and isomeric uronic acids, lowering the yield of the target products.

Micro- and macroalgae have been considered as feedstock with high potential for their use in a biorefinery [84]. As explained in the introduction, for the economic sustainability of a biorefinery, each fraction that constitutes the biomass

should be exploited, and a portfolio of different compounds can be obtained tailoring the reaction conditions. Aquatic biomass can be valorized looking at its lipidic fraction, wasting the carbohydrate part. This is why we decided to investigate the aqueous phase reforming (APR) of alginate, a compound closer to those present in the aqueous stream coming out from biorefinery processes. This is, indeed, the main target of aqueous phase reforming, as suggested from the very first work in which the APR was indicated as a strategic energetic-efficient process, useful for the generation of hydrogen rich fuel gas from carbohydrates extracted from renewable biomass [37]. The APR reaction in the case of alginate is the following



Please note that with this stoichiometry, the alginate is actually an anion, and the corresponding cation is sodium, in this work. We referred to the molecular formula of the repetitive unit of alginate (mannuronic or guluronic acid), without considering the first step of hydrolysis of the polysaccharide.

The influence of several reaction conditions has been evaluated (catalyst and alginate loading, reaction temperature and time, pH and hydrogen partial pressure). The results helped to validate the previous APR works done on simpler molecules, verifying its robustness in the case of a more complex feed; moreover, it permitted to move a step forward into the possible industrial application of this thermochemical process, trying to apply it with a complex feed similar to what expected in practical contexts, looking to a carbohydrate-based biorefinery.

This chapter (results, figures and tables) is based on the published work reported in [85].

## 3.2 Results and discussion

The tests were labelled according to the weight concentration of alginate in the starting solution (0.5, 1 or 2 wt.%) and the amount of catalyst (no cat, 0.4 or 0.8 g); moreover, the starting pH value was added when this parameter was investigated. Each test was performed at least in duplicate and the reported values are the average values (standard deviation was about 5%).

### 3.2.1 *Effect of the catalyst amount*

The influence of the catalyst amount on the APR of 1 wt.% alginate solution is reported in Table 2.

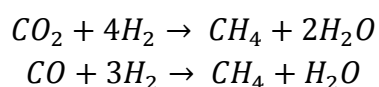
Table 2. Influence of the catalyst amount on the carbon conversion to gas, hydrogen yield, hydrogen selectivity and composition of the obtained gas phase. Reaction conditions: 1 wt.% alginate solution, T: 225 °C, reaction time: 6 h.

Test	Carbon to gas (%)	APR H <sub>2</sub> yield (%)	APR H <sub>2</sub> selectivity (%)	Gas concentration (%)					
				H <sub>2</sub>	CO <sub>2</sub>	CO	CH <sub>4</sub>	C <sub>2</sub> H <sub>6</sub>	C <sub>3</sub> H <sub>8</sub>
1%-no cat	8.5	1.3	15.5	19.9	77.8	2.9	0.3	0.0	0.1
1%-0.1	12.5	3.2	30.4	30.5	63.3	0.0	3.9	2.1	0.2
1%-0.2	16.5	4.3	32.3	31.4	61.3	0.0	4.3	2.6	0.4
1%-0.4	18.6	5.5	39.9	35.4	56.1	0.0	4.6	3.3	0.6
1%-0.8	22.5	6.0	36.1	32.7	57.2	0.0	4.8	4.5	0.8

The uncatalyzed test reported 8.5% of carbon conversion to gas, with 1.3% of hydrogen yield. The gas phase produced during the reforming was mainly constituted by carbon dioxide (77.8%). In a previous work in which the non-catalytic APR of glycerol was investigated, the gas phase obtained at 250 °C was entirely constituted by carbon dioxide [86].

According to Aida et al. [87], the uncatalyzed decomposition of alginate occurs under hydrothermal conditions through an acid hydrolysis pathway. At first, the monomer mannuronic acid is formed; afterwards, it decomposes giving water-soluble organic acids and gaseous species. The small organic acids can further react, being subjected to decarboxylation or decarbonylation reactions. In the first case, the oxygen from the molecule would be eliminated directly as carbon dioxide, while the latter would give a carbon monoxide molecule: for instance, the selective decarboxylation of the carboxylic group in the monomers would lead to xylose. The CO could react with water, giving hydrogen and carbon dioxide via water gas shift reaction (WGS). However, despite being the WGS thermodynamically favoured in these conditions of temperature, the absence of a catalyst make it difficult to occur. This is probably the reason why CO is still present at the end of the reaction in the uncatalyzed tests, contrarily to the ones in which Pt is present. It is worthy to mention the presence of hydrogen, although very small (19.9% of the produced gas phase).

The addition of 0.1 g of catalyst led to an increase both in the conversion to gaseous products and hydrogen production. This can be attributed to the more favourable C-C bond breaking reactions when a group VIII metal is used [39], together with the more favourable WGS. Methane was particularly sensitive to the presence of the catalyst, increasing its concentration by one order of magnitude (from 0.3 to 3.9%): this is probably due to methanation reactions, thermodynamically favoured at low temperature.





This outcome is important because it gives a general message when dealing with APR. In fact, while the presence of the catalyst has for sure a beneficent effect in the hydrogen production, it increases also the production of methane, whose presence was already thermodynamically favoured. Unfortunately, these reactions are hydrogen-consuming, therefore they will decrease the yield in the desired product and, at the same time, the selectivity.

The increase of the catalyst amount led to a constant increase in the carbon conversion to gas and hydrogen yield. If the homogeneous contribution to gaseous products is ideally removed, the improvement is still more evident. Therefore, it happens that, going from 0.1 to 0.2 g of catalyst, the conversion doubled, and the hydrogen had a production 1.5 times higher. The highest yield of hydrogen was obtained with the highest amount of catalyst used; however, a trade-off can be observed between the maximum conversion (obtained at 0.8 g) and the maximum selectivity (obtained at 0.4 g).

The beneficial effect of the increasing catalyst loading and the corresponding increase in the conversion can be explained with the increase of the number of active sites [46,88]. At the same time, as cited before, the greater availability may favour in a greater extent the production of small alkanes (methane, ethane and propane), whose increase can be seen constant in the whole range of catalyst amount investigated. Therefore, it can be inferred that there is a classic competition problem; we can assume that the reactions (methanation and Fischer-Tropsch reactions) that lead to the formation of alkanes have a greater dependence to the catalyst amount compared to the reactions that lead to the production of hydrogen, being platinum also an excellent hydrogenation catalyst.

### 3.2.2 Effect of alginate concentration

In Table 3 the results obtained with three different catalyst amounts (0, 0.4 and 0.8 g) are reported.

Table 3. Influence of the alginate amount on the carbon conversion to gas, hydrogen yield, hydrogen selectivity and composition of the obtained gas phase at different amount of catalyst. Reaction conditions: T: 225 °C, reaction time: 6 h.

Test	Carbon to gas (%)	APR H <sub>2</sub> yield (%)	APR H <sub>2</sub> selectivity (%)	Gas concentration (%)					
				H <sub>2</sub>	CO <sub>2</sub>	CO	CH <sub>4</sub>	C <sub>2</sub> H <sub>6</sub>	C <sub>3</sub> H <sub>8</sub>
0.5%-no cat	11.2	2.4	23.0	24.1	73.6	1.3	0.5	0.4	0.1
1%-no cat	8.5	1.3	15.5	19.9	77.8	2.9	0.3	0.0	0.1
2%-no cat	9.0	0.3	3.8	5.3	89.8	4.8	0.1	0.0	0.0
0.5%-0.4	21.9	5.8	36.1	32.6	56.8	0.0	4.8	4.9	0.8
1%-0.4	18.6	5.5	39.9	35.4	56.1	0.0	4.6	3.3	0.6
2%-0.4	13.8	3.4	30.4	30.1	62.8	0.0	4.3	2.5	0.3
0.5%-0.8	25.9	5.0	27.8	26.9	61.6	0.0	5.5	5.1	0.9
1%-0.8	22.5	6.0	36.1	32.7	57.2	0.0	4.8	4.5	0.8
2%-0.8	15.9	3.5	29.1	28.6	62.4	0.0	5.1	3.4	0.5

In the case of the uncatalyzed tests, a constant decrease in the hydrogen yield and selectivity with increasing the alginate initial concentration was observed, whereas the carbon to gas showed a less evident decrease. When the highest value of alginate concentration was used, only 0.3% of hydrogen yield was obtained, with just 3.8% of selectivity.

When the catalyst was added, the carbon conversion to gas had a stronger decrease with the increase in the alginate solution, both at 0.4 and 0.8 g of catalyst: it means that the positive effect of adding the catalyst, progressively disappears with the increase of the concentration of the alginate solution because of the more favourable homogeneous reactions. It has been reported in literature that in the case of thermochemical conversion of glucose in aqueous system at the investigated temperature interval, the sugar is subjected to homogeneous decompositions reactions that are first order in the glucose concentration [44]. On the other hand, the desirable reforming reactions are fractional order on the catalyst surface [43]: therefore, high glucose concentration leads to lower hydrogen selectivity. A difference also in the liquid product distribution was observed: again, it can be due to the difference in the orders of reaction between the desired and the parallel undesired reactions [89].

Making a comparison between two tests with the same alginate concentration and different catalyst amount, a higher conversion at 0.8 g of catalyst was reported. This is due to the beneficial influence of the higher ratio active sites/feed molecules. Looking at the hydrogen selectivity, a maximum was reported at 1% of alginate, both at 0.4 and 0.8 g of catalyst. In this case, at the same level of concentration, the higher the amount of catalyst used, the lower the hydrogen selectivity obtained. This is coherent with the results reported in the previous paragraph, where it was suggested that the catalyst has both a positive effect to increase the carbon conversion to gas, but at the same time a negative effect to decrease the final hydrogen production promoting parallel reaction pathways that consume the produced hydrogen.

A strong dependence of carbon monoxide from alginate concentration in the un-catalyzed test was observed, whereas it seemed insensitive in the case of the catalytic runs, remaining in each test not detectable. This is likely due to the effective water gas shift reaction that can entirely convert the produced carbon monoxide into carbon dioxide at these reaction conditions. The production of methane followed a trend like the one of carbon dioxide, with a minimum at 1 wt.%; on the other hand, ethane showed a decreasing behaviour with the increase in the alginate concentration.

In Table 4, the experimental results were re-elaborated ideally splitting the production of carbon dioxide into two contributions: the first one, named APR-CO<sub>2</sub>, is thought to come from the occurrence of the alginate APR and therefore calculated according to ideal reaction stoichiometry starting from the amount of hydrogen detected at the end of the test; the second one, named Excess CO<sub>2</sub>, is obtained as a difference between the total production of CO<sub>2</sub> and the APR-CO<sub>2</sub>

and refers to the production of carbon dioxide not directly linked to the reforming, such as decarboxylation.

Table 4. Contribution to the total CO<sub>2</sub> production coming from the APR reaction (evaluated from the reaction stoichiometry, APR-CO<sub>2</sub>) and from alternative pathways (Excess CO<sub>2</sub>), with the influence of the catalyst on the production of Excess CO<sub>2</sub> (Catalytic excess).

Test	Total CO <sub>2</sub> (mmol)	APR-CO <sub>2</sub> (mmol)	Excess CO <sub>2</sub> (mmol)	Catalytic excess CO <sub>2</sub> (%)
0.5%-no cat	1.52	0.25	1.27	-
1%-no cat	2.20	0.29	1.91	-
2%-no cat	5.00	0.19	4.81	-
0.5%-0.4	2.25	0.89	1.56	12.8
1%-0.4	4.27	1.70	2.57	15.4
2%-0.4	6.87	2.11	4.86	0.7
0.5%-0.8	2.77	0.77	2.00	26.3
1%-0.8	5.12	1.85	3.27	26.7
2%-0.8	7.40	2.14	5.26	6.1

In order to understand the influence of the catalyst on the excess CO<sub>2</sub> production, the values of the “catalytic excess CO<sub>2</sub>” are also reported, calculated as the ratio between the excess CO<sub>2</sub> in a catalytic test and the corresponding not-catalyzed test (e.g. 0.5%-0.4 and 0.5%-no cat). Looking at the results of this calculation, it can be observed that only a small contribution of the catalyst is in the fraction of excess CO<sub>2</sub>. In particular, it reaches a maximum when 1% of alginate solution is used. When the 2% alginate is used, the greater incidence of the homogeneous reactions led to a minimum difference between the catalyzed and uncatalyzed test. Moreover, as it can be understood from previous consideration, the catalytic excess CO<sub>2</sub> increased when the amount of catalyst increased, being equal the initial alginate concentration.

The influence of the homogeneous path can be understood further looking at the following results. If the CO<sub>2</sub> production is compared at low alginate concentration (i.e. 0.5%-0.4 and 1%-0.8), doubling reactant and catalyst leads to doubling both homogeneous and heterogeneous CO<sub>2</sub> mmoles. On the other hand, increasing the alginate concentration (i.e. 1%-0.4 and 2%-0.8) only the homogeneous CO<sub>2</sub> is doubled. This behaviour can be ascribed to the different reaction order between homogeneous (first order) conversion and heterogeneous (fractional order) conversion of the alginate.

### 3.2.3 Effect of the reaction temperature

In Table 5 the influence of the temperature on the process performance is shown, both in uncatalyzed and catalyzed tests.

Table 5. Influence of the reaction temperature with and without catalyst on the carbon conversion to gas, hydrogen yield, hydrogen selectivity and composition of the obtained gas phase. Reaction conditions: 1 wt.% alginate solution, reaction time: 6 hours.

				Gas concentration (%)
--	--	--	--	-----------------------

Test	Carbon to gas (%)	APR H <sub>2</sub> yield (%)	APR H <sub>2</sub> selectivity (%)	H <sub>2</sub>	CO <sub>2</sub>	CO	CH <sub>4</sub>	C <sub>2</sub> H <sub>6</sub>	C <sub>3</sub> H <sub>8</sub>
200-no cat	8.8	1.6	18.5	22.5	76.8	0.0	0.5	0.1	0.2
215-no cat	9.3	1.9	20.6	24.5	75.1	0.5	0.3	0.1	0.1
225-no cat	8.5	1.3	15.5	19.9	77.8	2.9	0.3	0.0	0.1
235-no cat	9.6	1.8	18.5	22.5	75.4	2.1	0.3	0.1	0.1
200-0.8	19.6	3.9	27.1	28.0	61.6	0.0	5.7	4.1	0.6
215-0.8	22.3	5.5	33.6	31.4	59.7	0.0	4.9	3.4	0.6
225-0.8	22.5	6.0	36.1	32.7	57.2	0.0	4.8	4.5	0.8
235-0.8	20.5	5.9	35.9	33.1	57.3	0.0	5.2	3.7	0.7

The reaction temperature seemed not to have an effect for the uncatalyzed tests, since the carbon conversion to gas was always around 9%, the hydrogen yield was about 1.5% and the hydrogen selectivity set at about 18%. Looking at the gas phase composition, it is noted that the concentration of carbon monoxide increased together with the temperature, with a maximum at 225 °C. No detectable changes were observed in the composition of the small alkanes.

When the catalyst was added, it was observed an increase in the hydrogen yield with the increase of the temperature, from 3.9 to 5.9% moving from 200 to 235 °C: this result is due to the more favourable C-C bond breakings [90]. The increase of temperature favoured the production of hydrogen with respect to carbon dioxide and it may be due to the promotion of the reforming reaction compared with undesired (hydrogenation) reactions.

However, the dependence from the temperature seemed smaller compared to what is reported in literature. Dumesic and coworkers reported an increase in the carbon conversion to gas from 8.6 to 21.0 moving from 210 to 225 °C, for APR of ethylene glycol using a 6% Pt/SiO<sub>2</sub> [48]. Because of the small dependence of the temperature, possible effects of transport limitations were considered. External mass transfer limitations were assessed performing an unstirred test. The observation of analogous results let us to conclude that the mass transport coefficient of the reactants from the bulk of the solution to the catalyst surface was high enough also in the unstirred case. Internal mass transport limitations may be generally evaluated in an empirical way, running the reaction on catalysts with progressively smaller particle sizes [91]. In the present work, the catalyst is in a powder form, so we could not follow this criterion. However, looking at the typical values of reaction rate obtained in the case of APR for simpler molecules, it can be inferred that the internal mass transport is fast enough not to limit the intrinsic kinetic. It should be observed, moreover, that we are focusing just on the gas phase, while the change in temperature could have an influence on the liquid product distribution.

#### 3.2.4 Effect of the reaction time

The influence of reaction time is reported in Table 6. A reference test, stopped when the reaction temperature was reached (about 30 minutes), showed negligible conversion and hydrogen yield. Please note that the results do not refer to a single

reaction because it was not possible performing periodic sampling; therefore, they have been obtained from different tests.

Table 6. Influence of the time reaction on the carbon conversion to gas, hydrogen yield, hydrogen selectivity and composition of the obtained gas phase. Reaction conditions: 1 wt.% alginate solution, 0.8 g catalyst, T: 225 °C.

Test	Carbon to gas (%)	APR H <sub>2</sub> yield (%)	APR H <sub>2</sub> selectivity (%)	Gas concentration (%)					
				H <sub>2</sub>	CO <sub>2</sub>	CO	CH <sub>4</sub>	C <sub>2</sub> H <sub>6</sub>	C <sub>3</sub> H <sub>8</sub>
1 h	20.9	5.1	33.5	31.4	59.2	0.0	4.9	3.8	0.8
2 h	23.2	6.4	36.7	33.3	57.6	0.0	4.7	3.8	0.7
3 h	22.3	6.3	36.7	32.5	58.2	0.0	4.4	4.2	0.7
4 h	21.9	6.5	37.3	34.1	56.4	0.0	5.1	3.7	0.8
6 h	22.5	6.0	36.0	32.7	57.2	0.0	4.8	4.5	0.8

It can be observed that the hydrogen yield increased up to 6.4% after 2 h, maintaining this value constant for the remaining reaction time. At the same way, the carbon conversion to gas reached 23.2% after 2 h, and then there was a plateau. Focusing on the composition of the gas phase, after 2 h, it was constituted mainly by hydrogen (33.3%) and carbon dioxide (57.6%), with this composition unchanged throughout the entire reaction time.

It was previously reported that a plateau can be observed in the case of aqueous phase reforming reactions, both for the gas and liquid products. Also in some precedent works a plateau in the conversion to gas and liquid products appears after 2 h of reaction [46,92,93]. Interestingly, an apparent stop of the reaction was observed also in the test of an actual biomass [69].

The observed phenomenon can derive from multiple reasons. The first one is due to thermodynamic motivations. This would mean that the observed plateau should be an indication of reaching the equilibrium conditions; however, this hypothesis does not seem satisfactory, because previous thermodynamic analysis reported that the APR reaction is completely favoured at the reaction conditions investigated in this work [39] leading to CO<sub>2</sub> and H<sub>2</sub>, or even methane, whose formation is only kinetically limited.

The deactivation of the catalyst may be a plausible reason: this argument will be largely explored and discussed in the sub-section 3.2.7.

Still another reason may be the simultaneous production of hydrogen thanks to APR, together with its consumption via hydrogenation/hydrogenolysis, methanation and Fischer-Tropsch reactions. The liquid phase collected at the end of the reaction was analysed by HPLC. APR typically produces a plethora of oxygenated compounds (aldehydes, alcohols, carboxylic acids) deriving from multiple reactions such as dehydration, isomerization etc. [94]. The complexity of the mixtures did not allow a complete identification of the species; despite of that, some key components were identified, based on previous works dealing with the hydrothermal treatment of an alginate solution [81,87].

Acetic acid and propionic acid, representatives of carboxylic acids, maintained, once formed, almost a constant concentration during the entire reaction time. This is a known phenomenon in literature, because they are recognized as stable compounds in the aqueous environment at this temperature. This result allowed us to explain what was reported in the previous section. In fact, being a fraction of the initial alginate molecule converted in these stable species, the possibility of further (and full) production of hydrogen is “locked” in these molecules that are unreactive from a kinetic point of view, despite being thermodynamically unstable and prone to the conversion to hydrogen and carbon dioxide. Therefore, we can assume that the kinetic constraints linked to the slow APR kinetics for these intermediate compounds blocked the hydrogen production. Nozawa et al. studied the APR of acetic acid over Ru/TiO<sub>2</sub> catalyst, observing that at 200 °C the H<sub>2</sub> formation stopped after 200 min; the authors reported also that the selective conversion to H<sub>2</sub> and CO<sub>2</sub> is easier starting from alcohols, because the C-C bond cleaving was activated by an adjacent OH group; conversely, the non-activated methyl group that is present in acetic acid (and generally in the carboxylic acids) is converted into CH<sub>4</sub> (or, generally, leading to alkanes) [95]. Two other key compounds detected were maleic and succinic acid, two dicarboxylic acids, with the former being with an unsaturated bond. The formation of dicarboxylic acids was studied in basic aqueous systems, where it was proposed that they are formed by β-elimination, Lorby de Bruyn–Alberta van Ekenstein Transformation (LBET) and other reactions (hydrolysis/dehydration) [96]. It was observed that the maleic acid decreased after the first hour: this could be caused by in-situ hydrogenation derived from APR, and this could be a general trend for all the unsaturated species. On the other hand, this decrease was not observed in the evolution trend of succinic acid, whose concentration was one order of magnitude higher than the concentration of the maleic acid, likely because of the fast hydrogenation of the double bond in the presence of the Pt-based catalyst. Instead, it is highlighted that the succinic acid tended to accumulate over time, because of its stability in hydrothermal conditions, in analogy with the already commented carboxylic acids. The trends observed for these species may be similar for other stable compounds and would explain the appearance of the plateau in the production of hydrogen and, generally, gaseous species. In the Chapter 5, further consideration on the APR of carboxylic and bicarboxylic acids will be reported, as they are representatives of another class of waste aqueous streams, i.e. derived from hydrothermal liquefaction of lignocellulosic biomass.

### *3.2.5 Effect of the hydrogen pressure*

Two tests at different hydrogen partial pressures were performed to investigate its influence on the APR performance. In Table 7 the results are reported, together with the standard test in inert atmosphere.

Table 7. Influence of the hydrogen partial pressure on the carbon conversion to gas, hydrogen yield and selectivity. Reaction conditions: 1 wt.% alginate solution, T: 225 °C, 0.8 g Pt/C, 6h.

Test	Carbon to gas (%)	APR H <sub>2</sub> yield (%)	APR H <sub>2</sub> selectivity (%)
0% H <sub>2</sub>	22.5	6.0	36.0
5% H <sub>2</sub>	22.3	5.1	27.6
100% H <sub>2</sub>	22.0	-	-

Please note that, in this case, the hydrogen yield was defined considering the amount of hydrogen produced, i.e. calculating the difference between the moles of hydrogen measured at the end of the reaction and the moles initially present in the headspace. While the carbon conversion to gas is not affected by the hydrogen partial pressure, it hindered the hydrogen yield, causing even a “negative” production in the case of 100% H<sub>2</sub>. Being valid the Henry’s law, it was estimated that 1 mol of hydrogen are dissolved per 50 moles of alginate. It means that it should not have a kinetic influence to explain these results. However, it can be constantly consumed by hydrogenation/hydrogenolysis reactions, worsening the selectivity and causing that the final pressure was lower than the initial (with about 10% of the initial moles of hydrogen being consumed). The characterization of the liquid phase should valorize the hypothesis finding more reduced compounds compared to the case in which only the nitrogen atmosphere was used. Huber et al. reported that the rate of hydrogen production in the case of APR of ethylene glycol is negative (-0.7 order), suggesting that it is due to the blockage of the active sites [54]. At the same time, it negatively affects the water gas shift equilibrium, going to the direction of reducing the production of hydrogen [43]. Neira D’Angelo and co-workers showed in their works the positive effects of improving the mass transfer of hydrogen, removing it as fast as possible from the catalytic surfaces. For example, they stripped hydrogen using a nitrogen flow, decreasing the production of hydrogenated liquid products and leading to higher hydrogen yield [64,65]. It is enough to think that working with hydrogen pressure has been suggested as an alternative process to aqueous phase reforming, with the aim of producing alkanes starting from oxygenated biomass: in fact, this process has been commercialized (Virent). This outcome has been showed by Huber et al., where they reported that increasing the hydrogen partial pressures contributed to increase the carbon conversion to liquid products (and not gaseous species), repressing the C-C bond cleavages [97].

We decided to investigate this phenomenon, despite working with a batch reactor. The continuous-like conditions were approximated performing a series of tests in which the produced gas was periodically purged each two hours (after cooling down). It was observed that, after the first step, the production of hydrogen increased from 3.2 to 3.8 mmol, whereas in the case of the test performed without intermediate purging, the hydrogen production stopped at 3.2 mmol, as reported in the previous paragraph. Such an occurrence would indicate that the plateau observed after 2 h cannot be connected to a deactivation of the catalyst, but it is more likely due to the complex reaction scheme and kinetic constraints that involve the formation of recalcitrant intermediate compounds. In

this case, the kinetic constraint would be overcome thanks to the purge of the gas atmosphere, helping to eliminate the block due to the hydrogen adsorption on the active sites. The second purge, performed after 4 h from the beginning (i.e. after 2 h from the first purge), gave no detectable effects on the hydrogen production, that remained approximately constant. This behaviour can be due to the lower concentration of alginate in the solution at this point, which influences directly the rate of hydrogen production. Indeed, the plateau cannot be due to thermodynamic constraints, because the removal of the products should have influenced the equilibrium, pushing the reaction towards the conversion of the substrate. At the same way, it cannot be only due to a kinetic reason linked to the concentration of hydrogen in the gas atmosphere, as suggested previously. Indeed, if a high hydrogen concentration had been maintained, it would have led to hydrogenation with the formation of intermediate species, that will not further react by reforming reactions. For this reason, we inferred that, after 4 h, most of the starting feed has been converted into liquid by-products that are not subjectable to give hydrogen with consistent kinetics, as carboxylic or dicarboxylic acids.

### 3.2.6 Effect of the pH

The influence of the pH on the product distribution is well noted in the study of APR of model compounds [39]. For this reason, three tests at different pH were carried out to evaluate this effect also in the case of the catalytic APR of alginate. The autogenous value of the pH was equal to 6.3.

The Table 8 shows that the carbon conversion to gas slightly decreased with the increasing pH, going from 24.3% at pH = 3 to 20.4% at pH = 12; on the other hand, the hydrogen yield increased by one order of magnitude, moving from 1.2% up to 10.9% at basic conditions. The same trend was observed for the hydrogen selectivity, that reported a disruptive increase from 5.7% to 70.9%.

Table 8. Influence of the pH on the carbon conversion to gas, hydrogen yield, hydrogen selectivity and composition of the obtained gas phase. Reaction conditions: 1 wt.% alginate solution, 0.8 g catalyst, T: 225 °C, time: 6 h.

Test	Carbon to gas (%)	APR H <sub>2</sub> yield (%)	APR H <sub>2</sub> selectivity (%)	Gas concentration (%)					
				H <sub>2</sub>	CO <sub>2</sub>	CO	CH <sub>4</sub>	C <sub>2</sub> H <sub>6</sub>	C <sub>3</sub> H <sub>8</sub>
pH = 3	24.3	1.2	5.7	6.7	75.7	0.0	5.7	3.6	1.5
pH = 6.3	22.5	6.0	36.1	32.7	57.2	0.0	4.8	4.5	0.8
pH = 12	20.4	10.9	70.9	46.8	41.7	0.0	5.9	1.9	0.4

The lowest performance at acidic condition can be explained following the mechanism proposed by Dumesic et al. for ethylene glycol [39]. The acid pH promotes dehydration reactions of the feed leading to unsaturated compounds; afterwards, they are easily hydrogenated (at expense of the produced hydrogen) on the metal site to give alcohols. Furthermore, the alcohol can react, leading not



only to hydrogen, but also to alkanes, reducing in a drastic way the hydrogen yield and selectivity. Avoiding this path becomes still more challenging starting from a complicated feed as alginate, where the presence of several by-products allows many side reactions to occur.

### 3.2.7 Catalyst reutilization and characterization

Since a plateau in the production of gaseous species was observed at long reaction times, the reuse of the catalyst was performed to assess the possibility of deactivation. The results are reported in Figure 13.

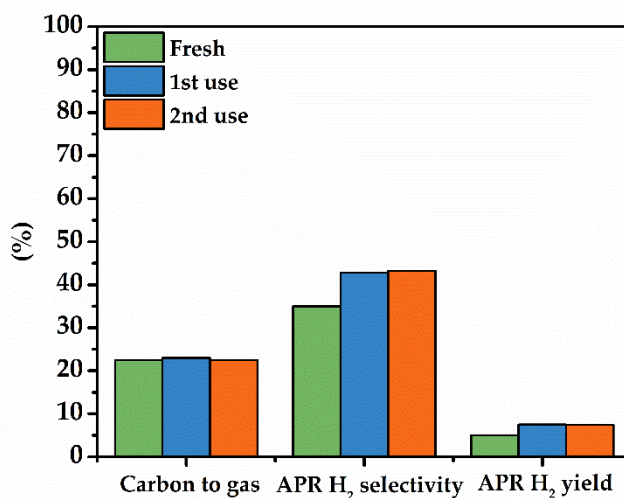


Figure 13. Carbon conversion to gas, hydrogen selectivity and hydrogen yield with catalyst after first, second and third use. Reaction conditions: 1 wt.% alginate solution, T: 225 °C, 0.8 g Pt/C, 6h.

When reused up to three times, the catalyst did not show any sign of deactivation, with a constant carbon to gas conversion and a slightly higher hydrogen selectivity. As shown in the following, the platinum particles increased their size after its first use. The result reported in Figure 13 seems therefore coherent with the observation reported by Lehnert et al., which showed that higher size particles led to similar glycerol conversion and higher hydrogen selectivity [98]. This is an important result because it means that the catalyst did not suffer from any modification than could affect its stability. It is trivial to highlight that this is a fundamental feature for ensuring the application of a catalyst at the industrial scale.

The link between the apparent stop of the reaction and the worsening of the catalyst performance has been investigated also from another point of view. The liquid product obtained from a conventional test was completely recovered and subjected to a new APR test with a fresh catalyst. The results are depicted in the Figure 14.

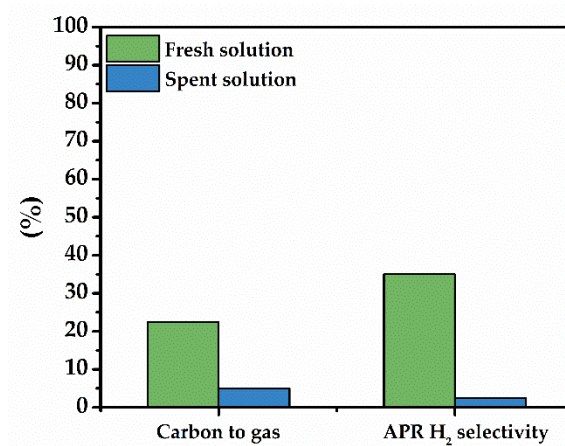


Figure 14. Carbon conversion to gas and hydrogen selectivity obtained after the APR of the liquid effluent and comparison with the fresh one. Reaction conditions: 1 wt.% alginate solution, T: 225 °C, 0.8 g Pt/C, 6h.

A very small carbon to gas conversion and hydrogen selectivity were obtained when the solution was re-tested with a fresh catalyst. This result clearly states that the observed plateau cannot be ascribed to the catalyst, because, if it was the case, comparable performances should have been obtained re-using the solution after the first test. On the other way around, it seems to confirm that the organic compounds present in the liquid phase are not prone to the production of hydrogen, and globally recalcitrant to APR, as suggested in the previous paragraph.

XRD analysis were performed on the fresh and spent catalyst to assess possible structural change in the catalyst, and the results are depicted in Figure 15.

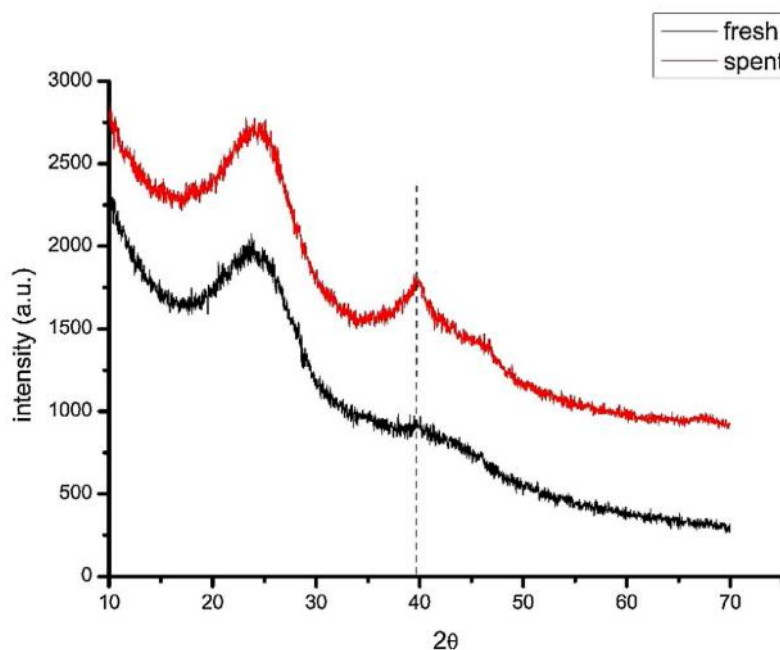


Figure 15. XRD spectra of fresh and spent catalyst after APR of 1 wt.% alginate solution, T: 225 °C, 0.8 g Pt/C, 6h.

The broad peak observed at 22 derives from the graphitic component of the activated carbon. The characteristic peak of Pt is located at 40°. It was barely detected in the case of the fresh catalyst: this is an indication that the active sites were highly dispersed. On the other hand, it was easier to identify the peak in the case of the spent catalyst, likely due to the sintering of the particles.

The hydrothermal stability of the support is a fundamental issue when dealing with catalysts which deal with the APR reaction conditions [99]. For this reason, the textural characteristics of the fresh and spent catalyst (after 6 hours of reaction) were measured. A substantial decrease of the surface area was observed, moving from 1271 to 903 m<sup>2</sup>/g, together with a decrease of the pore volume, from 0.987 to 0.703 m<sup>3</sup>/g. Despite of these modification, no decrease of the performance was observed.

The leaching of platinum from the support was investigated by ICP-MS. The analysis showed an effective 3.2 wt.% Pt loading with the fresh catalyst; at the end of the reaction, the loading of the active metal remained almost constant, with just 0.0036% of the initial platinum lost in the aqueous solution: therefore leaching was excluded as a possible mechanism of the catalyst deactivation.

Finally, the deposition of coke on the catalyst was investigated [48]. A small carbon deposition was reported on the first APR paper and it is generally considered as a possible cause of deactivation, despite it should be minimal working at such low temperature [37,42]. On the other hand, Luo et al. observed that the carbon content reached up to 7.18 wt.% in the used alumina-supported catalyst after glycerol APR [100]. The influence of the support on APR performance has been reported not only for the hydrogen yield, but also for the resistance to coke formation [42]. Alumina-supported catalysts are prone to deactivation by sintering and carbonaceous deposits on the catalyst surface; on the other hand, carbon-supported catalysts showed slighter deactivation and higher resistance. Working with a carbon-supported catalyst, it is complex to assess the presence of carbonaceous species on the surface. Nevertheless, a thermogravimetric analysis was performed on a fresh and spent catalyst, and the results obtained are reported in Figure 16.

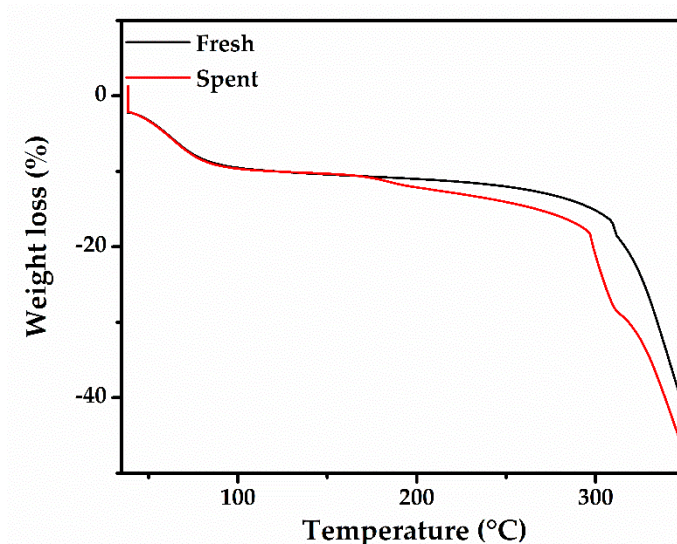


Figure 16. TGA spectra of the fresh and spent catalyst after APR of 1 wt.% alginate solution, T: 225 °C, 0.8 g Pt/C, 6h.

The spent catalyst started to lose weight at lower temperature compared to the fresh catalyst, at about 170 °C. It can be due to the volatilization of small organic compounds on the catalyst surface. At 300 °C, both the catalysts started to lose most of their weight, and it is due to the decomposition of the support and it is not possible to explore the presence of coke above this temperature. Together with this information, it is worthy to mention that at the end of the reaction we recovered 0.83 g of solid phase (after the drying step), compared to initial 0.8 g of catalyst. This means that there is at least a slight increase of the weight due to the presence of organics on the surface.

Together with this kind of depositions, the presence of carbonates due to the sodium and carbon dioxide in the aqueous reaction environment (confirmed by the results of inorganic carbon analysis) may lead to inorganic deposits. In fact, water at high temperature is a solvent with lower dielectric constant, therefore the salts are less soluble and may interfere with the catalytic activity.

### 3.3 Conclusions

The catalytic aqueous phase reforming of alginate was investigated to produce hydrogen, looking to a representative compound of by-product aquatic biomass processing. The variations of several parameters were analysed (effect of alginate, catalyst loading, temperature, time reaction, pH, hydrogen partial pressure) to examine their influence on the carbon conversion to gas, the yield and selectivity of hydrogen. It was observed that there is an increase of the carbon to gas with the increasing catalyst amount and that the maximum hydrogen selectivity was reached at 0.4 g of catalyst; at the same way, there was a beneficent effect of the increasing temperature, with a maximum of performance at 225 °C. On the other hand, there was a negative effect increasing the alginate concentration, since the carbon conversion to gas decreased because of side reactions that take place in the liquid phase. The analysis of the evolution of the gas products with time showed a

plateau after 2 h for hydrogen: this phenomenon was ascribed mainly to the formation of products that have low tendency to react and give hydrogen, even though its production would be thermodynamically favoured. The variation of pH showed a strong positive effect when the APR is carried out in basic conditions, increasing by one order of magnitude the hydrogen selectivity. Therefore, it was confirmed what is present in literature, where working at low pH gave rise to problems of competitiveness of the produced hydrogen with other reactions, such as dehydration/hydrogenation or hydrogenolysis. Finally, the characterization of the catalysts showed a modification of the surface area and pore volume under hydrothermal conditions, together with a slight deposition of coke and sintering of the Pt particles; on the other hand, leaching of the active metal was not observed. Our study confirmed the dependence of the typical reaction conditions on the performance obtained by the APR of a more complex feed respect to the typical ones investigated, giving validation also to previous results in terms of representability of complex systems. With this work, we tried to enlarge the portfolio of molecules that can be investigated for hydrogen production. Even if the results are less positive than the ones present in literature, further research efforts will be assessed to have a better comprehension of the phenomena involved in the catalytic aqueous phase reforming of alginate: the sustainable exploitation of both the liquid (with value-added molecules) and gas phase (with a high energetic value) would be essential with the aim of developing a biorefinery for a carbohydrate-based economy.

# Chapter 4 Exploitation of sugar-based biorefinery streams

## 4.1 Introduction

Lignocellulosic biomass is the most abundant biomass and, for this reason, it plays a key role to replace fossil oil [101]. It is constituted by approximately 50% cellulose, 30% hemicellulose, with the remaining being mostly lignin. Cellulose is a highly ordered homopolymer of  $\beta$ -linked glucose; hemicellulose is an amorphous polymer containing typically five different C5-C6 sugars; lignin is a complex three-dimensional phenolic polymer.

The interest in lignocellulosic biomass is increasing thanks to the possibility to consider it as a feed to produce bioethanol. Indeed, it offers several advantages compared to the first generation-based bioethanol (mainly from edible sugarcane): lignocellulosic biomass is often a waste, it can be found at low price, and it does not raise ethical dilemmas, being not in overlap with the food chain [102]. Bioethanol production consists of several steps: briefly, it begins with the pretreatments necessary to destroy the complex linkage between cellulose, hemicellulose and lignin. Afterwards, the carbohydrates are subjected to hydrolysis (enzyme- or acid-catalyzed) leading to a mixture of simple sugars (hydrolysate). Finally, the hydrolysate is later fermented by dedicated yeasts or bacteria producing ethanol, which is ultimately distilled and purified [103].

In order to ensure the economic sustainability of a process based on biomass, the utilization of each component of the feed should be maximized. The lignin is mainly used to generate electricity, even if many efforts are put to convert it into biofuels and/or commodity chemicals [104].

Despite their utilization in the fermentation step, the hemicellulose-derived sugars are not effectively exploited, as *S. cerevisiae* yeasts are unable to utilize pentoses [105]. For this reason, a lot of effort has been put in the modification of the conventional strains to allow them also the fermentation of the pentoses [106]; anyway, the efficient exploitation of these sugars is still ongoing. Studying the most effective way to separate the hemicellulose from the other fractions in a bioethanol plant is also an important research theme, necessary to taking advantage of the entire organic content [107].

Butanol is an option as product from the hemicellulose fraction, used, for example, as drop-in biofuel. Lessard et al. valorized the C5 sugars producing high octane oxygenates blended in the gasoline pool [108]. Another alternative is pentoses fermentation to lactic acid by using *Lactobacillus plantarum* [109]. Furthermore, furfural synthesis is one of the most interesting path as it would lead

to a sustainable way to produce an important intermediate for solvent, plastics, fuel additives etc. [110].

Moreover, it has been proposed to utilize the xyloses to produce bio-hydrogen, namely through dark fermentation [111].

In this chapter, the valorization of the hemicellulose fraction via aqueous phase reforming will be reported.

Among the several possible molecules of interest, sorbitol (i.e. glucose's corresponding sugar alcohol) has been thoroughly studied as model compound for APR [65,90,112–118], while xylitol (the xylose's corresponding sugar alcohol) has been studied with less extent [113,119–122]. Moreover, apart from the first works, glucose has been poorly investigated, possibly due to the low thermal stability and hydrogen production compared to the corresponding alcohol [37,123,124]. Meryemoglu et al. performed the wheat straw hydrolysis, followed by APR of the derived solution with precious (Pt, Pd, Ru) and non-precious catalysts (Ni Raney), with platinum showing the best results among the former ones, and Ni reporting the highest hydrogen production [125]. Surprisingly, to the best of our knowledge, xylose has never been subjected to APR.

We evaluated for the first time the production of hydrogen from xylose, the most abundant C5 sugar in hemicellulose, therefore seen as representative compound of a biorefinery stream (i.e. pentoses sugars) not yet well valorized, following the scheme reported in Figure 17. In the scheme it is assumed to follow the pretreatments necessary to maximize the recovery of the hemicellulose fraction, as reported in [105]. Afterwards, the C6 sugars can be effectively converted to bioethanol through fermentation using conventional yeasts, while the C5 sugars can be addressed to aqueous phase reforming. A systematic approach was used globally to evaluate the influence of temperature and concentration on the reforming of glucose, xylose and corresponding sugar alcohols. Moreover, we subjected to APR a stream from a bioethanol plant after the hydrolysis step (from here on referred as hydrolysate). A model mixture glucose-xylose, imitating the composition of the hydrolysate, has been tested as well. As it is known from literature, and confirmed here, the sugar alcohols are more prone to hydrogen production [76]. For this reason, we compared the performance obtained with the sugar mixture with a sorbitol-xylitol solution. A two-step process hydrogenation-APR was studied in order to evaluate if a total positive production of hydrogen was obtained; this scheme has been investigated for the hydrolysate as well. Finally, a study on the reuse of the catalyst and its characterization has been carried out, looking for deeper information on the solid phase obtained during the reaction.

This chapter (results, figures and tables) is based on the published work reported in [126].

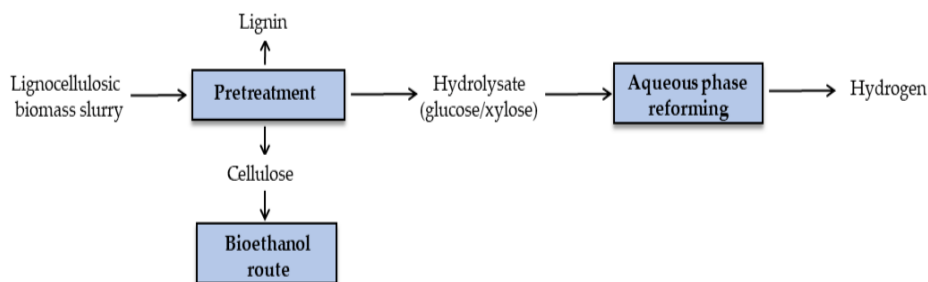


Figure 17. Block-flow diagram of a bioethanol plant with valorization of the C5 sugars via APR.

## 4.2 Results and discussion

### 4.2.1 Characterization hydrolysate

Wheat straw hydrolysate was kindly furnished by Beta Renewable S.p.A. In the following Table 9, its characterization is reported. The pretreated biomass with PROESA technology generally provides an aqueous solution with the following composition (ranges according to pretreatment operating conditions): glucose 50-75 g/kg, xylose 20-30 g/kg, arabinose 0.7-1.5 g/kg, glycerol <0.3 g/kg, formic acid 0.5-1.2 g/kg, lactic acid <0.5 g/kg, acetic acid 1.8-2.5 g/kg, 5-HMF <0.2 g/kg, furfural <0.3 g/kg. Oligomers of the above-mentioned might be present. The pH of the solution was around 5.1.

The main characterized monosaccharides were glucose and xylose, whose concentration fall in the lower boundary of the formerly presented ranges (5.3 wt.% for glucose and 2.2 wt.% for xylose), being the aqueous solution quite diluted. These values were used to mimic the real hydrolysate in the preparation of synthetic mixtures of the two sugars (as later described), adopting the same relative concentrations of glucose and xylose (70% and 30% respectively).

The TOC of the hydrolysate was 4.24 wt.% (Table 9), of which 70% carbon comes from the contribution glucose + xylose. The remaining 30% carbon may be constituted by the oligomers and it was not identified by HPLC analysis. Other compounds identified by chromatography were present in traces (e.g. acetic acid). Finally, the hydrolysate contained some inorganics, originally present in the biomass.

Table 9. Characterization of the wheat straw hydrolysate.

TOC (mg C/L)	Monosaccharides (wt.%)		Inorganics (ppm)		
	Glucose	Xylose	Na	K	Ca
42400	5.3	2.2	3585	504	351



## 4.2.2 Influence of the reaction temperature and carbon concentration

### *Influence of the reaction temperature on the model compounds APR*

In this section, the influence of the reaction temperature in the range 230-270 °C is discussed, working at 0.9 wt.% carbon in the feed.

In Figure 18, the trend of the indicators is reported for each model compound. Looking at the glucose (18-A), the carbon conversion to gas slightly increased with the temperature, due to the more favourable C-C cleavage step that leads to gaseous products. The H<sub>2</sub> gas distribution and APR H<sub>2</sub> selectivity had a steep increase between 250 and 270 °C. This is due to two phenomena: from one side, less alkanes were obtained in the gas phase, leading to an increase of the H<sub>2</sub> gas distribution; on the other side, the H<sub>2</sub>/CO<sub>2</sub> ratio increased, leading to higher APR H<sub>2</sub> selectivity. To the best of our knowledge, only Dumesic and coworkers looked at the influence of temperature on the APR of glucose at 225 and 265 °C [37]. Coherently with Dumesic, there is a positive effect of increasing temperature on the carbon conversion, but different trends in the selectivity were obtained. Nevertheless, it is difficult to perform a direct comparison between the two results because of the differences in the reaction condition. As reported in the previous chapter, where alginate was studied, the increase of the temperature showed similar results, with a slight increase of the carbon conversion to gas and the increase of the selectivity to hydrogen production [85]. The gas phase was mainly constituted by CO<sub>2</sub>, at each temperature investigated (from 90% at 230 °C to 75% at 270 °C), despite a strong increase is observed in the hydrogen concentration (Figure 19-A). It may indicate that higher temperatures favour more the reforming path than decarboxylation-like reactions. Koklin et al. showed also that, in similar conditions, carbon dioxide is the main component of the gas phase produced by the transformation of glucose in aqueous solution in an inert environment [127].

In the liquid phase glucose reached complete conversion already at the lowest investigated temperature. Among the by-products, glycolic, acetic and lactic acid decreased their concentration with the increase of temperature. Therefore they contributed to the increase of the conversion to gaseous products, as they are prone to be reformed to produce hydrogen and alkanes [128].

As it is known from literature, sugar decomposes at high temperature in hydrothermal conditions, giving a solid residue. It was the case also during the current experimental campaign and it is likely the main cause for the expectation to reach carbon balance closure if only the contribution of gaseous and liquid organic products is considered. A decreasing tendency to produce a solid residue was observed, going from 255 mg at 230 °C to 170 mg at 250 °C and 150 mg at 270 °C. It worths being highlighted that these amounts were calculated as the difference between the solid phase recovered after drying and the initial amount of catalyst at the same conditions. This is an important information as it would

complete what is known in literature regarding the production of the solid phase only according to different concentration. This result is in accordance with the trend of the increasing selectivity with higher temperature, that should favour the reforming instead of decarboxylation/decomposition. Further information on the solid phase are reported in the paragraph 4.2.5, where its effect on the stability of the catalyst is discussed.

Aqueous phase reforming of xylose was investigated in this work for the first time. It had a small increase in the carbon conversion to gas, from 25 to 37%, with a trend similar to the one of glucose, but with relatively higher values. This result may be due to the smaller length of the molecule, that may favour the production of gas more than liquid products. In fact, reducing the molecular weight of the starting compound helps to increase the probability to obtain carbon containing gaseous compounds, enabled by the C-C bond breaking reactions. Looking at the composition of the gas phase, we observed a strong influence of the temperature on the alkanes formation, that is reflected in the H<sub>2</sub> gas distribution (Figure 19-B). In fact, at 230 °C propane was present in high concentration (about 20%), decreasing at 17% at 250 °C and 13% at 270 °C. It may be obtained from consecutive decarboxylation reactions that lead to the production of gaseous products other than the expected H<sub>2</sub> and CO<sub>2</sub>. Interestingly, the higher the temperature the lower is the production. At first, it may be hypothesized that higher temperature may lead to cracking reactions. On the other hand, methane and ethane did not increase appreciably. Therefore, we may conclude that the increase of the temperature changed the reaction pathways, not favouring the production of alkanes but rather the production of hydrogen (as seen also for glucose previously).

In the liquid phase, it can be observed that xylose exhibited a considerable conversion already at 230 °C; the HPLC chromatogram showed a pattern similar to the one of glucose. About 60% of the liquid compounds was identified, with hydroxyacetone being to main compound (about 6% of the starting carbon), followed by glycolic and lactic acid (3%) at 230 °C; anyway, their concentration decreased with temperature: at 270 °C the carboxylic acids were the main compounds, i.e. propionic acid (3.5%), acetic acid (2.3%) and butanoic acid (1.9%). The acids may come from the rearrangement of C-O bonds, as happens in the isomerization of poly-alcohols leading to the corresponding carboxylic acid [94].

Sorbitol has been studied in much higher detail in the past, as compared to glucose. It was anyway studied in this work to make a rigorous comparison with its corresponding sugar and similar compounds thanks to the fact that the experimental campaign has been performed in the same set-up, without the influence of many possible variables other than the different reaction conditions whose influence was under investigation.

The carbon conversion to gas moved from 20 to 50%, and the gas composition seemed uninfluenced by the reaction temperature. In fact, contrary to the corresponding sugar, the composition of the gas phase remained constant at each temperature, with H<sub>2</sub> (55%) and CO<sub>2</sub> (35%) as main component. The

selectivity of the aqueous phase reforming was not affected as well, therefore the increase of the yield of hydrogen is ascribed substantially to the higher conversion obtained (Figure 19-C). So, dealing with the sugar alcohol, the increase of the temperature had the effect of increasing the activity, without substantially affecting the selectivity.

Sorbitol converted 50% at 230 °C, 80% at 250 °C and completely at 270 °C. At 270 °C there were many more molecules coming from the feed fragmentation; in this case, in contrast with the glucose, alcohols and poly-alcohols were the main compounds, i.e. propylene glycol, ethylene glycol, ethanol, coming likely from the successive dehydrogenation and C-C bond cleavage of the molecule. It is likely that higher reaction time would have led to higher hydrogen production, as these by products are known to be prone to give hydrogen in the current reaction conditions. This is probably the reason why a decrease in the selectivity was not observed. Indeed, the reaction path lead to the production of beneficent by-products, not recalcitrant to further APR, that keep going on the reforming pathway, contrary to the case of glucose, where carboxylic acids were obtained. The number of compounds was lower as compared to other works in literature, presumably due to the longer reaction time and higher temperature used in this work. For example, Kirilin et al. reported the identification of hundreds of compounds in the liquid phase, but much fewer by-products were obtained in our reaction conditions [90].

As in the case of sorbitol, xylitol reached about 55% of carbon to gas conversion at 270 °C. The APR hydrogen yield exceeded 30%, higher than the C6 sugar alcohol. The temperature did not affect the gas composition, with hydrogen and carbon dioxide remaining the main gaseous products (Figure 19-D).

In the liquid phase, xylitol reached 40% of conversion at 230 °C, 80% at 250 °C and complete conversion at 270 °C. Even then, C2, C3 and C4 poly-alcohols were the main liquid by-products.

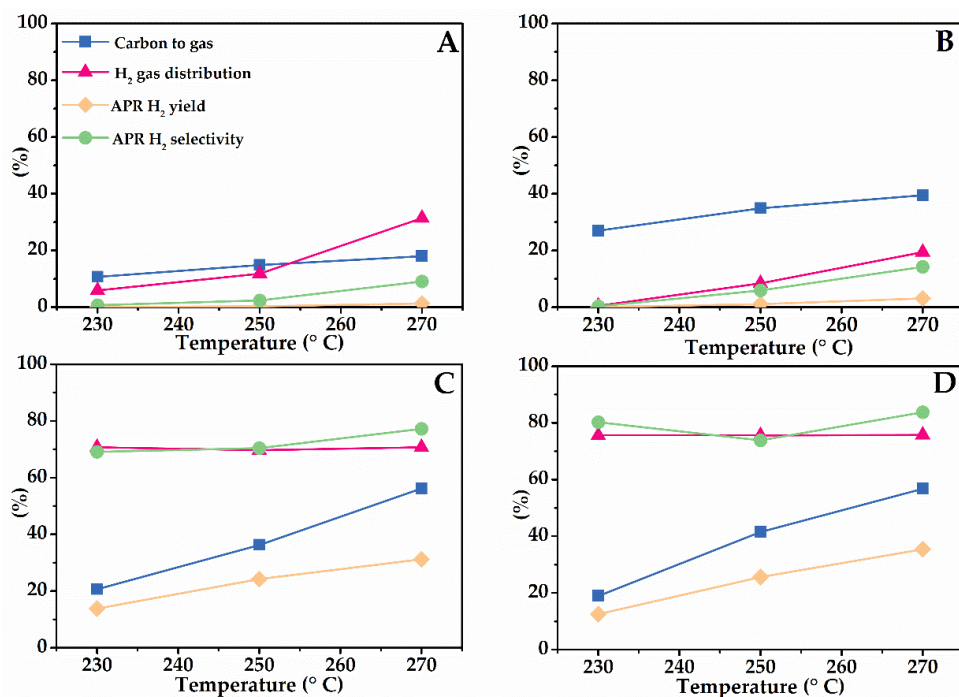


Figure 18. Influence of temperature on the APR performance of glucose (A), xylose (B), sorbitol (C) and xylitol (D). Reaction conditions: 0.375 g Pt/C catalyst, 2 hours reaction time, 0.9 wt.% carbon concentration.

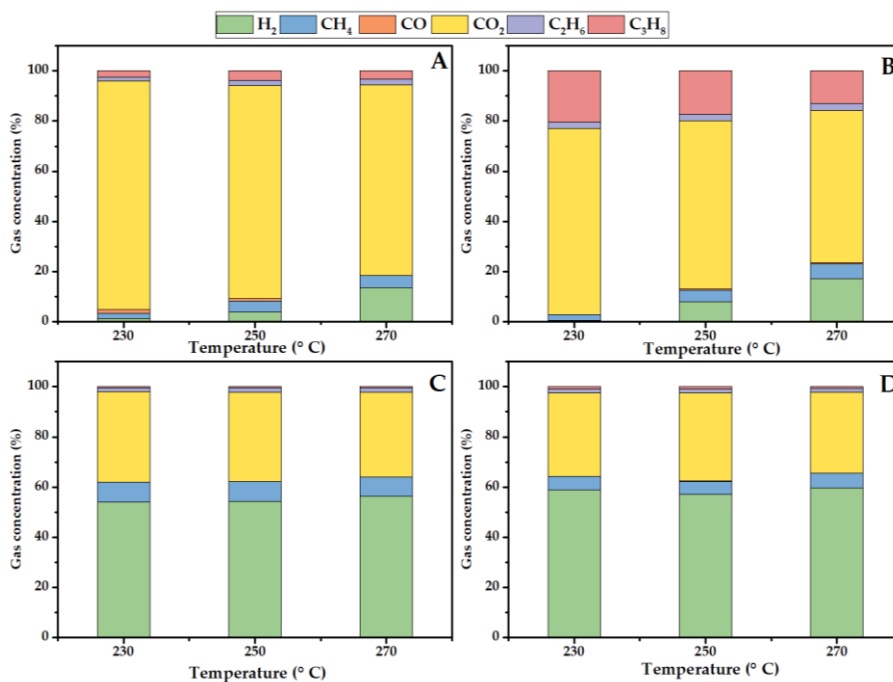


Figure 19. Influence of the reaction temperature on the composition of the gas phase obtained after APR of glucose (a), xylose (b), sorbitol (c) and xylitol (d). APR reaction conditions: 2 h reaction time, 0.9 wt.% carbon.

### *Influence of the reaction temperature on the hydrolysate APR*

The influence of the reaction temperature was evaluated for the hydrolysate looking only to the carbon to gas and the H<sub>2</sub> gas distribution, as the other indicators would need a complete knowledge of its composition to define a reaction stoichiometry (Figure 20).

It was observed that the temperature had no effect on the carbon to gas conversion: this was unexpected as glucose and xylose alone showed, despite slightly, a clear increase with temperature. One explanation may be given referring to the carbon present in the feed as oligomers, constituting about 30% of the total carbon. Probably this fraction of carbon was not activated in these reaction conditions and does not contribute to the pool of carbon that may go in the gas phase. A confirmation of this hypothesis may come from the results that will be showed in the paragraph 4.2.3, where a model mixture constituted only by glucose and xylose had results that are totally coherent with the single compounds (i.e. with a slight but evident increase of the carbon conversion to gas with higher temperature). Therefore, as the fraction of carbon that can undergo reforming decreased from the model compounds to the real stream, the small increase of the production of gaseous products could not be observed. Moreover, the influence of pH should be taken into account. Indeed, the lower pH of the hydrolysate feed may have hindered the production of short-chain molecules, reducing the carbon to gas conversion [39]. The hydrogen gas distribution showed an evident increase. Indeed, looking at the gas composition, the trend observed agrees with the one reported for the model compounds. This result, that can be ascribed to the glucose/xylose fraction, seems to confirm that higher temperatures are beneficial towards reforming reactions, as compared to side reactions.

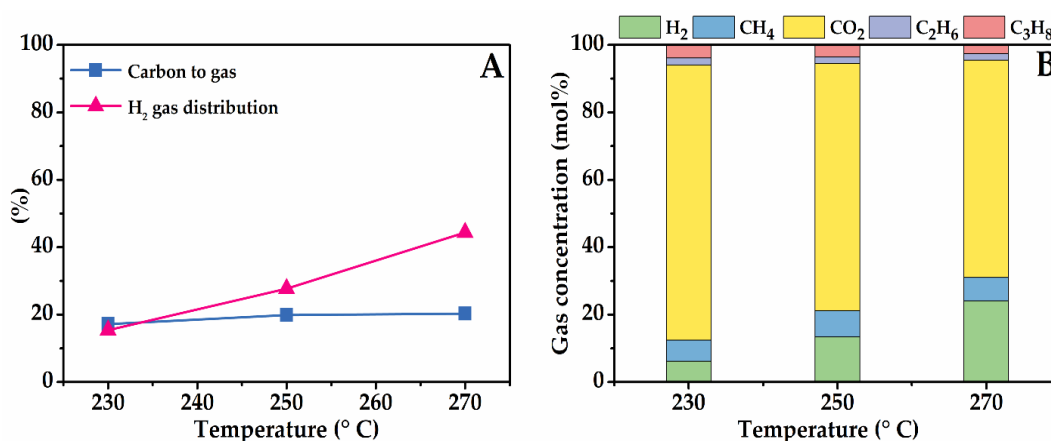


Figure 20. Influence of reaction temperature on APR performance of wheat straw hydrolysate (A) and composition of the produced gas phase (B). Reaction conditions: 0.375 g Pt/C catalyst, 2 hours reaction time, 0.9 wt.% carbon concentration.

### *Influence of the carbon concentration on the model compounds APR*

Being 270 °C the temperature leading to the highest hydrogen production, the influence of the concentration was investigated only at this temperature in the 0.3-1.8 wt.% carbon range (i.e. 0.75-4.5 wt.% of the feed).

Glucose reported a dramatic decrease of the performance working at higher concentrations, in terms of carbon conversion to gas, hydrogen selectivity and therefore, globally, on the hydrogen yield (Figure 21-A). This phenomenon can be ascribed to the more favourable homogenous side reactions in contrast to the reforming reactions: indeed, the former ones have first-order dependence on the feed concentration, while the latter have fractional-order dependence. The gas composition was strongly influenced by the concentration (Figure 22-A). Indeed, while hydrogen was present at 40% in the diluted conditions, it reached less than 10% at 1.8% of carbon, with the main compound being CO<sub>2</sub>.

At the diluted conditions, the small carboxylic acids were the main compounds (acetic acid, propionic acid). As reported in the previous section, glucose reforming led to the production of a solid phase. It was evident as the weight of the solid phase recovered on the filter after the drying step was higher than the one that may be attributed only to the catalyst. Indeed, it has been recovered up to 770 mg at 1.8 wt.%, 460 mg at 0.9 wt.% and 150 mg at 0.3 wt.% of carbon concentration composed by solid residue and 375 mg of original catalyst.

In analogy with glucose, carbon conversion to gas of xylose decreased from 60% at 0.3 wt.% of carbon to less than 30% at 1.8 wt.%. The gas composition was influenced by the starting concentration as well, as a constant decrease of hydrogen was observed; on the other hand, carbon dioxide increased up to 70%, with 16% also of propane.

In the liquid phase, xylose completely reacted at each concentration. Acetic acid was the main identified liquid product, constituting about 20% of the total carbon identified in the condensed phase.

The solid phase of xylose moved from 80 mg at 0.9% C to 360 mg at 1.8% C (it was not appreciable at 0.3% C): therefore, it is evident that more concentrated solutions favour condensation reactions, producing likely high molecular weight compounds, maybe with a more pronounced hydrophobic nature. Indeed, as reported later, during a washing step performed on the catalyst, ethanol was able to better extract organic compounds as compared to water: this may be an indication of a different chemical characteristic of the deposit on the surface of the catalyst, being ethanol less polar than water.

The hydrogen gas distribution of sorbitol was not influenced by the carbon concentration, that is, the production of alkanes was not favoured at high concentrations, differently to glucose. On the other hand, the APR-H<sub>2</sub> selectivity decreased for the higher production of carbon dioxide, globally leading to the half of the hydrogen yield at the highest concentration investigated. The reason may be due to a higher presence of intermediates at high concentration, that can be subjected to hydrogenation, leading to a consumption of the produced H<sub>2</sub>, eventually decreasing the selectivity. Sorbitol converted at 80% at 1.8 wt.%, while it converted completely at lower concentrations; hydroxyacetone was the second

most present compound in these conditions. When sorbitol was tested, a solid phase was not observed apart from the used catalyst. This implies that the involved reactions are completely different from the APR of glucose. Thus, working with the reduced form of the sugar is of paramount importance. For this reason, Davda et al. proposed to use a hydrogenative pretreatment to overcome the side reactions that involve the sugars and not the sugar alcohols [89]. The results obtained studying this reaction configuration will be reported in the paragraph 4.2.4

Xylitol behaved analogously to sorbitol: even in this case, the hydrogen gas distribution was constant, while the APR H<sub>2</sub> selectivity, involving the relative production of hydrogen and carbon dioxide, decreased with the concentration.

In the liquid phase xylitol converted at 78% at 1.8%, but quantitatively at lower levels of concentration. Xylitol, at the same way of sorbitol, did not produce a solid phase that may be ascribed to the formation of high molecular weight compounds.

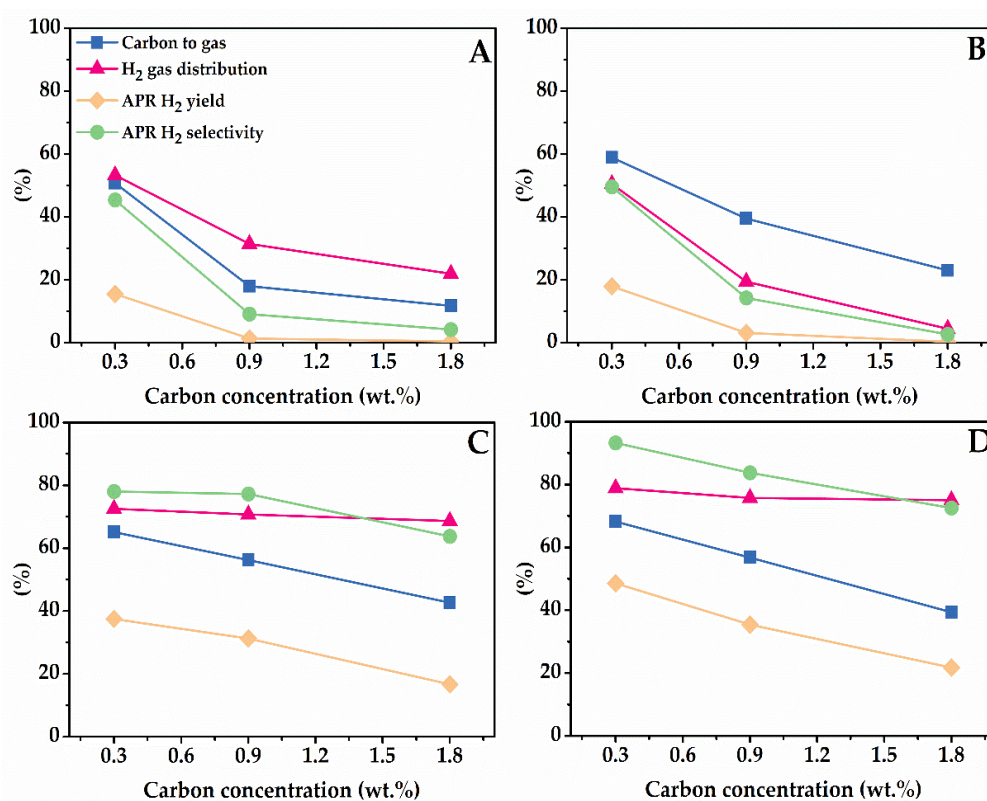


Figure 21. Influence of the carbon concentration on the APR performance of glucose (A), xylose (B), sorbitol (C) and xylitol (D). Reaction conditions: 0.375 g Pt/C catalyst, 2 hours reaction time, 270 °C reaction temperature.

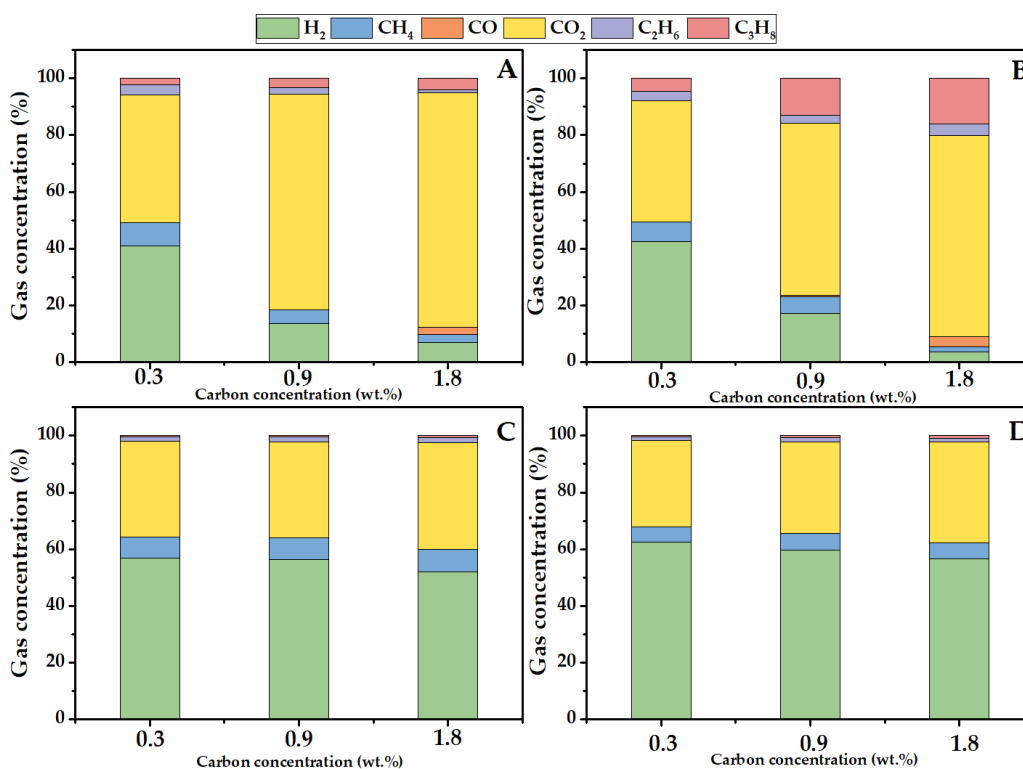


Figure 22. Influence of the carbon concentration in wt.% on the composition of the gas phase obtained after APR of glucose (a), xylose (b), sorbitol (c) and xylitol (d). APR reaction conditions: 2 h reaction time, 270 °C.

### *Influence of the carbon concentration on the hydrolysate APR*

In accordance with the study of the model compounds, increasing the concentration hindered the conversion to carbon-containing gaseous species (Figure 23). Hydrolysate is constituted mainly by glucose and xylose; therefore, this result can be ascribed to the homogeneous phenomena in which they are involved. Also, the hydrogen distribution decreased, as the production of gaseous alkanes became more favourable working at higher concentrations. This outcome can be highlighted looking at the distribution of the gaseous products.

In the liquid phase, both glucose and xylose were converted considerably. The main identified liquid products are carboxylic acids (acetic acid, propionic acid, butanoic acid). The test performed at 1.8 wt.% showed also isomers of glucose and xylose, as the isomerization is known to be one of the first reactions in hot aqueous systems [44]. Comparing the chromatograms obtained with the hydrolysate and the model compounds, we observed that there are approximately the same peaks. This may be an indication that only glucose and xylose effectively contributed to the reaction, while the remaining 30% of carbon present in the oligomers did not influence the product distribution.

Hydrolysate produced a solid phase; the amount recovered increased up to 375 mg at 1.8 %, coherently with the decreasing carbon conversion to gas. Therefore, working at higher concentration shifted the fate of carbon from the gas



phase, where it is mainly under the form of carbon dioxide, to the liquid and solid phase.

It is important to highlight that the effect of the inorganics on the APR performance cannot be excluded at this stage. This issue has not been fully addressed by the available literature and opposing outcomes have been reported. Lehnert et al. reported for the first time the APR of crude glycerol [98]. They ascribed the deactivation and the lower hydrogen production to the inorganics (e.g. NaCl). Conversely, Boga et al. reported, using a synthetic mixture to imitate the composition of a crude glycerol, that the salts of the fatty acids are likely the main responsible for the worsening of the performance [129]. This aspect has not been deeply analyzed in the present work; however, we may suppose, following Boga's outcomes, that the only presence of inorganics may have not influenced drastically the obtained results. Further investigation should be addressed to confirm this hypothesis.

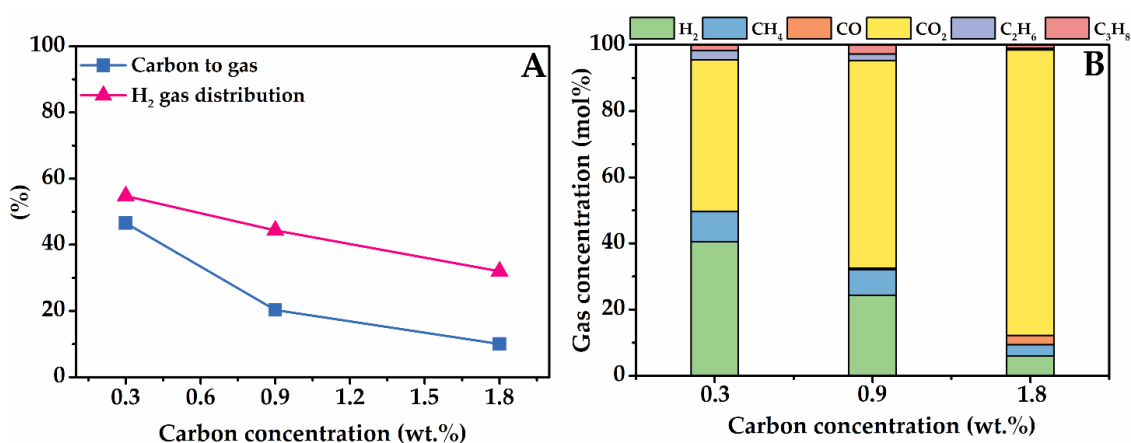


Figure 23. Influence of the carbon concentration on APR performance of wheat straw hydrolysate (left) and composition of the produced gas phase (right). Reaction conditions: 0.375 g Pt/C catalyst, 2 hours reaction time, 270 °C reaction temperature.

#### 4.2.3 Mixtures of model compounds

In the view of an industrial application, a mixture of sugars rather than a single compound will be the feedstock for the process. For this reason, a synthetic binary mixture of glucose and xylose was subjected to APR. This is an important step because collateral inhibitory phenomena (e.g. competitive adsorption) may happen. Moreover, we tested a synthetic mixture of the corresponding sugar alcohols, i.e. sorbitol and xylitol.

The mixture is constituted by 70% of glucose and 30% of xylose (and with the same ratio in the case of the sorbitol-xylitol mixture), in order to have results as close as possible to the hydrolysate and facilitate the comparison of the results. It is worthy to underline that the acids have not been included for modelling the hydrolysate. This choice has been justified by the about twenty times higher

concentration of the sugars compared to the acids (acetic acid, lactic acid), and by the low hydrogen yield obtained by the latter, both alone and in mixtures, as reported in [128].

In Figure 24, the results of the influence of the temperature on the APR of glucose-xylose mixtures at 0.9 wt.% carbon are reported.

All the indicators increased with temperature, at the same way of the single compounds, as reported in the relevant section. We compared the results with the linear combination of the single test and plotted the outcomes. The linear combination related to the carbon to gas conversion (CtoG) was calculated according to the following equation (in an analogous way the calculations for the hydrogen yield and for the sorbitol-xylitol mixture were performed).

$$\text{CtoG}_{\text{linear combination}} (\%) = 100 * (0.7 * \text{CtoG}_{\text{glucose}} + 0.3 * \text{CtoG}_{\text{xylose}})$$

It is highlighted that the points coming from the linear combination are close to the experimental results (the points of the H<sub>2</sub> selectivity were not reported for the sake of clarity of the figure). This is an interesting result because it should imply that there are no inhibitory phenomena between the compounds, as on the other hand we observed with small organic acids [128]. This means, for example, that there is not a competitive adsorption on the surface of the catalyst. Therefore, the mixture can be thought as a pseudo-compound, whose results are the combination of the results from the components of the mixture itself.

In order to complete this piece of knowledge, we investigated also the sorbitol-xylitol mixture at different temperatures. Even in this case, the linear combination points are close to the experimental results. Moreover, xylitol may be thought as the result of the first dehydrogenation/decabonylation of sorbitol [114] and the liquid by-products of sorbitol are the same of xylitol. For this reason, the sorbitol-xylitol mixture can be considered, even more than the glucose-xylose one, a pseudo-component. This information may give an indication for the modelling and design of a plant that may valorize this feed.

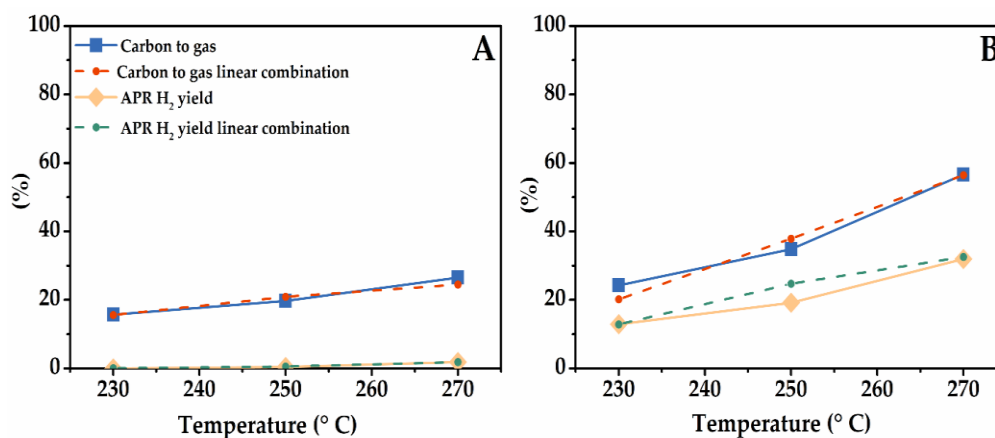


Figure 24. Influence of reaction temperature on the performance of APR of a glucose-xylose (A) and sorbitol-xylitol (B) mixture. The points jointed by a dotted line are referred to the linear combination of the singular components. Reaction conditions: 0.375 g Pt/C catalyst, 2 hours reaction time, 0.9 wt.% total carbon concentration.

At the same way of the model compounds, we investigated also the influence of the carbon concentration on the performance of the synthetic mixtures.

In the Figure 25-A the experimental results for the glucose-xylose mixture are reported, together with the linear combination of the single compounds results linked with a dotted line. First of all, also in the case of different concentrations, it has been observed a similar trend of all the indicators with the single compounds. The carbon conversion to gas and the APR-H<sub>2</sub> selectivity almost halved between 0.3 and 0.9 %, leading to a negligible APR-H<sub>2</sub> yield already at 0.9%. Moreover, not only the yield, but also the amount of hydrogen decreased substantially despite the increase in the amount of the feed (Figure 26, left). The linear combination reflected the experimental outcomes also in this case, evidencing the absence of collateral phenomena of interference between the compounds not only at different temperatures, but also at different concentrations.

The sorbitol-xylitol reported analogous results (Figure 25-B). The indicators had the same trend reported for the single compounds, with the decreasing carbon conversion to gas main responsible for the decreasing APR-H<sub>2</sub> yield. Anyway, despite of this decrease, the amount of H<sub>2</sub> produced increased, contrarily to the glucose-xylose mixture (Figure 26, right). Also, with the sugar-alcohol mixture, the linear combination points are in perfect agreement with the experimental results, pointing out the similar reactivity of the components related to the possible reaction pathways at the experimental conditions investigated.

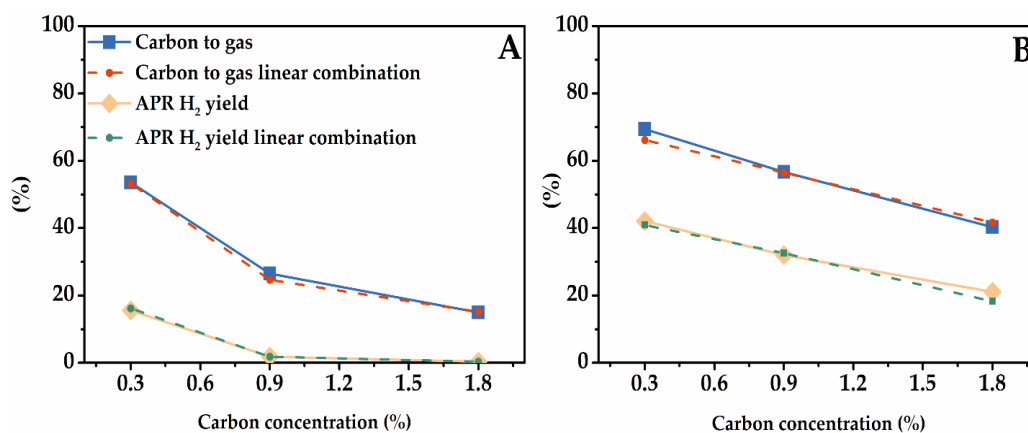


Figure 25. Influence of carbon concentration on the performance of APR of a glucose-xylose (A) and sorbitol-xylitol (B) mixture. The points joined by a dotted line are referred to the linear combination of the singular components. Reaction conditions: 0.375 g Pt/C catalyst, 2 hours reaction time, 270 °C reaction temperature.

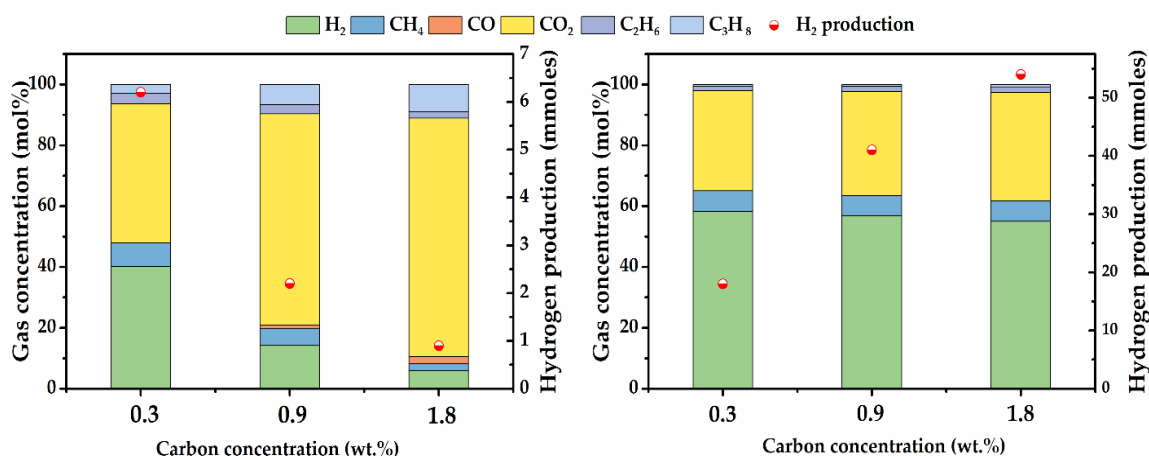


Figure 26. Influence of carbon concentration on gas phase composition and hydrogen production of a glucose-xylose (left) and sorbitol-xylitol (right) mixture. Reaction conditions: 0.375 g Pt/C catalyst, 2 hours reaction time, 270 °C reaction temperature.

#### 4.2.4 Hydrogenation-APR tests

From the previous results, it has been clear that the mixture of sugar alcohols led to much higher hydrogen production compared to the corresponding sugars. This is due to the possibility to work at higher concentration with the alcohols, without losing in productivity because of the homogeneous reactions. On the other hand, the alcohols are not the primary feedstock, as only the sugars would be available if we think to the bioethanol plant. The approach suggested by Dumesic and co-workers was followed to evaluate the feasibility of a two-step process, in which the APR is preceded by a selective hydrogenation to convert the sugars in sugar alcohols, trying to prevent the homogenous reactions that hinder the hydrogen production [89]. Irmak et al. tested a similar configuration with kenaf biomass hydrolysate reformed with an alumina supported catalysts, showing better performance of the hydrogenated feed [130]. Aim of this section is evaluating if the total hydrogen production is higher in the two steps process than in the one-pot (i.e. without pre-hydrogenation). As reported in the experimental section, the hydrogenation tests were performed with a commercial 5% Ru/C catalyst.

##### *Hydrolysate-like mixture*

The synthetic glucose-xylose mixture (referred also as hydrolysate-like mixture) was tested with the same composition reported in the previous section (i.e. 70% glucose, 30% xylose). In the Figure 27 (left) the results of the hydrogenations are reported at different concentrations. Both sugars were converted at a high extent, also for the highest concentration. The selectivity to the sugar alcohols was almost complete, with sorbitol and xylitol being the main

products, but with the presence also of arabitol and traces of threitol (C4 sugar alcohol). The effective hydrogenation of sugars is a known process and its good performance is of paramount importance for the success of the process scheme, as the consumption of hydrogen in side-reactions must be minimized in this step.

After the hydrogenation, the solution was filtered to remove the catalyst and put in the APR reactor, with the catalyst used for the reforming (i.e. 5% Pt/C). The results obtained are reported in Figure 27 (right). The carbon to gas conversion and the hydrogen gas distribution reflected in a good way the results obtained with the sorbitol-xylitol mixture, indication of the effective hydrogenation. The important results come from the comparison between the hydrogen production in the two steps and the one pot process. In fact, while the former has an increasing trend, leading to about 32 mmoles of hydrogen (namely, the difference between the hydrogen produced in the APR step and the one consumed during the hydrogenation step), the latter has the trend reported in the section regarding the APR of the glucose-xylose mixture, with a negligible hydrogen production (about 1 mmole) due to the homogeneous phenomena previously reported. Godina et al. recently compared the APR performance between a sorbitol solution and a sorbitol/mannitol solution obtained by hydrogenation of sucrose [131]. They did not observe difference between the model and technical feeds, however the hydrogen production in the APR step was not enough to perform the hydrogenation of sucrose. The discrepancy with the present work can be due to the lower reaction temperature and higher feed concentration used by Godina, that lead to a lower hydrogen yield.

From these results it is highlighted that a process that aims to valorize sugars through APR, with the necessity to work in concentrated solutions to reduce the reactor size, should foresee a pre-hydrogenation step to “stabilize” the feedstock, producing the corresponding sugar alcohols, leading to satisfactory hydrogen production and, possibly, increasing the life of the catalyst (see paragraph 4.2.5).

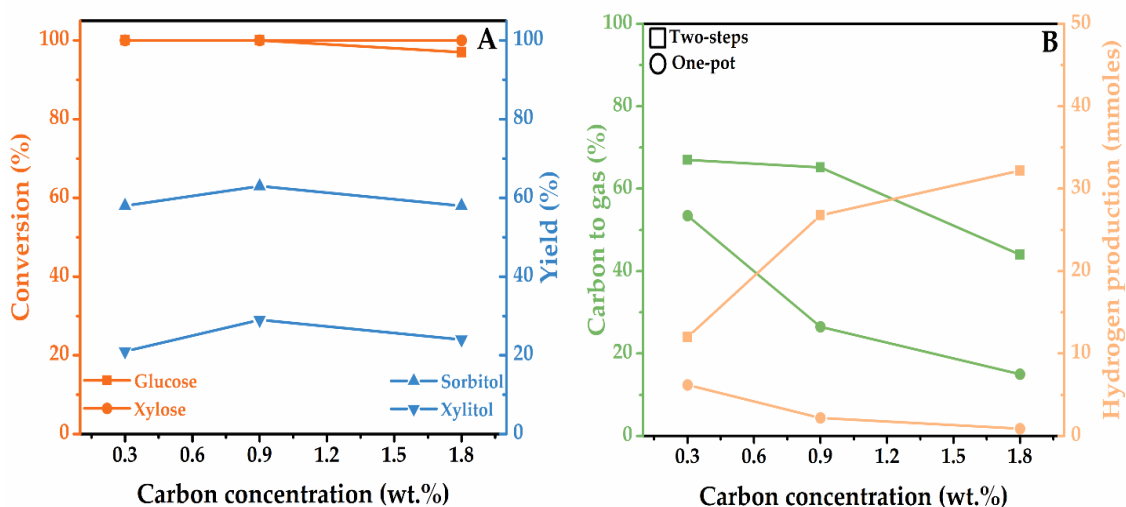


Figure 27. Influence of carbon concentration on the hydrogenation of a glucose-xylose mixture (A) and on the APR of the hydrogenated feed (B). Hydrogenation reaction conditions: 0.188 g Ru/C catalyst, 1 h reaction time, 180 °C, 15 bar H<sub>2</sub> pressure. APR reaction conditions: 0.375 g Pt/C catalyst, 2 h reaction time, 270 °C.

### Hydrolysate

After the study of the synthetic mixture, the hydrogenation of the hydrolysate was performed, and the results are reported in Figure 28.

It can be observed that the hydrogenation of the hydrolysate is much more difficult than the synthetic mixture. Maximum glucose conversion is 60% at 0.3%, and about 70% for the xylose, whereas it was complete with the hydrolysate-like. In addition, there is a strong dependence with the feed concentration, with a strong decrease of all the indicators working in more concentrated solutions. This important difference may be referred to the presence of oligomers in the solution. The valorization of polysaccharides passes through the formation of the monomer via hydrolysis, followed by the hydrogenation of the latter to the alcohol [132]. In our reaction conditions, using Ru/C as catalyst, there is a lack of acidic sites. Therefore, the carbon present in the oligosaccharides is not available for the production of the alcohols; at the same way, adsorbing on the catalyst, it may reduce the available sites for glucose and xylose and may participate to parasite hydrogenation reactions that consume hydrogen, but not leading to the final desired sugar alcohol.

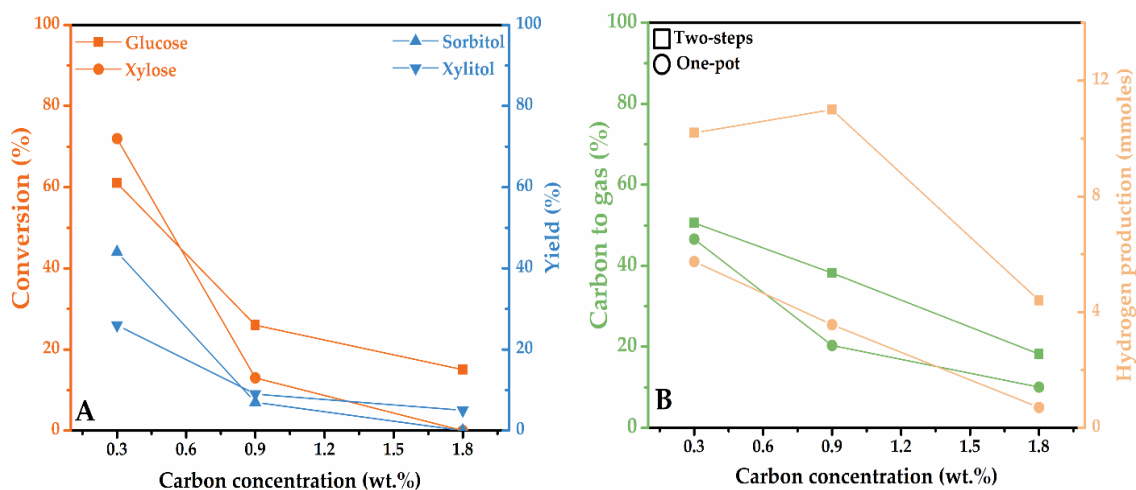


Figure 28. Influence of carbon concentration on the hydrogenation of the hydrolysate (A) and on the APR of the hydrogenated feed (B). Hydrogenation reaction conditions: 0.188 g Ru/C catalyst, 1 h reaction time, 180 °C, 15 bar H<sub>2</sub> pressure. APR reaction conditions: 0.375 g Pt/C catalyst, 2 h reaction time, 270 °C.

#### 4.2.5 Reuse of the catalyst

The stability of the catalytic system has a paramount importance in a process, therefore tests in which the catalyst was reused at different reaction temperatures were performed.

Blank experiments (not reported) in which only the spent catalyst was present in the system were performed as references, leading to negligible but still more than zero carbon containing gaseous species. This is an interesting result because it highlights the presence of organic deposits on the surface of the catalyst, that can further react, although with low activity.

In the Figure 29 the results for the hydrolysate-like mixture are reported. A decrease of the carbon conversion to gas was reported after the reuse of the catalyst at each temperature. It was observed that the lower the temperature, the higher the deactivation. This result is coherent with the observation that at lower temperature a higher amount of residue was produced, leading to a higher deactivation. At 270 °C, both the selectivity and the hydrogen yield are inferior to the results with the fresh catalyst; on the other hand, at lower temperatures, the hydrogen gas distribution and selectivity were higher than the fresh test (especially at 230 °C). During the reforming, a series-selectivity challenge involves the hydrogen, as it may be consumed by following reactions once it is formed. One possible reason for this result is that the presence of the organics, blocking the pores, reduced the activity (as fewer active sites were available), but on the other hand increased the selectivity, as most of the reaction did not involve the pores and hydrogen could escape more easily preventing consecutive hydrogenation.

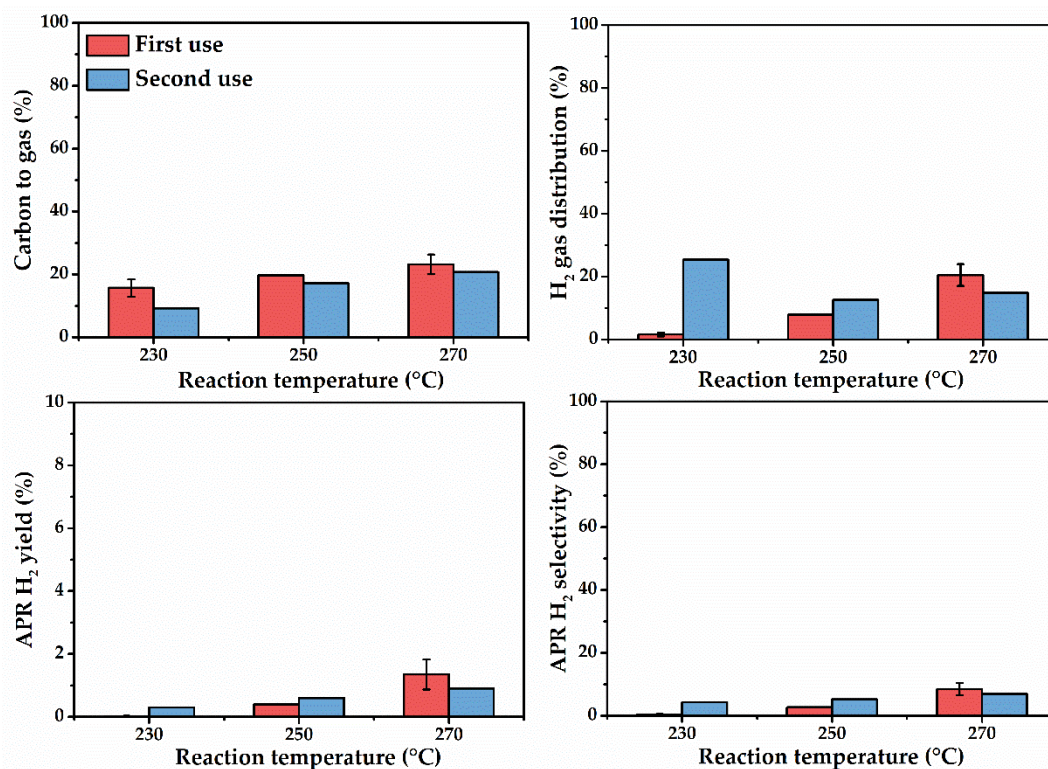


Figure 29. Influence of the reaction temperature on the reusability of the catalyst with a glucose-xylose mixture. APR reaction conditions: 270 °C, 2 h reaction time, 0.9 wt.% C.

Figure 30 shows the results obtained when hydrolysate was used as feedstock. The carbon conversion to gas almost halved at each temperature investigated. It indicates that the temperature had not an influence on the degree of deactivation when the hydrolysate was used. On the other hand, the hydrogen gas distribution was only slightly affected by the reuse. Therefore, it seems that the lack in stability of the catalyst led mainly to lower conversion of the feed, maybe because of less available sites on the surface of the catalyst.

The catalyst recovered after the reaction performed at 270 °C underwent to a washing treatment with ethanol and/or water (Figure 31). It was observed that the organic solution (named as E) allowed the solubilization of adsorbed compounds, leading eventually a dark brown ethanolic solution. However, when water was used for the washing (named as W) of the already washed catalyst with ethanol, it did not experience a change in colour: as a matter of fact, an HPLC analysis of the latter did not show the presence of any compounds. Subsequent catalyst washings with ethanol further enhanced the organic compounds extraction in the liquid phase (E2-5).

This outcome suggested the presence of hydrophobic compounds on the surface of the catalyst, that may cause the observed deactivation. It is likely that these compounds are humic acids (humins), that are water insoluble and derive from the polymerization and condensation of furfurals, phenols and acids during the reaction [133,134].



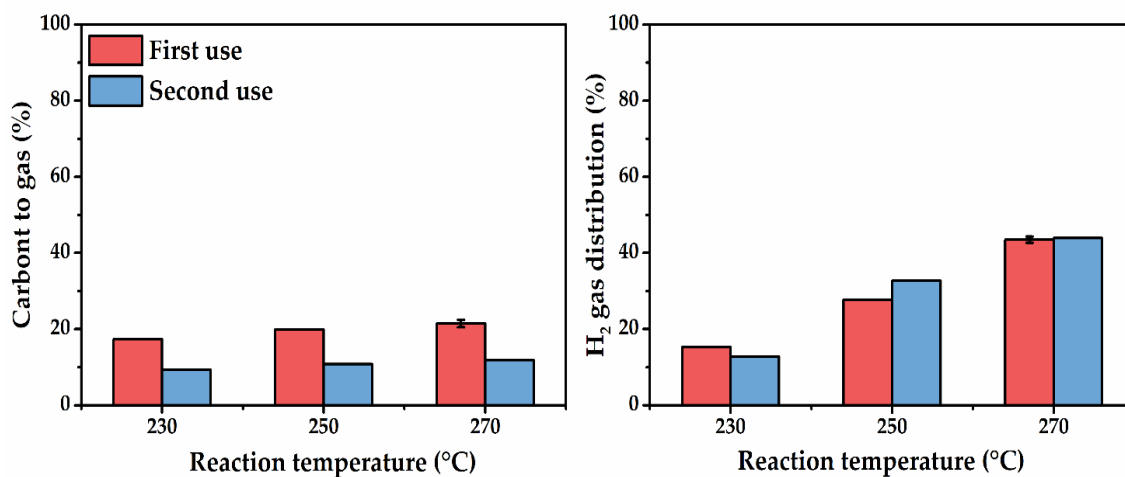


Figure 30. Influence of the reaction temperature on the reusability of the catalyst with the hydrolysate. APR reaction conditions: 270 °C, 2 h reaction time, 0.9 wt.% C.



Figure 31. Washing treatment of a spent catalyst after APR of hydrolysate 0.9 wt.% C at 270 °C.

Two tests performed with the treated catalysts after APR of glucose-xylose mixture and hydrolysate reported the same results of the un-treated ones (Figure 32). It is possible that the washing step removed only the organics on the external surface of the catalyst, not affecting the pores, therefore without changing the global performance.

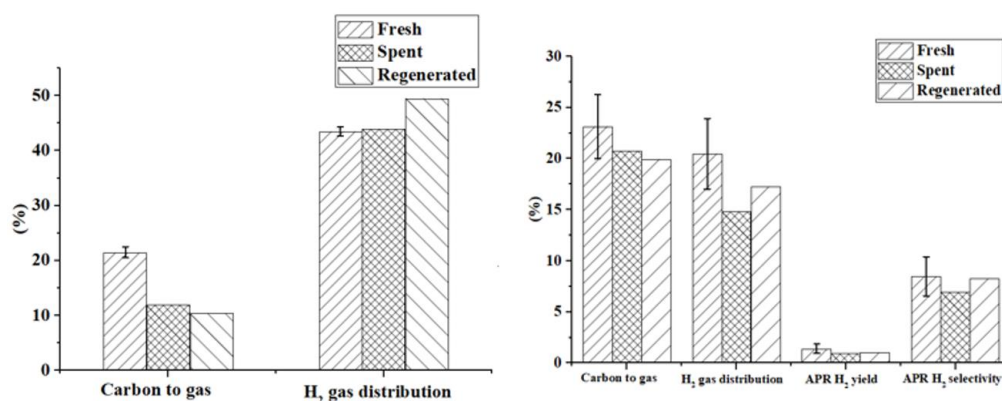


Figure 32. APR performance of hydrolysate (left) and glucose-xylose mixture (right) with fresh catalyst, spent catalyst and regenerated (after ethanol washing) catalyst. APR reaction conditions: 0.9 wt.% C, 270 °C reaction temperature, 2h reaction time.

### *Catalyst characterization*

Although it is widely accepted that sugar solutions may be unstable in the APR reaction conditions, due to the formation of a solid residue, few works looked at the effects on the catalyst [135].

N<sub>2</sub> physisorption isotherms have been performed on the fresh and spent catalysts to evaluate the influence of the feedstock on the textural modifications (Table 10). It is observed that after the first use there is a dramatic decrease of the surface area and pore volume, likely due to the fouling caused by the humins. The re-use of the catalyst led finally to the complete loss of the original textural characteristics of the catalyst, having less than 1 m<sup>2</sup>/g as surface area and negligible pore volume. On the other hand, when the sugar mixture was hydrogenated to sorbitol and xylitol, the decrease of the surface area is much less evident (about 15%), together with the pore characteristics (both volume and average size).

Analogous results were obtained with the hydrolysate. Indeed, there was a decrease of 90% of the surface area with the untreated feedstock, while it was 70% in the case of the hydrogenated one, a result that must be improved in view of a practical application. It is evident that the conversion to the sugar alcohols allows to maintain in a greater extent the stability of the catalyst, as they do not lead to the deposition phenomena. This is due to the avoidance of dehydration reactions, involving the formation furfural and hydroxy-methyl furfural starting from glucose and xylose, which are catalysed by an acid environment. For this reason, the pH of the solution or of the catalytic surface may play a key role in the selectivity towards solid by-products.

Finally, it can be observed that the concentration of the feed plays a key role in the stability of the catalyst. Indeed, reducing the carbon concentration to 0.6 wt.% allowed to maintain a higher surface area and pore volume, one order of magnitude higher than in case of 0.9 wt.%.

Table 10. Textural characteristic of the fresh and spent catalysts. All tested mixtures were at an overall 0.9wt.% of carbon, except for the last line that was at 0.6 wt.%. Reaction conditions: 270 °C, 2 h reaction time.

Sample	BET surface area (m <sup>2</sup> /g)	Pore Volume (cm <sup>3</sup> /g)	Average pore size (nm)
Fresh	923	0.632	5.1
Glucose-Xylose	35	0.121	10.1
Glucose-Xylose II use	0.9	0.002	10.4
Glucose-Xylose hydrogenated	772	0.606	5.1
Glucose-Xylose hydrogenated II use	750	0.583	5.1
Hydrolysate	76	0.208	7.8
Hydrolysate hydrogenated	247	0.411	5.5
Glucose-Xylose 0.6 wt.% C	567	0.538	5.2

FESEM images of the fresh and spent catalysts used for the hydrolysate APR are reported in Figure 33. It was observed that the fresh catalyst (A) showed the typical morphology of an activated carbon, with microporosity on the surface. When the catalyst was used (B), the surface seemed much flatter and less porous, as if the solid deposits cover homogeneously the catalyst, blocking the pores and strongly reducing the performance of the reaction. The catalyst used with the hydrogenated feed (C) apparently showed an intermediate morphology. Despite there was not an equal distribution of micropores as evident in the fresh one, it maintained a partial porosity, as it was confirmed in the N<sub>2</sub> physisorption analysis.

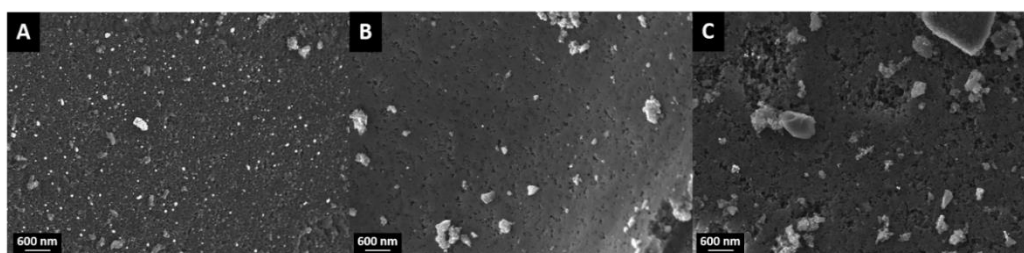


Figure 33. FESEM images of the fresh catalyst (A) and spent catalyst after the aqueous phase reforming of hydrolysate solution (B) and hydrogenated hydrolysate solution (C). APR reaction conditions: 270 °C, reaction time 2 h, 0.9 wt. % C.

Spectroscopic analysis (ATR) was used to derive information on the nature of the organic deposits, while the TGA was functional to the determination of the deposit fraction that decomposes under inert conditions. It is worth highlighting that the amount of decomposed deposit in the TGA is always lower than the one obtained from the weighting procedure of the spent catalyst.

The ATR analyses on the fresh catalyst showed a band at around 1550 cm<sup>-1</sup> and 3450 cm<sup>-1</sup> likely associated to the presence of absorbed water on the surface (Figure 34). No other major bands are observed for the fresh catalyst.

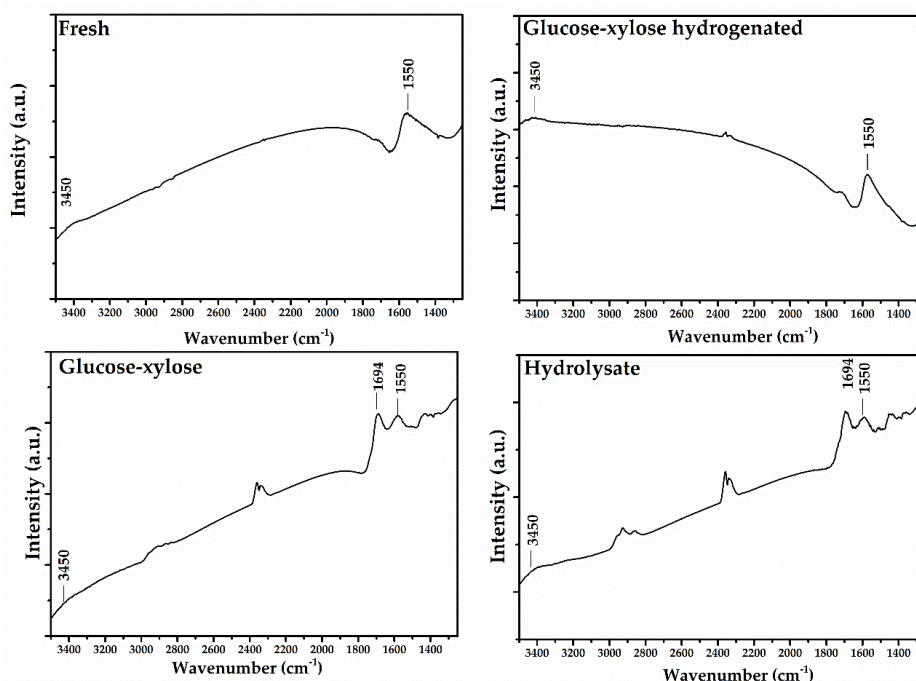


Figure 34. ATR-IR spectra of fresh catalyst and spent catalyst after the aqueous phase reforming of a glucose-xylose hydrogenated solution, a glucose-xylose solution and a hydrolysate. APR reaction conditions: 270 °C, reaction time 2 h, 1.8 wt. % C.

The ATR analyses of the other catalyst samples are strictly depended from the substrate used in the APR reaction: hereafter, the results on spent catalysts from the aqueous phase reforming of a glucose-xylose hydrogenated solution, a glucose-xylose solution and the hydrolysate are presented.

The catalyst used with the glucose-xylose hydrogenated mixture showed a spectrum similar to the one of the fresh catalyst, indicating the absence (or small) amount of organic deposits. On the other hand, when sugar (glucose-xylose or the hydrolysate) solutions were used as substrate, an intense band with maximum at 1694  $\text{cm}^{-1}$  appeared, together with the appearance of a shoulder at 1730  $\text{cm}^{-1}$ . 1694  $\text{cm}^{-1}$  can be attributed to species originated from the decomposition of glucose at high temperature in water, with the formation of insoluble compounds such as humins [136]. Indeed, this band is related to the carbonyl group stretches derived from adsorbed acids, ketones and aldehydes, that were not observed in the liquid phase obtained from glucose-xylose hydrogenated APR [133].

At the same time the presence of organic fragments is confirmed from the absorption between 3000 and 2800  $\text{cm}^{-1}$  with the symmetric and asymmetric stretching of  $-\text{CH}_2-$  and  $\text{CH}_3$  groups. Please note that the absorption at around 2300  $\text{cm}^{-1}$  is referred to a noise due to a not perfect compensation of atmospheric  $\text{CO}_2$ .

Thermogravimetric analyses of the catalysts led to conclusions coherent with the previous ones from ATR (Figure 35). The fresh catalyst showed a total weight loss of about 15 wt.%, concentrated in three different steps: the first one with a maximum at 80 °C associated to a loss of adsorbed water; the second step, between 200 °C and 600 °C, can originate from the initial decomposition of the carbon support of the catalyst, which is composed from a certain percentage of

oxygen, with the formation of carbon dioxide; the third step is a further decomposition of the carbon support, with the formation of carbon monoxide. This hypothesis is confirmed from the infrared analysis (Figure 36) of the developed gasses: the curve shows a maximum for water absorption around 100°C, a maximum at 600°C for CO<sub>2</sub> adsorption and an increase in CO concentration over the 600°C.

The catalyst used for APR of hydrogenated glucose-xylose showed comparable results with the fresh catalyst, with a total loss of about 19 wt.%, slightly higher than the pristine catalyst. The degradation was similar except for the initial water loss, probably for the process of drying of the used catalyst and the presence of a small quantity of carbonyl functionalities at low temperature (around 200-300 °C) derived from the low amount of organics still present. The carbon dioxide curve was instead almost equivalent to the one obtained for the fresh catalyst.

All the other spent catalysts had a higher weight loss, around 40 wt. % (Figure 35). This means that, after normalization, the amount of deposits generated in the glucose-xylose APR was more than seven times higher than the one from the hydrogenated glucose-xylose APR, clearly explaining why the catalyst in the latter conditions was much more stable than in the former ones.

A similar weight loss and degradation in three main steps was noticed: the first one with a maximum below 100 °C and where only water was produced; the second step had usually a maximum around 300 °C and aliphatic substances with carbonyl groups were mainly produced. At higher temperature, the aliphatic compounds slowly decreased with an increase of CO<sub>2</sub>, water and methane production, all of them being typical products of organic compounds pyrolysis. Therefore, the TGA with infrared analyses of the produced gases confirmed the presence of organic material that is formed only in the presence of sugars, and at a much lower extent with sugar alcohols (Figure 36).

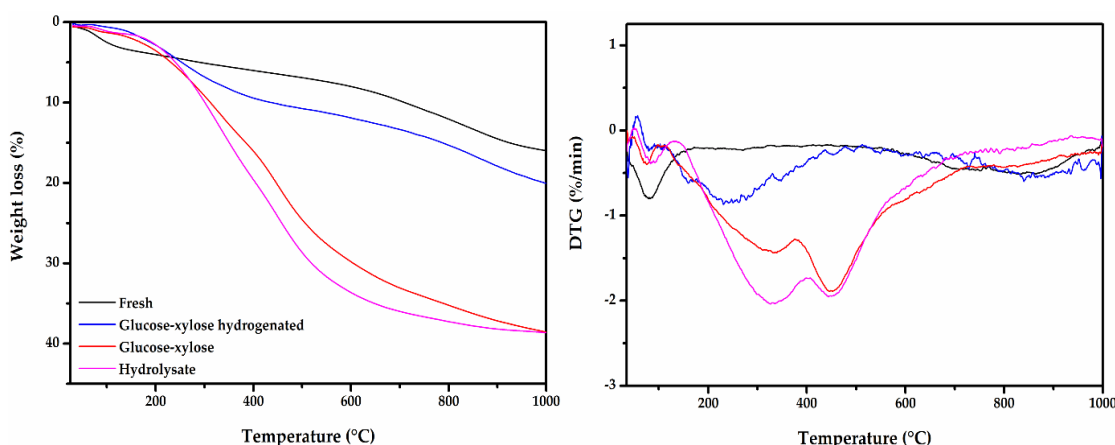


Figure 35. Thermogravimetric analysis of fresh catalyst (black line) and spent catalyst after the aqueous phase reforming of a glucose-xylose hydrogenated solution (blue line), a glucose-xylose solution (red line) and a hydrolysate (purple line). APR reaction conditions: 270 °C, reaction time 2 h, 1.8 wt. % C. TGA temperature program: heat from 30 °C to 1000 °C @ 20 °C/min in nitrogen atmosphere with a purge rate of 20 mL/min.

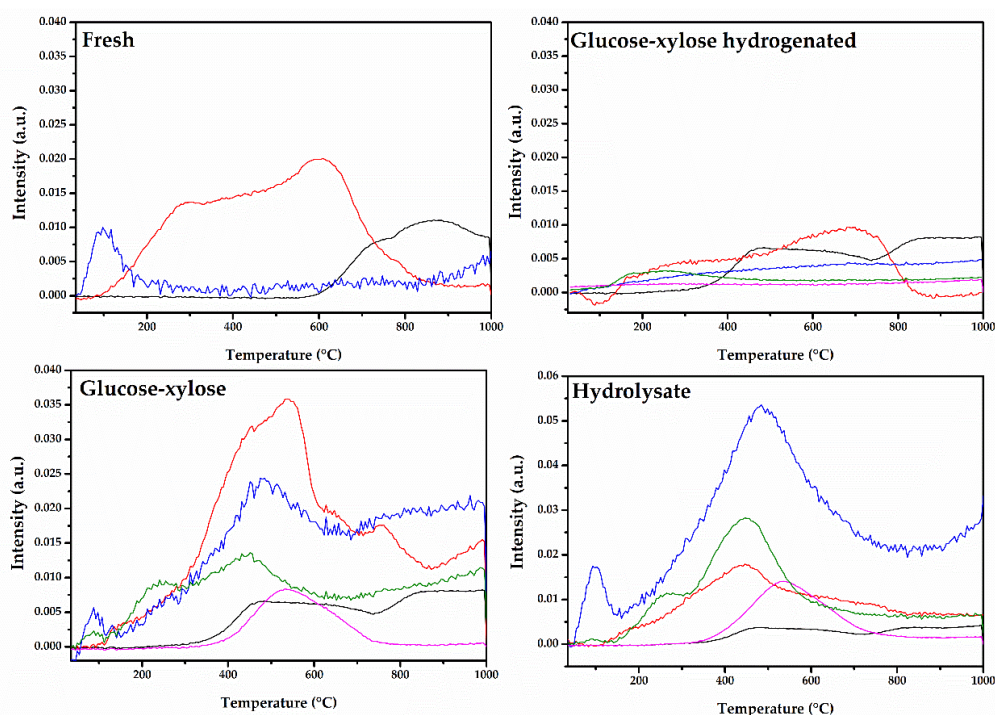


Figure 36. IR analysis of evolving gas from fresh and spent catalysts reported in Figure 13; water (blue line), carbon dioxide (red line), carbon monoxide (black line), methane (purple line), carboxylic groups (green line).

### 4.3 Conclusions

A stream coming from the hydrolysis treatment of a bioethanol plant and its representative model compounds were subjected to APR to produce hydrogen. For the first time, in this work, we tested xylose as strategic compound for the valorization of the hemicellulose fraction in lignocellulosic biomass. The influence of the reaction temperature and carbon concentration were systematically investigated to evaluate their impact on the APR performance, mainly in terms of carbon conversion to gas and hydrogen yield. The increase of the reaction temperature favoured the hydrogen production of each compound, leading also to less solid residue formation by the sugars. The same results were obtained with the binary mixtures investigated, showing a behaviour strictly close to the linear combination of the constituents. On the other hand, the increase of the carbon concentration had a detrimental effect towards hydrogen production from both glucose and xylose, while it was not observed with sorbitol and xylitol. For this reason, a pre-hydrogenation step carried out on the sugar mixture showed a higher hydrogen production, even taking into consideration the amount consumed for the hydrogenation. Although this step was performed also on the hydrolysate, it showed worse performance than the synthetic mixture, maybe due to the presence of oligomers. The catalyst used for hydrolysate APR underwent deactivation phenomena, that caused mainly the decrease of the carbon

conversion to gas, while maintaining almost the same selectivity. The catalyst characterization showed the presence of organic deposits (humins) that blocked the pores of the catalyst in the case of the sugar-rich feeds, while the hydrogenated mixture allowed a longer life of the catalyst. Further studies in the optimization of the reaction configuration hydrogenation-APR, or in the reaction conditions (i.e. pH modification) may allow to make a step forward in the exploitation of the pentoses, at the same time helping to satisfy the need of renewable hydrogen of a biorefinery.

# Chapter 5 Hydrothermal liquefaction-derived aqueous streams

## 5.1 Introduction

The hydrothermal processing of biomass has gained interest in the last decades mainly with the aim of producing alternative fuels [1]. Water near critical or at supercritical conditions becomes a peculiar reaction medium thanks to the drastic change of its physical-chemical characteristics. For example, at subcritical conditions the pH-value strongly decreases, enabling to carry out acid-catalyzed reactions without the use of a dedicated catalyst; moreover, water polarity changes thanks to the diminishing dielectric constant, being able to dissolve non-polar substances [138]. Apart from the actual properties of water, the exploitation of a hydrothermal process allows the use of biomass with high moisture content, without the need for a drying step that would limit the overall process economy [139].

Depending on the temperature of the process, three main hydrothermal processes can be classified: hydrothermal carbonization (below 520 K), hydrothermal liquefaction (between 520 and 647 K, the latter being the critical temperature of water) and hydrothermal gasification (above 647 K) [140].

Focusing on the liquefaction, it has been investigated mainly with the goal of producing an organic product, often related as biocrude, with a relatively high heating value [141,142]. Its high oxygen content compared with the commercial fuels though, arises the necessity of an upgrading step.

Nevertheless, in order to make the whole process economically sustainable, the other products should be exploited and valorized as well. To confirm this point, it was estimated that the disposal of the aqueous waste is second only to the feedstock costs [32].

Despite of the strategic importance of this issue, there are just few examples in literature where attention is put on the aqueous phase obtained after a hydrothermal process [143]. The major efforts have been carried out at the PNNL (Pacific Northwest National Laboratory) in the USA, where the aqueous samples obtained from many different feedstocks (lignocellulosic, algae, municipal wastes) were characterized [144–146].

Panisko et al. analysed the hydrothermal liquefaction of pine forestry residuals or corn stover and from the hydrotreatment of fast pyrolysis bio-oils [144]. The experiments showed that the aqueous phase coming from the latter process contained negligible amounts of organic carbon; on the other hand, the



samples coming from the former contained about 2 wt.% of organic carbon. It was mainly constituted by organic acids, such as glycolic acid (i.e. a hydroxyacid) and acetic acid. Moreover, alcohols (methanol and ethanol) were present, together with numerous ketones (acetone and cyclopenta-ones). The same research group performed a quantitative characterization of the aqueous fraction from the HTL of four fresh water and four seawater algae, identifying also nitrogenous compounds, in addition to the compound found from the lignocellulosic feedstocks [145].

A recent work started from municipal and food industry wastes, and it was highlighted the influence of the chosen feedstock on the classes of compounds that can be found, after the hydrothermal treatment, in the aqueous phase [146].

Many organic species present in the aqueous by-products are high valuable, so it may be interesting their selective recovery. However, they are present in low concentrations, therefore the stream should be subjected to a drying step that would be not economically feasible in an industrial scale. For this reason, it seems reasonable to consider a process that valorizes the entire family of substances present in the stream.

Anaerobic digestion and catalytic hydrothermal gasification (CHG) have been suggested as possible processes for the valorization of the aqueous stream [147]. Elliott et al. carried out the CHG of the HTL aqueous by-product, producing a high methane content gas [148].

In this chapter, we want to investigate the possibility to exploit the aqueous phase reforming (APR) conditions for producing a high-value gas in terms of hydrogen concentration.

Several model compounds belonging to the different classes found in the aqueous phase of lignocellulosic feed were screened. Main attention was put on the composition of the gas phase, looking at the tendency of each compound to be reformed at different reaction temperatures; however, a big effort was put also to investigate the composition of the liquid phase after the reaction, searching for key intermediates or final by-products in the reaction mechanism that could be defined as “bottleneck-species” for the production of hydrogen. To the best of our knowledge, this is the first work in which the current set of compounds, belonging to various classes and being representative of the aqueous phase post-HTL, was investigated in one experimental system, including gas and the liquid phase characterization. Attention was put also on the characterization of the alumina-supported platinum catalyst recovered after the reaction. Furthermore, mixtures of two and three compounds were tested to analyse possible synergic or inhibiting effects, making a step forward in the direction of the investigation of a real biorefinery stream.

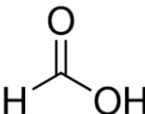
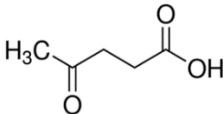
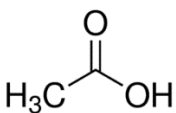
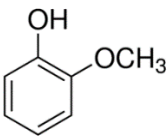
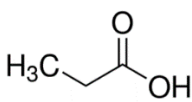
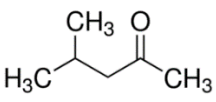
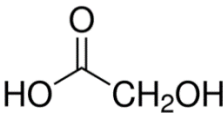
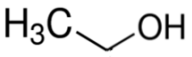
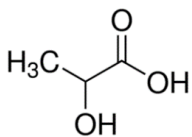
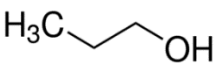
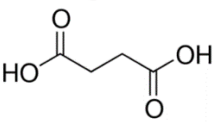
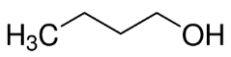
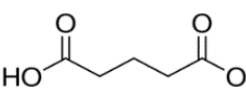
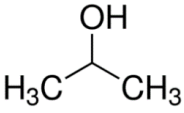
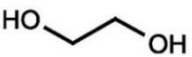
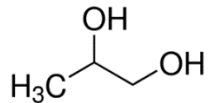
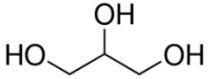
This chapter (results, figures and tables) is based on the published work reported in [128].

## 5.2 Results and discussion

### 5.2.1 Influence of the reaction temperature

The APR of seventeen characteristic compounds was performed at three different temperatures: 230, 250 and 270 °C. These species were chosen accordingly to the work of Panisko et al., selecting the most representatives in terms of abundance in the aqueous solution post-HTL, for our scope [144]. The list of the molecules is reported in the Table 11. As it can be observed, at least one compound from the main classes possibly found in the aqueous stream was investigated. It is noteworthy that some of them (e.g. glycolic acid, 4-methyl-2-pentanone, guaiacol) were subjected to APR for the first time. As reported in the experimental section, the solutions were prepared without modifying the pH, leading to an autogenous starting pH different from one compound to another according to the relevant pKa. In literature the influence of pH is reported [39], and basic values of pH are beneficial towards hydrogen production. As a consequence, the starting pH of the solution may affect the comparison of the screening compounds. Nevertheless, as highlighted, aim of the present work is performing an evaluation of the reactivity and tendency to give hydrogen by compounds present in aqueous side-streams; in order to be as close as possible to the real application, it was decided not to modify the pH in the reactive solution.

Table 11. List of investigated model compounds.

Carboxylic acids		Ketoacids, aromatics, ketones	
Formic acid		Levulinic acid	
Acetic acid		Guaiacol	
Propionic acid		4 methyl 2 pentanone	
Hydroxyacids and dicarboxylic acids		Alcohols	
Glycolic acid		Ethanol	
Lactic acid		1-propanol	
Succinic acid		Butanol	
Glutaric acid		2-propanol	
Polyalcohols			
Ethylene glycol		Propylene glycol	
	Glycerol		

### Carboxylic acids

The carboxylic acids were the first compounds to be investigated. As reported from Panisko, they are the second most abundant class in the aqueous phase post-HTL [144]. Moreover, they can be considered representative also in other contexts, like bio-oil pyrolysis: therefore, their study may be interesting not only to our purposes. The results regarding the gas phase are reported in the following Figure 37-A. First of all, it was observed that formic acid differs from the other

acids. There was almost no influence of the temperature on all the parameters, and they were globally higher than the other carboxylic acids. Also, the gas composition remained unchanged at every temperature investigated. A not catalyzed test showed almost the same result, with 70% of carbon to gas, 69% hydrogen yield and 99.8% as hydrogen gas distribution. These observations supported the idea that a thermic decomposition is responsible for these results and not an actual reforming process. This outcome is coherent with the work of Yasaka et al. [149]. CO is present in relatively high amount (12000 ppm at 270 °C) compared to the other tested molecules (maximum 1000 ppm at 270 °C) and it may be due to the high production of carbon monoxide by decarbonylation, so that the catalyst is not able to convert it completely by water gas shift. In the liquid phase, the total conversion of the molecule was observed.

Acetic acid and propionic acid showed different behaviour compared to formic acid. They exhibited an increase of the carbon conversion to gas, together with the hydrogen yield, with a drastic rise at 270 °C. Anyway, despite of the moderate carbon conversion to gas, the hydrogen yield was particularly low. Carboxylic acids have been rarely investigated in the aqueous phase reforming process, but as it was observed, they are important by-products in post-HTL aqueous stream. Some research have been focused more in the steam reforming of acetic acid, where the reaction mechanism has been studied on platinum-based catalysts [150]. The difficulty for reforming may be due to the presence of a methyl group that is not activated by a hydroxyl one, as suggested from the original work of Dumesic that hypothesized the first reaction mechanism for APR [37]. Looking at the gas composition, it is observed an almost 1:1 ratio between carbon dioxide and methane for acetic acid; at the same way, for the propionic acid, the ethane is the most abundant gaseous alkane (Figure 38). This means that the C-C bond with the carboxylic group was preferably broken. In this case it is not possible to think that a thermal phenomenon is ongoing: in fact, a not catalytic test with acetic acid a 270 °C showed 1% of carbon conversion to gas and 97% of hydrogen gas distribution.

In the liquid phase, the conversion of acetic acid was 22% at 230 °C and it increased up to 56% at 270 °C, being almost the only compound (Figure 37-B). This observation let us think a possible reaction mechanism based on the observation of Matas Güell et al. on the steam reforming of acetic acid at 320 °C on Pt/C [150]. At first, acetic acid adsorbed on the Pt sites, with CO<sub>2</sub> that is primarily set free; then the recombination of CH<sub>3ads</sub> and H<sub>ads</sub> may be the main pathway, with the formation of CO<sub>2</sub> and CH<sub>4</sub> in equimolar amount. Looking at the run at 270 °C, it was observed that, compared to this ideal mechanism, 88% of methane and 84% of carbon dioxide is obtained, supporting the idea that this path may be the main reaction route for acetic acid in these reaction conditions. The small presence of hydrogen may be due to the minor path of recombination of the H<sub>ads</sub> (Figure 37-A), but this would be not sufficient to explain still great part of the hydrogen present. This means that other mechanisms, such as dehydrogenation of the feed, may be present, even if less important than the main route leading to methane and carbon dioxide. The same behaviour may be reported for propionic

acid, where the ethyl group may be recombined with the atomic adsorbed hydrogen, giving ethane (Figure 37-B). In this case, other paths may be expected because the ratio is not exactly as hypothesized looking at the previous mechanism.

Propionic acid conversion goes from 7% at 230 °C to 39% at 270 °C. In line with the previous case, the feed was the main liquid compound, representing 93% of the carbon remained in the liquid phase; acetic acid was the second most important liquid compound, and its importance increased with the reaction temperature, from 1% to 7% of the carbon in the liquid phase. Its concentration may be the result of two competitive phenomena: its production because of the higher conversion of propionic acid and its consumption, because of the higher reactivity of acetic acid itself at higher temperature, as reported previously. In fact, despite of the constant concentration of methane, its amount increased consistently, more than six times from 230 to 270 °C, perhaps reflecting the increase of acetic acid in the liquid phase.

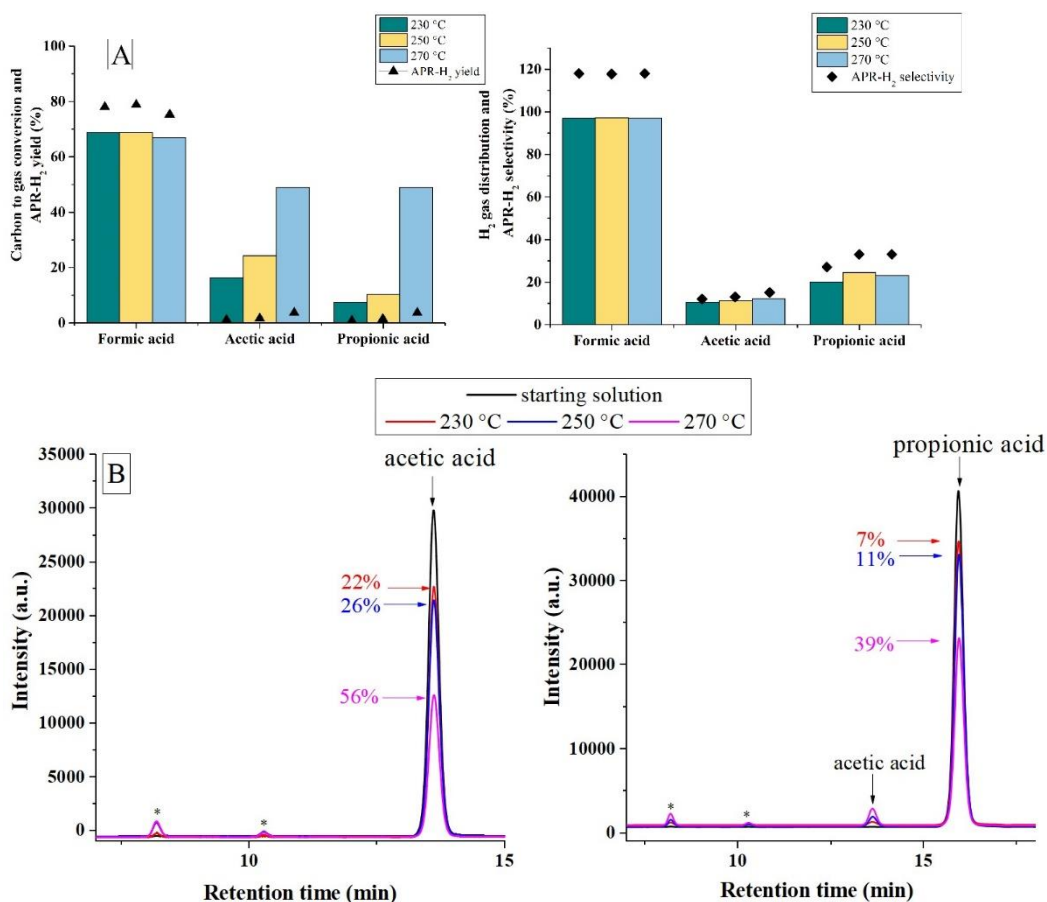


Figure 37. Influence of the reaction temperature on the APR of carboxylic acids (A) and composition of the liquid phase of acetic acid (B-left) and propionic acid (B-right); the numbers in the figure close to the reagent peak refers to the conversion; \*: unknown. Reaction conditions: 0.133 M feed, 0.375 g 5% Pt/Al<sub>2</sub>O<sub>3</sub>, reaction time 2 h.

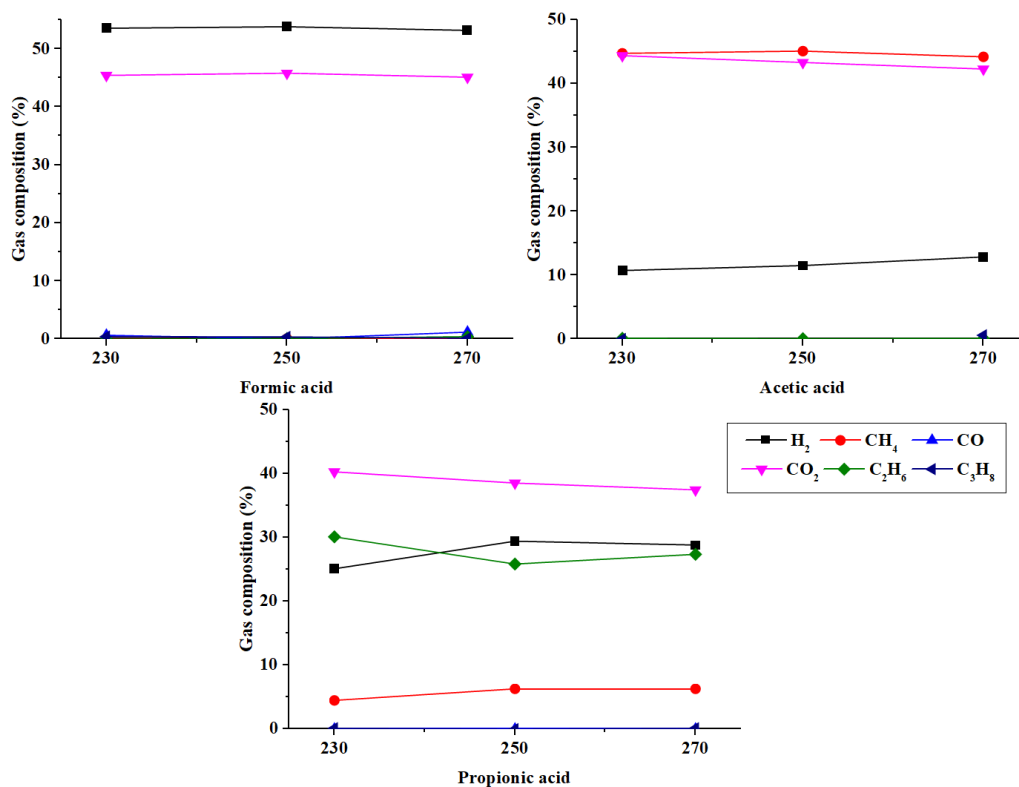


Figure 38. Influence of the reaction temperature on the composition of the gas phase from APR of carboxylic acids. Reaction conditions: 0.133 M feed, 0.375 g 5% Pt/Al<sub>2</sub>O<sub>3</sub>, reaction time 2 h.

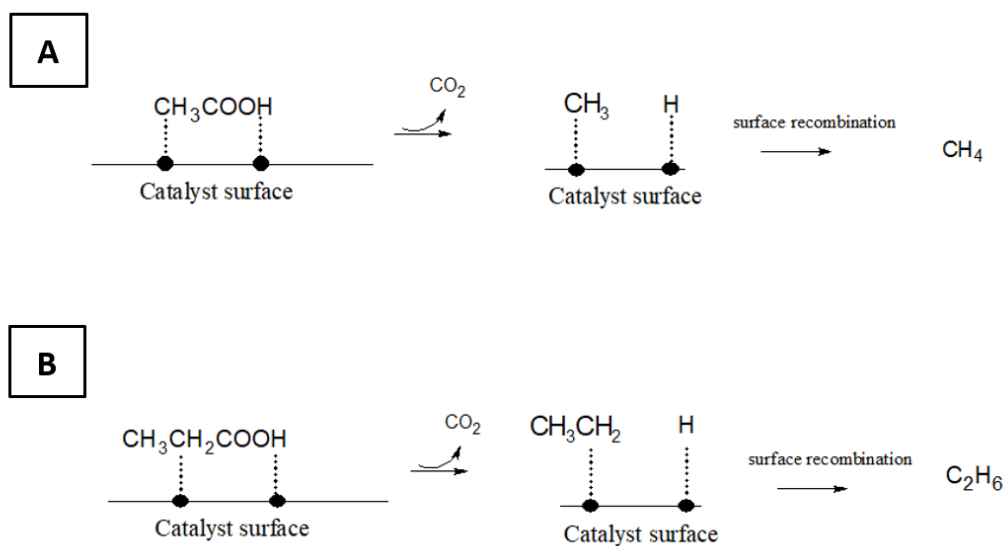


Figure 39. Hypothetic mechanism for the reforming of acetic acid (A) as suggested from [150] and propionic acid as proposed in this work (B).

### *Hydroxyacids and dicarboxylic acids*

In Figure 40 the results for two hydroxyacids (glycolic and lactic acid) and two dicarboxylic acids (succinic and glutaric acid) were reported. These

compounds are particularly interesting because, as reported by Panisko et al., the post-HTL aqueous phase, at least in the conditions cited in their work, contained glycolic acid as main product [144]. Therefore, it was worthy in our opinion starting the investigation on this compound and, to the best of our knowledge, this work was the first to perform this study.

Glycolic acid reported about 70% of carbon conversion to gas at 270 °C, with about 74% of hydrogen yield. Looking at Figure 41-A it can be observed that no alkanes were produced, and the gas is composed just by hydrogen (60%) and carbon dioxide (40%). Please note that the fact that APR H<sub>2</sub> selectivity exceeds 100% is an indication that not just the APR is in progress, therefore the relative contribution of H<sub>2</sub> and CO<sub>2</sub> lead to this apparently atypical result. Working with an integral reactor, it is not straightforward to study the reaction mechanism, but some analogies starting from the behaviour of acetic acid can be highlighted. Indeed, glycolic acid contains a carboxylic group, as acetic acid, so it may be inferred that the first step involves a decarboxylation. After that, the two radicals present on the surface may recombine leading to the production of methanol, not found in the liquid phase. However, this would not be surprising, as it is known that methanol can be easily reformed following the path suggested by Dumesic's research (Figure 42-A) [39]. The proposed mechanism would explain also the 3:2 ratio hydrogen:carbon dioxide present in the gas phase.

In the liquid phase glycolic acid was completely converted at each investigated temperature, but as it is reported, not all the carbon is in the gas phase (Figure 41-B). Indeed, 90% of the carbon in the liquid phase was present as acetic acid. This may be due to the hydrogenation of the hydroxyl group, so it may arise a problem of series-selectivity: part of the produced hydrogen is consumed in hydrogenation reactions. It is fundamental to control and minimize this phenomenon: as it is observed, it may have consequences on the performance of the process, as 30% of the starting carbon remained in the liquid phase as acetic acid, that we reported before as a recalcitrant molecule. Despite of these observations, the obtained results with glycolic acid are encouraging for the idea of exploiting APR for the valorization of these streams.

Lactic acid carbon conversion to gas was strongly less than the glycolic acid. Despite of the small values, it is highlighted the strong dependence of the hydrogen yield from the temperature, which increased about one order of magnitude, ranging from 0.3 to 2.9% at 270 °C. Together with this increase, there is a decrease of the percentage of carbon dioxide and methane, with a global increase of the hydrogen selectivity.

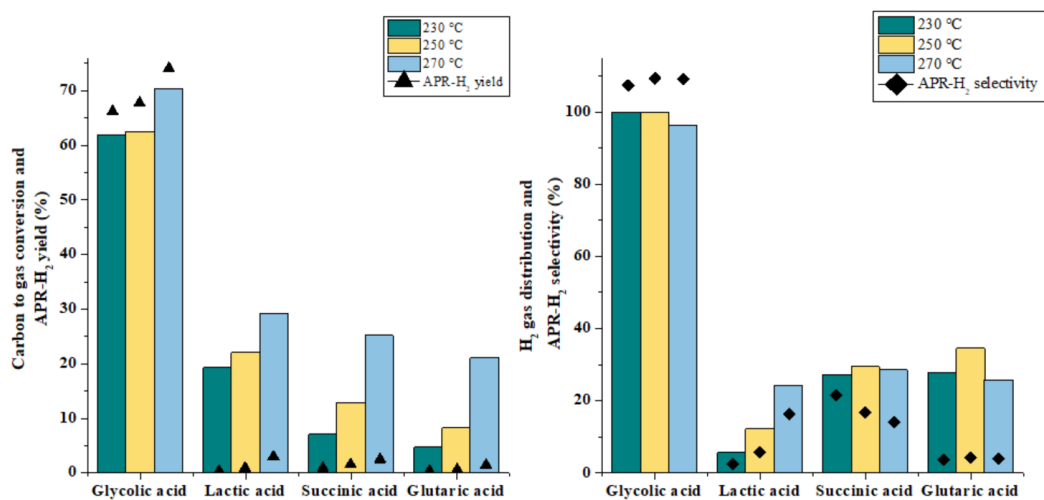
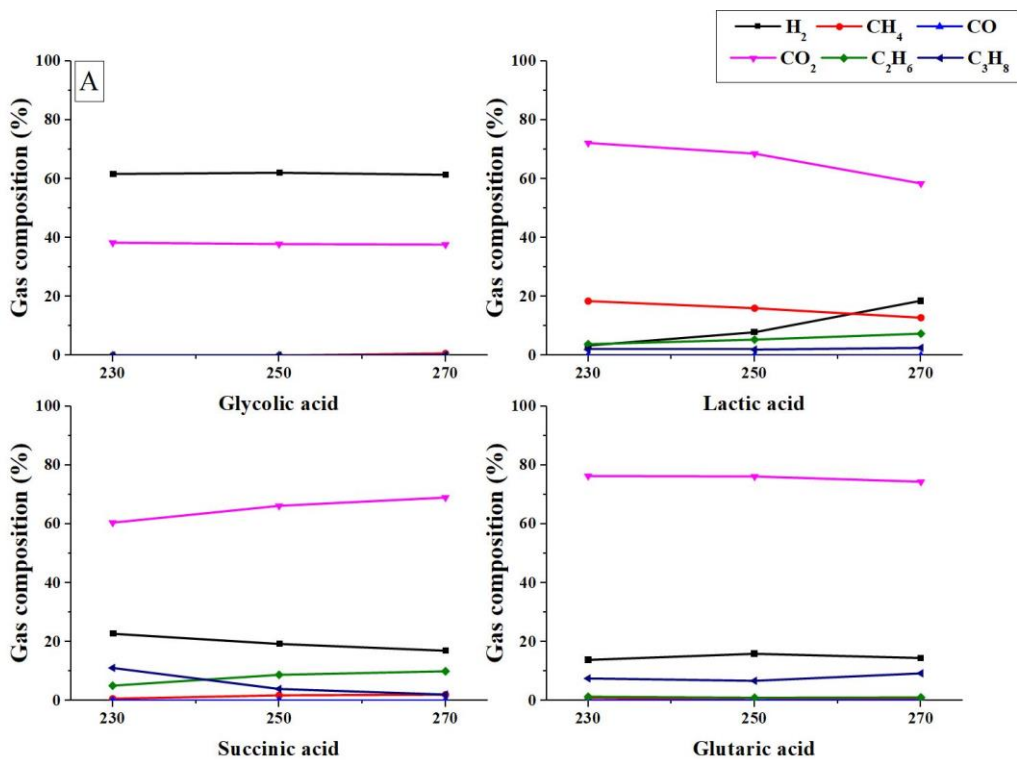


Figure 40. Influence of the reaction temperature on APR of hydroxyacids and bicarboxylic acids. Reaction conditions: 0.133 M feed, 0.375 g 5% Pt/Al<sub>2</sub>O<sub>3</sub>, reaction time 2 h.





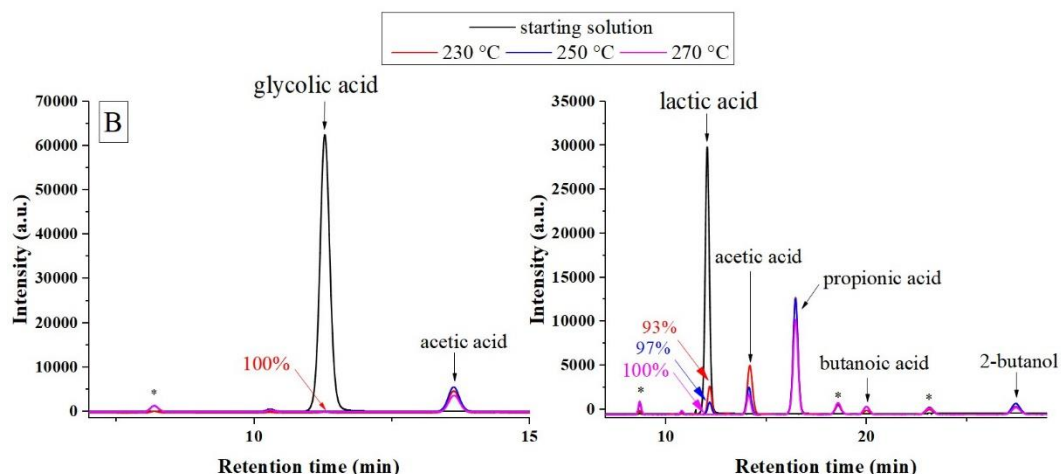


Figure 41. Influence of the reaction temperature on the composition of the gas phase from APR of hydroxyacids and bicarboxylic acids (1) and on the composition of the liquid phase from APR of glycolic acid (B-left) and lactic acid (B-right); the numbers in the figure close to the reagent peaks refer to the conversion; \*: unknown. Reaction conditions: 0.133 M feed, 0.375 g 5% Pt/Al<sub>2</sub>O<sub>3</sub>, reaction time 2 h.

Possible reaction schemes for lactic acid can be inferred in analogy with the glycolic acid and carboxylic acid mechanisms (Figure 42-B). If decarboxylation was the first step, then ethanol may be produced that, in turn, would lead to the production of hydrogen, carbon dioxide and methane (as reported in the following paragraph). Propionic acid was the most abundant product in the liquid phase (70% of the carbon at 270 °C): therefore, it is reasonable to assume that a fraction of the lactic acid may be converted to propionic acid through two possible reaction paths. One would involve the C-O hydrogenolysis on the Pt site; the other would involve also the nature of the support, that may cause dehydration followed by hydrogenation on the Pt site [151]. In addition, thermodynamic consideration reports that hydrogenation of lactic acid to propionic acid is nine order of magnitude more favourable compared to the production of propylene glycol near the present reaction conditions: in fact, the latter compound was not observed in the liquid phase [152]. Either of the two would anyway require a molecule of hydrogen, and for this reason the path has been lumped in the step 2. In turn, propionic acid can lead to ethane and carbon dioxide as reported in the previous paragraph, explaining also the presence of the C<sub>2</sub> alkane in the gas phase.

Acetic acid accounts for 10% of the carbon in the liquid phase, and a small but still 5% is butanoic acid, indication that condensation reactions are involved.

Succinic and glutaric acid, bicarboxylic acids with four and five carbon atoms respectively, showed low performance toward APR, with a maximum H<sub>2</sub> yield of 2.5 and 1.4% respectively. The reason may be the stability that the acids show even at these temperatures.

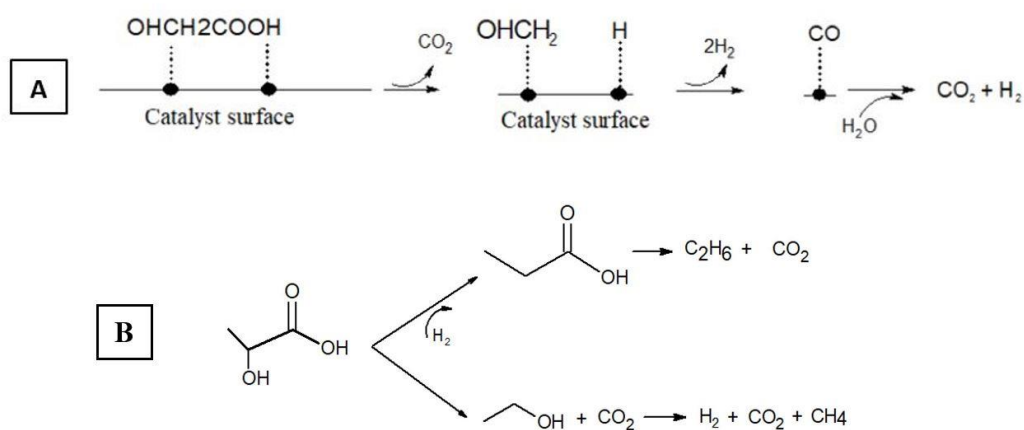


Figure 42. Suggested reaction mechanism for the APR of glycolic acid (A) and lactic acid (B).

Succinic acid converted from 26% at 230 °C to 78% at 270 °C. The increase in the temperature affected in this case also the APR selectivity, that decreased because of the increase in the carbon dioxide production compared to hydrogen. CO<sub>2</sub> is the main gaseous product, and the reason may be the path of decarboxylation in which the succinic acid is involved. Indeed, in the liquid phase propionic acid is the main product, accounting for 65% of the carbon. A confirmation of this hypothesis is that ethane is the most present alkane at 270 °C: so, it seems that the mechanism included first the formation of propionic acid by decarboxylation, followed by the production of ethane from the latter, as it was reported also in the section dedicated to the carboxylic acids. Butanoic acid, that would be the product of direct hydrogenation of the carboxylic acid, was present in negligible amounts (30 times less than propionic acid).

Glutaric acid reported, as in the case of succinic acid, a strong dependence of the conversion with the temperature, ranging from 35% at 230 °C to a maximum conversion of about 88% at 270 °C. In the liquid phase, 80% of the remaining carbon is constituted by butanoic acid. In line with the previous hypothesis, it may be produced if we think to decarboxylation mechanisms: these would explain the carbon dioxide as main gaseous component. The propane is another gas component with higher percentage than usual, and it may be produced by successive reactions of the butanoic acid. It is interesting to observe that, despite glutaric acid and glycolic acid solutions has similar pH (2.6 vs 2.3), the latter had an APR H<sub>2</sub> yield 30 times higher. This may be a confirmation that the intrinsic reactivity of the molecule might have a higher impact on the performance as compared to the pH values.

In definitive, despite of the low tendency of the bicarboxylic acids to the production of hydrogen, they are quite reactive, but the main issue is that their intermediates (the relative mono-carboxylic acids) have also low reactivity. The efforts of the research therefore should be in maximizing the yield of the carboxylic acids, because they seem the key-compounds in the pathway to produce renewable hydrogen.

## Mono-alcohols

In Figure 43 the results of four mono-alcohols are reported. Ethanol, 1-propanol and butanol were chosen because representatives as present in aqueous phase and also because their similar behaviour may give a hint on the mechanisms of reaction; 2-propanol, as will be shown later, behaved in a drastic different way, underlining the importance of the position of the hydroxyl group in the structure of the molecule. Ethanol reached about 68% of carbon conversion to gas, while its global conversion increased from 78% at 230 °C to almost complete conversion (99%) at 270 °C. As it is reported in Figure 44-A, hydrogen constituted 50% of the gas phase, with methane and carbon dioxide almost 25% each. About 30% of the carbon from ethanol remained in the liquid phase (Figure 44-B). 60% of the carbon is acetic acid, that is the corresponding carboxylic acid of the starting alcohol. However, it is just 6% of the initial moles of ethanol, so it may be considered as a minor by-product, involved in side-reactions of hydrodehydrogenation. This result agrees with previous works in literature. Tokarev et al. [118] reported double production of hydrogen compared to methane and carbon dioxide from the APR of 10% of ethanol.

1-Propanol obtained the same results of ethanol regarding the carbon conversion to gas and the selectivity; also, the absolute amount of hydrogen produced was the same, but it resulted in less yield considering the higher presence of hydrogen in the starting molecule. Ethane and carbon dioxide have the same molar ratio, and hydrogen accounts for half of the gas phase, as was the case with ethanol. In the liquid phase it reached 96% of conversion at 270 °C and in this case 20% of the carbon remained as propionic acid, its relevant carboxylic acid. The analogies in the results keep going on with butanol. In fact, in this case we put our attention on the  $C_3H_8:CO_2$  ratio, that is again a bit more than unity; again, hydrogen is 50% of the gaseous product species.

Butanol reached 98% of conversion at 270 °C. As observed in the Figure 43-left, 73% of the carbon goes to the gas phase. 58% of the remaining carbon in the liquid phase was constituted, in agreement with the previous alcohols, by butanoic acid.

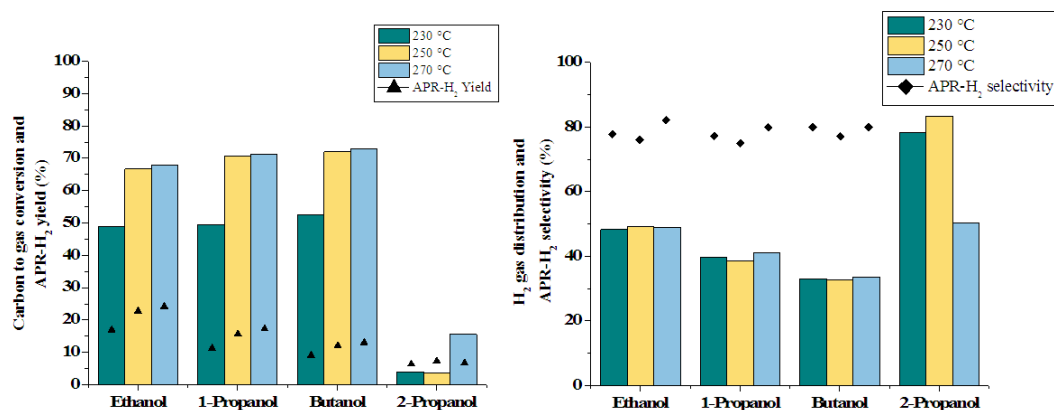


Figure 43. Influence of the reaction temperature on APR of monoalcohols. Reaction conditions: 0.133 M feed, 0.375 g 5% Pt/Al<sub>2</sub>O<sub>3</sub>, reaction time 2 h.

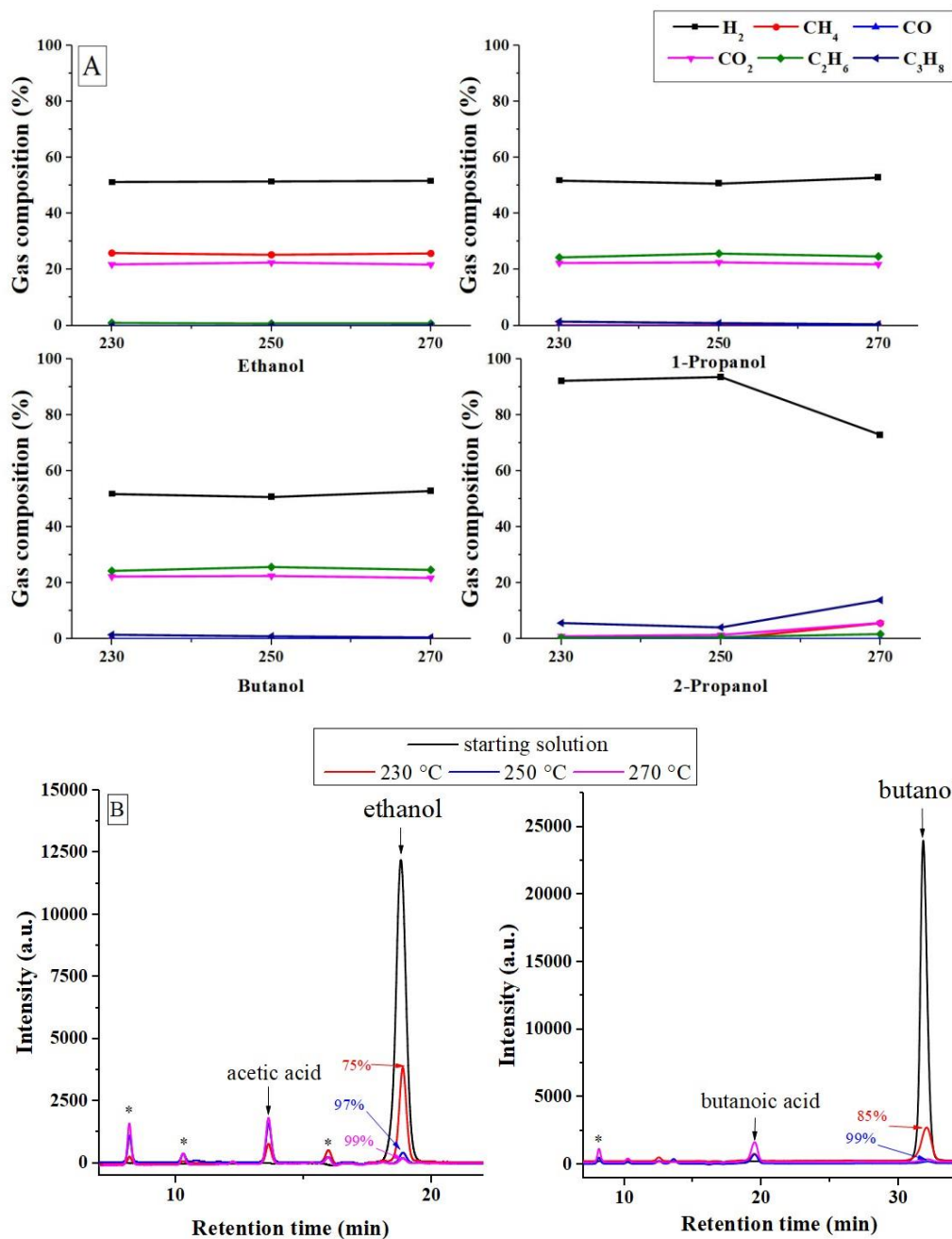


Figure 44. Influence of the reaction temperature on the composition of the gas phase from APR of monoalcohols (A) and on the liquid phase of ethanol (7-B left) and butanol (7-B right); the numbers in the figure close to the reagent peak refers to the conversion; \*: unknown compounds. Reaction conditions: 0.133 M feed, 0.375 g 5% Pt/Al<sub>2</sub>O<sub>3</sub>, reaction time 2 h.

The analogy between ethanol, 1-propanol and butanol allowed us to propose a similar reaction pathway, despite out of the scope of this work (Figure 45). As suggested by Dumesic, the first step of the reforming is the dehydrogenation of the molecule to give adsorbate intermediates [39]. A key difference in our case is that we are dealing with the presence of alkyl groups. Gursahani et al. performed a DFT study for ethanol on Pt in which they proposed the initial dehydrogenation of the alcohol leading adsorbed acetaldehyde [153]. Subsequently, the C-H scission

may lead to an  $\text{CH}_3\text{CO}$  intermediate that, after C-C bond cleavage, produces methane and carbon monoxide; finally, the latter would produce hydrogen and carbon dioxide via WGS in our reaction conditions. As outlined in the cited work, the  $\text{CH}_3\text{CO}$  intermediate is present also in the catalytic conversion of acetic acid, creating a link between the two pathways. As it was observed in the analysis of the liquid phase, acetic acid was indeed the main liquid product in the APR of ethanol. An analogous reaction pathway can be suggested for 1-propanol and butanol, where the corresponding carboxylic acids were found at the same way. It is important to observe that in our conditions the aldehydes relevant to the studied alcohols were not found, contrarily to a recent published work that investigated the APR of ethanol and propanol with different nickel-based catalysts [154]. The discrepancy may be due either to the longer reaction time in our work, that would allow a complete conversion of these reactive intermediates; or to the different used catalyst, as in the cited work is highlighted that the catalytic systems affected the obtained product distribution.

1-propanol and butanol may follow an analogous mechanism, leading respectively to ethane and propane as main alkanes in the gas phase.

2-propanol showed a completely different behaviour, compared to the previous series and, for some aspects, also to all the other investigated molecules. It had strongly less carbon conversion to gas (maximum 16%) but almost complete conversion was reached in the liquid phase (98%). It has high hydrogen gas distribution, since almost no alkanes were present, except propane at about 20%. This result may be due to hydrodeoxygenation pathways, that removed the oxygen leading to propane. The APR- $\text{H}_2$  selectivity was up to two orders of magnitude higher than the usual values, and for this reason it was not reported in the relative graph. This result, that is at first sight illogical, may hide an indication on the mechanism of the production of hydrogen. We may infer that in this case it is not associated to a reforming path, that would lead to the contemporary production of hydrogen and carbon dioxide in similar amount, but to a dehydrogenation mechanism. Confirming this hypothesis, acetone was the main compound present in the liquid phase, accounting for 90% of carbon. It can be the result of the catalytic dehydrogenation of 2-propanol on the catalyst [155]. This path would explain the high value of the APR- $\text{H}_2$  selectivity.

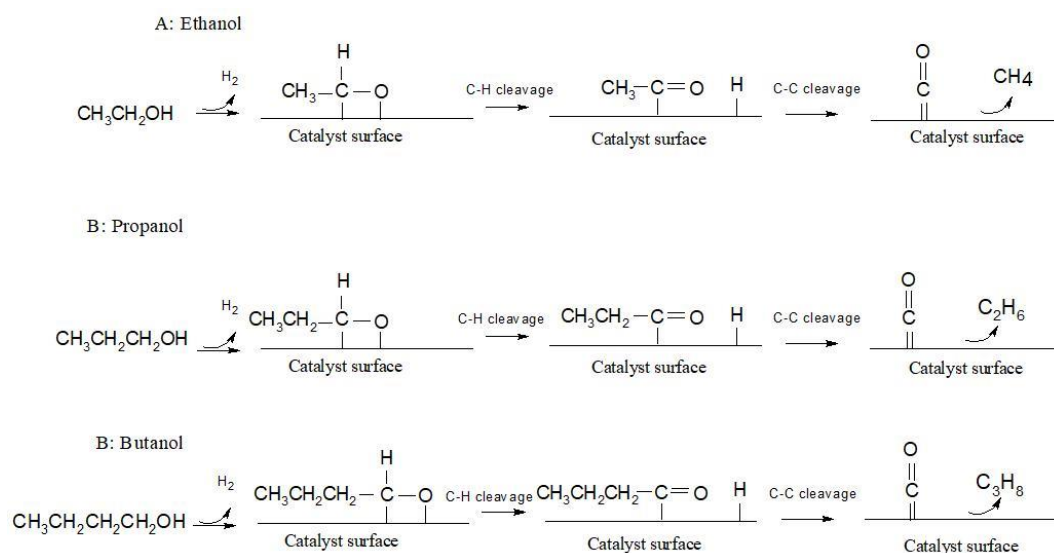


Figure 45. Suggested reaction mechanisms for monoalcohols.

## Polyalcohols

In the following Figure 46 the performance obtained by the reforming of three polyalcohols were reported. Ethylene glycol is one of the most studied compounds for aqueous phase reforming [43,48,54]. In this work we showed that it maintained the same selectivity for the production of hydrogen, and temperature had an effect mainly on the conversion. Therefore, in these conditions, selectivity seemed not a significant challenge and phenomena of side reactions were not important, contrarily to what is reported in literature. The reason may be due to the dilute conditions in which the experiments are carried out. In the liquid phase, ethylene glycol reached 100% of conversion at 270 °C, but also in this case the effect of temperature is visible because the conversion was 42% at 230 °C and 73% at 250 °C.

Propylene glycol had also a strong increase of the carbon conversion to gas with the temperature, and, thanks to the constant selectivity, of the hydrogen yield. In the liquid phase it converted quantitatively (99.8% at 270 °C). The APR-H<sub>2</sub> selectivity was lower compared to ethylene glycol maybe because of the methyl group that is not activated by a hydroxyl group. This causes the presence in the gas phase of methane (more than 10%) at expense of hydrogen production (Figure 47). In the liquid phase, ethanol is the main product at 230 °C, but its importance decreases with temperature, so that acetic acid becomes the main component at 270 °C (70% of the remaining carbon).

Similar consideration to ethylene-glycol may be reported for glycerol. The selectivity was not affected by temperature and the increase in the conversion led to a strong increase in the hydrogen yield. In the liquid phase glycerol converted up to 49% at 230 °C, but this value increase to 93% at 250 °C, reaching 100% at 270 °C. In the case of glycerol, the liquid composition changed drastically among the investigated temperatures. At 230 °C, the main liquid product is propylene-glycol, after glycerol, followed by ethanol and ethylene-glycol. At 250 °C,

propylene-glycol remains the most present compound, but acetic acid started to be present in consistent amount. This is consistent with the result reported in the previous paragraph, where starting from the diol, acetic acid was produced as main intermediate; also, ethanol and lactic acid still increase their presence, maybe because of the higher glycerol conversion. Finally, at 270 °C, acetic acid was the liquid compound with the highest concentration.

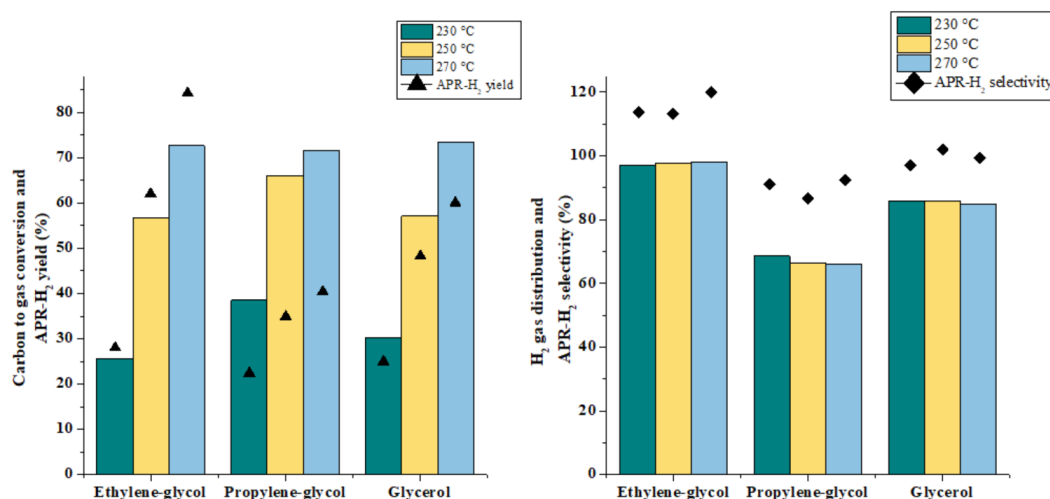


Figure 46. Influence of the reaction temperature on APR of polyalcohols. Reaction conditions: 0.133 M feed, 0.375 g 5% Pt/Al<sub>2</sub>O<sub>3</sub>, reaction time 2 h.

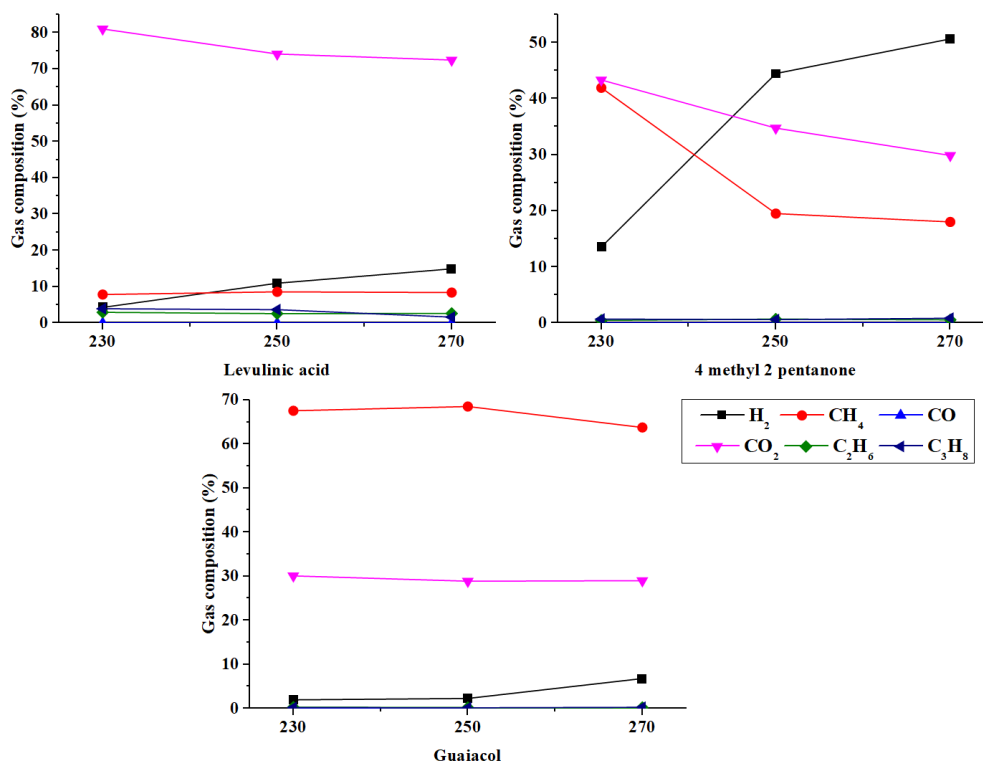


Figure 47. Influence of the reaction temperature on the composition of the gas phase from APR of polyalcohols. Reaction conditions: 0.133 M feed, 0.375 g 5% Pt/Al<sub>2</sub>O<sub>3</sub>, reaction time 2 h.

### *Ketoacids, ketones and aromatics*

Finally, in the following Figure 48 the results regarding levulinic acid, 4-methyl-2-pentanone and guaiacol are reported, respectively a ketoacid, a ketone and an aromatic. This is the first time that such compounds are investigated for aqueous phase reforming. In general, it is observed that the performance of these compounds were the worst among all the tested classes. The reason could be ascribed to the presence of recalcitrant groups (ketonic, carboxylic, aromaticity) that do not have any reactivity for hydrogen production, reducing drastically the APR-hydrogen yield. In Panisko's work, a plethora of ketones were present, despite with low concentration; the same can be reported for aromatics, where phenol was present as main aromatic compound [144]. For this reason, it is important investigate also these classes of compounds if APR should be used as a process that aims to exploit as much as possible the organic compounds present in the aqueous phase.

Levulinic acid's conversion was from 7% at 230 °C to 23% at 270 °C. The carbon conversion to gas was 4.6% at 270 °C, and the main product was carbon dioxide (Figure 49). This result suggests that decarboxylation reactions may give these products in the liquid phase, but this would give rise to the presence of small amount of MEK (2-butanone) in the liquid phase; actually, it was not present, but 2-butanol was observed indeed, moving from 3% to 9% of carbon in the liquid phase in the investigated range of temperature, with carbon dioxide that increased 2.8 times in the same range. This hypothesis seems reasonable because it is known that MEK is 100% selective to 2-butanol under reaction conditions milder than the ones present in this work [156]. Other minor products were propionic and butanoic acid, accounting for about 1% of carbon each at 270 °C.

4-methyl-2-pentanone showed the lowest gas production among the molecules screened in this work at each investigated temperature. Within the low amount of gaseous products, interestingly the gas phase contained methane (from 40 to 20% going at higher temperatures), maybe because of the breakage of the methyl group present in the structure of the molecule. The analysis of the liquid phase was not as effective as in the other cases, and a small percentage of the carbon present was recognized. This may be seen as an indirect indication that the ketone does not produce the usual compounds that were recognized before (carboxylic acids, monoalcohols), so the reaction path is not trivial and requires further studies to allow the identification of the liquid by-products. In general, ketones behave as strong recalcitrant compounds for APR and would necessitate further efforts to improve its performance, using more severe reaction conditions, for example.



Compared to the previous compounds in this section, guaiacol reported the highest carbon conversion to gas, but it is not associated to a reforming path, i.e. to hydrogen and carbon dioxide production, but mainly to the presence of methane. This is likely due to the breakage of the ether group present in the molecule. Methane is present up to about 70% in the gas phase, giving the formation of catechol, that was identified in the liquid phase.

Despite the poor performance of these representative compounds, it is worth to highlight the importance of better understanding the possible reaction pathways for these recalcitrant molecules because of their presence in the aqueous stream coming from lignocellulosic biomass. One of the main reasons may be the scarce presence of hydroxyl groups in the investigated molecules.

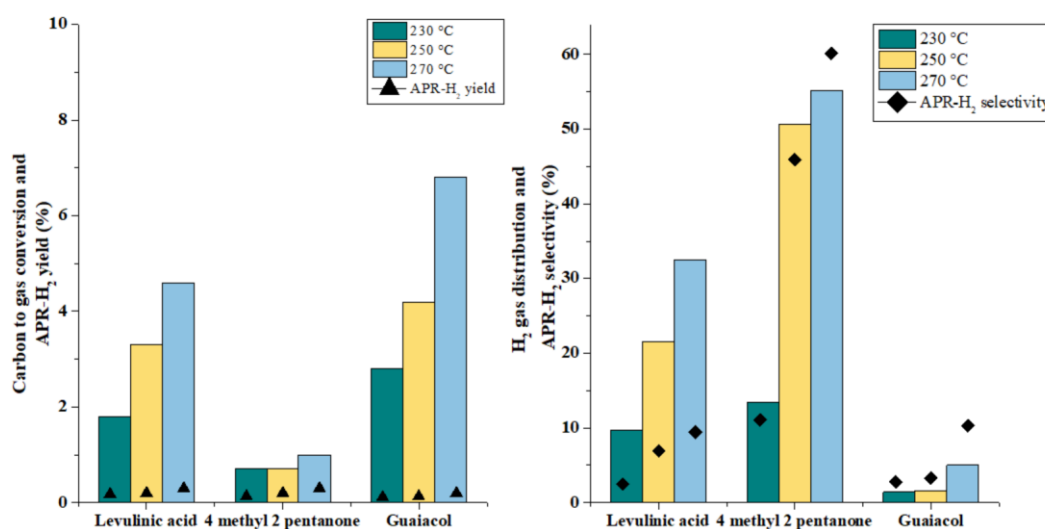


Figure 48. Influence of the reaction temperature on APR of levulinic acid, 4-methyl-2-pentanone and guaiacol. Reaction conditions: 0.133 M feed, 0.375 g 5% Pt/Al<sub>2</sub>O<sub>3</sub>, reaction time 2 h.

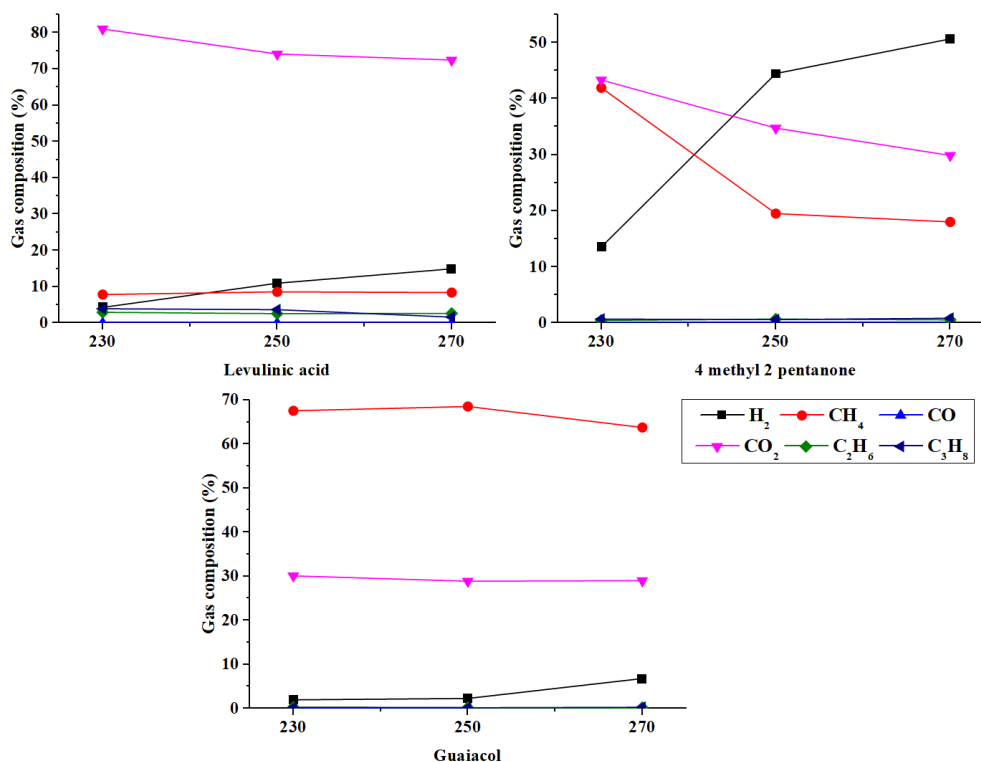


Figure 49. Influence of the reaction temperature on the composition of the gas phase from APR of levulinic acid, 4 methyl 2 pentanone and guaiacol. Reaction conditions: 0.133 M feed, 0.375 g 5% Pt/Al<sub>2</sub>O<sub>3</sub>, reaction time 2 h.

### 5.2.2 Study of binary and ternary mixtures

The screening of the seventeen model compounds helped to understand how the reactivity of the single molecule changes according to the reaction temperature, outlining the compounds easily reformed and the ones that have been reported as recalcitrant.

In this section, we performed tests of binary and ternary mixtures of four selected compounds. Four binary solutions and two ternary solutions were tested to examine if the reactivity changes and to go into the direction of the test of a representative biorefinery stream. The tests were carried out maintaining the global same molarity (133 mM). The results were evaluated according to the same indicators used in the screening. For comparison, we performed also tests in which the components of the mixtures were investigated at the concentrations used in the mixture (67 and 44 mM)

The performances of the mixture were also compared with two ideal values of linear combination, whose equation is reported in the paragraph 2.4.

In the Figure 50 the influence of the concentration of the single substrate on the performance is reported.

First of all, we observed that glycolic acid maintained almost the same performance for all the parameters reported; in the liquid phase its conversion remained quantitative. Regarding ethanol, comparable results, can be observed.

Fewer liquid products from ethanol at 67 mM are present compared with 133 mM, and the conversion of ethanol was similar (96.7%).

On the contrary, acetic acid increased steeply the carbon conversion to gas working at lower molarity and, as a consequence, the hydrogen selectivities decreased for the higher concentration in the gas phase of both CO<sub>2</sub> and CH<sub>4</sub>. It is highlighted that also in the runs with different carbon concentrations, carbon dioxide and methane maintained almost the same molar ratio of 1:1.

The conversion of acetic acid increased from 56% to 99.8% going towards lower molarity. This means that the ratio catalyst/acetic acid plays a fundamental role in its reactivity in the investigated reaction conditions. Dealing with a catalytic reaction, the decrease of the conversion with the increase of the concentration may be an indication that a limit value on the saturation of the catalyst was reached. Therefore, increasing the starting molarity would not affect the productivity because the catalyst is saturated and the superficial phenomena (adsorption of the reagents, chemical reaction, desorption of the products) may be the rate determining steps.

Finally, it is interesting to analyse the effect of the concentration on the lactic acid. It is observed that the concentration has an effect not only on the conversion but also on the selectivity of the hydrogen production, meaning that the reaction pathways are sensitive in different way to the concentration of the reagent, so it would be a positive effect working in dilute conditions for the sake of the higher selectivity. The higher selectivity is reflected in the liquid phase with lower amount of propionic acid, which is actually the product of hydrogenation of the hydroxyl group, that is 30% of the moles of lactic acid in the 133 mM test and it decreases at 10% in the 67 mM one.

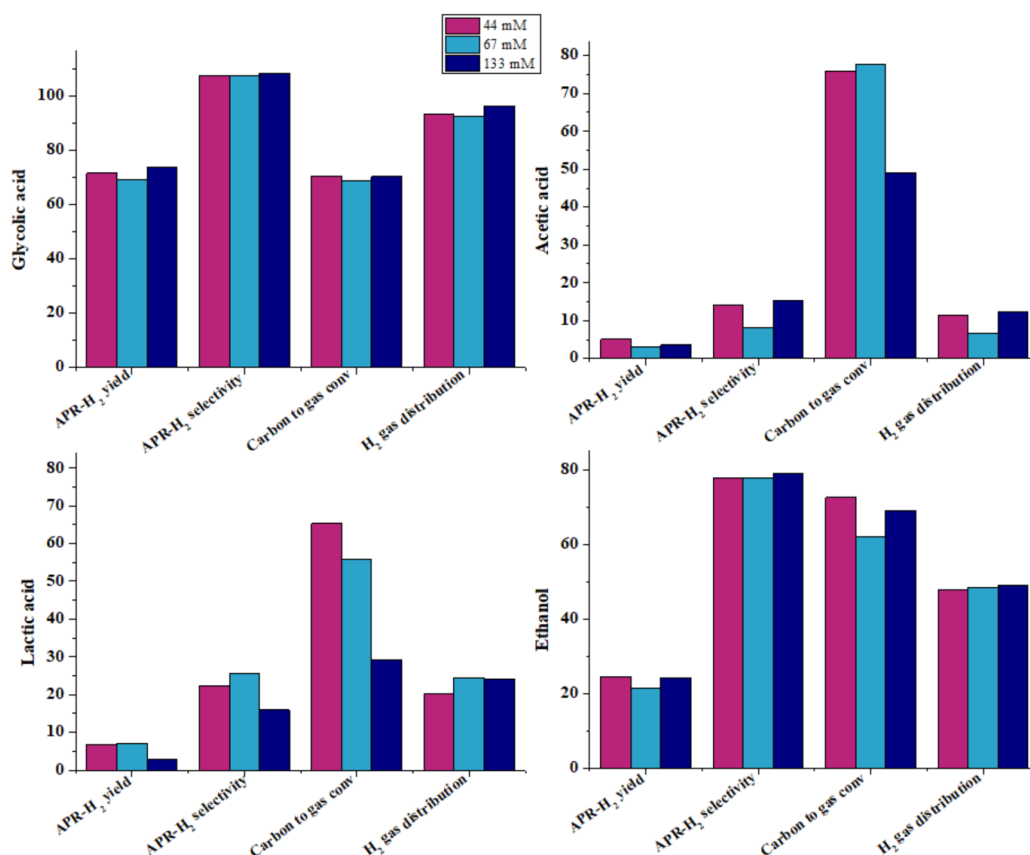


Figure 50. Influence of the concentration of feed on the performance of APR. Reaction conditions: 270 °C, 0.375 g 5% Pt/Al<sub>2</sub>O<sub>3</sub>, reaction time 2 h.

### Binary mixtures

The results obtained from the binary mixtures are reported in the Figure 51. Each parameter is compared with the linear combination points, as explained before.

In the glycolic acid and acetic acid mixture test an interesting result was identified. Indeed, while the conversion of glycolic acid remained 100%, the one of the acetic acid decreased sharply to 3.5%. It is important to observe that acetic acid can be formed from the glycolic acid, so we should pay attention when we evaluate the conversion of acetic acid that may be actually produced during the reaction from glycolic acid. Even considering the highest production (133 mM test) the conversion would increase up to 16%, still too low compared to the test with acetic acid alone.

Moreover, looking at the amount of each gaseous compound, we observed that the moles of hydrogen in the mixture test are almost equal (just 2% more) of the test with glycolic alone at 67 mM and the same is for the carbon dioxide (6% more). This behaviour may indicate a selective adsorption of the glycolic acid at expense of the acetic acid. Because of this apparent lack of interaction between the catalyst and acetic acid, it is not surprising that the results obtained in the mixture were so far from the linear combination: actually, only glycolic acid is reacting.

This is an important information, and to the best of our knowledge, this work showed this behaviour for the first time. It has important consequences not only when acetic acid is in the mixture, but also when it is an intermediate of reaction. In fact, if it had lower adsorption kinetics than the other molecules, it would not interact with the catalyst, increasing its concentration during the reaction time and not being converted. To better understand this phenomenon, it is interesting to observe the results obtained with other mixtures.

The results obtained from the equimolar mixture ethanol/acetic acid showed that, even in this case, acetic acid behaved differently from the mono-compound solution, reaching 8.9% of conversion. Here the problem of the intercorrelation between the two compounds is less evident, because acetic acid was obtained from ethanol with a less extent comparing to the case of glycolic acid. Similar to the previous result, the carbon conversion to gas is less than expected from the linear combination, while the selectivity is higher. This outcome suggests that also in the case of the binary mixture acetic acid – ethanol there is an issue of selective adsorption.

The third investigated mixture was the glycolic and lactic acid binary system. Conversely to the acetic acid, the lactic acid converted completely in the liquid phase; looking at the composition of the liquid phase, propionic acid was the most present compound, reaching 93% of the carbon in the liquid phase. This was an unexpected result because, when the lactic acid was tested alone at 67 mM, gave propionic acid with less selectivity, as reported previously. So, it may come from the hydrogen that is produced from glycolic acid that, in this case, would hydrogenate selectively the lactic acid more than itself, giving acetic acid, that constituted just the remaining 7% of carbon. This would lead, as observed, to a decreased of carbon to gas and hydrogen yield compared to the runs with one component.

Because of the peculiar results obtained when acetic and lactic acid were used, we were interested in investigating a binary mixture constituted by these two compounds. Indeed, the acetic and lactic acid mixture behaved differently from the others. It was observed that the performances obtained in the test were closer to the linear combination of the singular results. It is reasonable to assume that this is because there is not competitive adsorption between the two species. It means that each molecule can interact with the catalyst as if it was the only compound in the reaction system. Indeed, it is observed that the conversion of the acetic acid is indeed higher than in the other cases, reaching 68%.

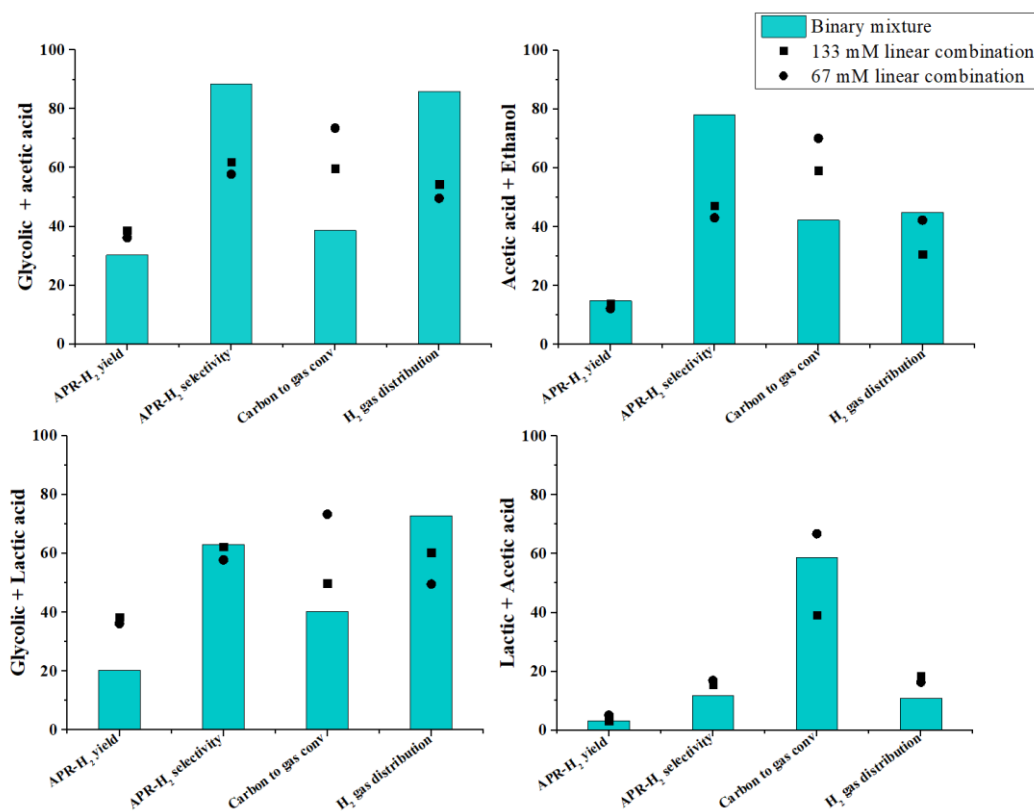


Figure 51. Results of four equimolar binary mixtures. Reaction conditions: 270 °C, 0.375 g 5% Pt/Al<sub>2</sub>O<sub>3</sub>, reaction time 2 h.

### *Ternary mixtures*

In order to make a step forward in the valorization of a post-HTL aqueous stream, we investigated two ternary mixtures. In the first one we tested glycolic and acetic acid and lactic acid; in the second one, we analysed the results of the ternary mixture constituted by glycolic acetic acid and ethanol. The obtained results are shown in Figure 52.

Studying the first mixture, we observed that glycolic and lactic acid converted completely; on the other hand, acetic acid reached 27.6% of conversion. It was still higher compared to the binary mixture with the glycolic, but lower compared to the one with lactic acid. This is an interesting result because gives indication on the necessity of working on the nature of the catalyst to improve acetic acid adsorption. Indeed, being a representative compound of the water stream, and being a common intermediate component, it is necessary to develop strategies for improving its chemical affinity with the adopted catalyst.

In the glycolic-acetic-ethanol mixture it was observed a higher hydrogen selectivity compared to the linear combination, but a lower carbon to gas: taking into accounts these considerations, the yield of hydrogen reached the theoretical one. In the liquid phase glycolic and ethanol converted quantitatively; on the other hand, confirming the previous outcomes, the acetic acid conversion dropped from almost 100% (acetic acid conversion in the test at 44 mM) to 6.4%.

Therefore, it can be concluded that acetic acid especially is a key component in the study of mixture because its adsorption may be a limiting step in the reactions conditions to perform its reforming. Further studies are suggested to improve the catalyst and its interactions with acetic acid.

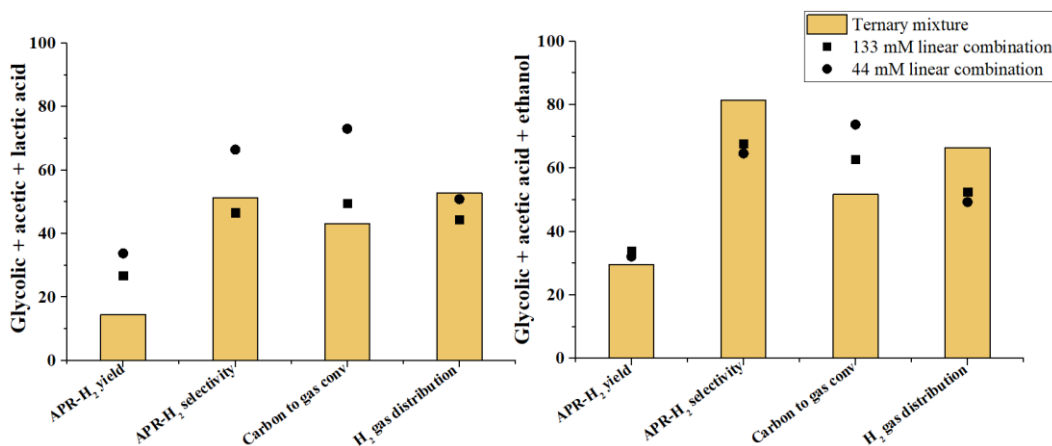


Figure 52. Results from ternary mixtures constituted by glycolic acid, acetic acid and lactic acid (left) and glycolic acid, acetic acid and ethanol (right). Reaction conditions: 270 °C, 0.375 g 5% Pt/Al<sub>2</sub>O<sub>3</sub>, reaction time 2 h.

### 5.2.3 Characterization and stability of the catalyst

The Pt/Al<sub>2</sub>O<sub>3</sub> commercial catalyst, after its drying, was characterized by several techniques to address if some deactivation mechanisms occurred. First of all, we investigated if leaching phenomena may occur in our reaction conditions. To investigate this option, ICP analysis were carried out in the liquid solution that was recovered after the reaction. The results reported the absence of platinum dissolved in the solution; therefore, we can exclude that leaching of the catalyst may happen during the experiment.

Coking is one of the possible deactivation mechanisms during aqueous phase reforming. The TGA in inert and oxidizing environment of the catalyst used for APR of acetic acid at 250 °C is reported in the Figure 53 (left). The test was performed at first using nitrogen; then, after natural cooling, using air. As it is reported, only the inert test presented a clear peak at 500 °C (apart from a small speak at about 50 °C ascribed to the presence of water physisorbed on the surface of the catalyst). When the oxidizing test was carried out, no peak indicating losing weight was observed. The inert test cannot decompose the coke possibly present on the surface; therefore, if high-molecular weight compounds were present, they should have been decomposed by the following treatment in air. As it was not the case, we assumed the absence of coking phenomena.

Therefore, we ascribed this behaviour to something that would be insensitive to the chemical nature of the flow, but just to its thermal properties. To go deeper in this issue, we evaluated if a structural change of the support was present by XRD.

The results reported in the Figure 53 (right) show the diffractograms of a fresh catalyst sample and a spent catalyst, after APR of acetic acid at 250 °C. Cristobalite was used as internal standard to quantify the conversion to boehmite. The diffractogram of the fresh sample reported the peak of the defective spinel structure at 45.8° and 67° corresponding to the (400) and (440) crystal planes of gamma alumina. On the other hand, the hydrothermal conditions at which the catalyst was subjected caused the appearance of new peaks. The characteristic angle of the new peaks (28.2°, 38.3°, 49°) allowed to ascribe these peaks to the formation of a crystalline phase, boehmite. The information coming from the quantification of the boehmite phase was compared with loss weight obtained in the TGA analysis, assuming that, between 400 °C and 600 °C, it can be ascribed to the loss of water. The matching between the two results (i.e. about 40% conversion of alumina to boehmite) excluded the presence of coke on the surface of the catalyst.

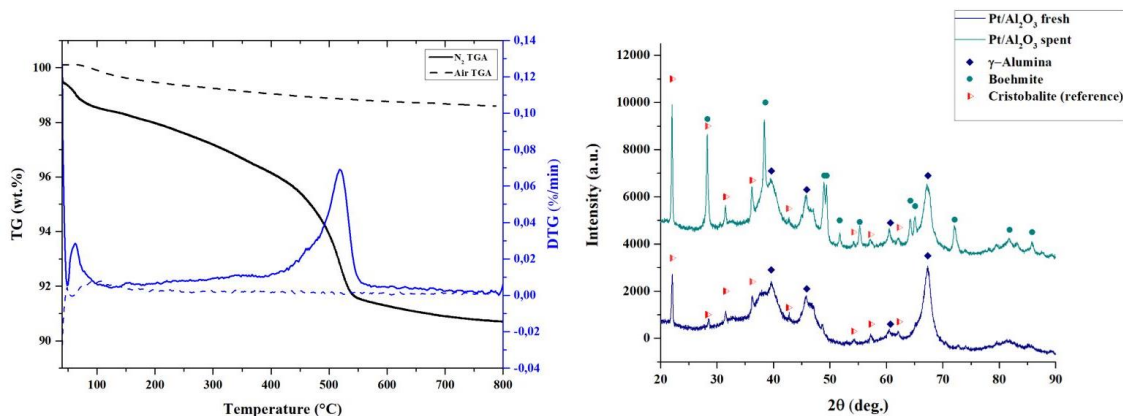


Figure 53. Thermogravimetric analysis of the spent catalyst performed in nitrogen and air (left) and XRD analysis of the fresh and spent catalyst with cristobalite as internal standard (right).

In order to complete the characterization, morphological and textural features were analysed by FESEM and adsorption/desorption N<sub>2</sub> isotherms respectively. The latter gave no appreciable changes in the value of the surface area, pore volume and pore size distribution, maybe because of the small reaction time.

In the Figure 54 there is a comparison between the fresh catalyst and the spent one, after APR of lactic acid at 230 °C.



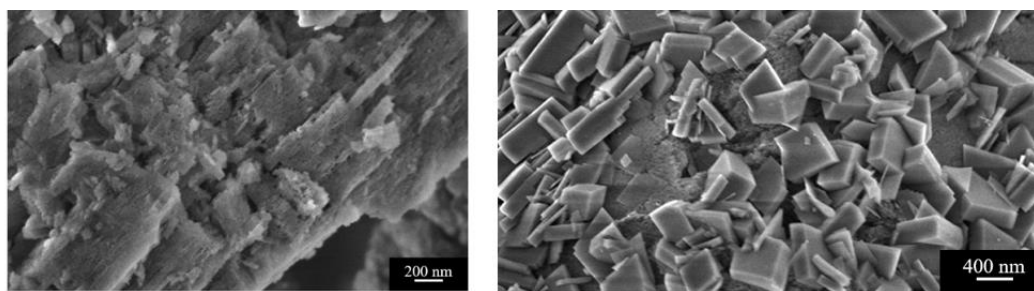


Figure 54. FESEM images of the fresh (left) and spent catalyst (right) after APR of lactic acid at 230 °C.

In the figure on the right it was observed the presence of nanocrystals, with sizes at around 200-400 nm. It is interesting to observe as this phenomenon appears on the surface of the catalyst, while it can be seen still the original structure on the bottom. As it was reported by Carrier et al., the transformation of  $\gamma$ -alumina into boehmite can occur via two mechanisms: one involves a surface hydration mechanism, the other one a dissolution of alumina, followed by its precipitation [157]. Because of the homogeneous covering of the surface we may propose that the first mechanism was the most likely in our experimental conditions, but a definite answer cannot be reported just with this information.

The alumina-boehmite transition is a known phenomenon when dealing with hot liquid water. The stability of alumina support is therefore a known issue and it is one of the challenges for heterogenous catalysis applied to biomass valorisation. Interestingly, we observed that this phenomenon, despite dependent mainly on the solvent and the temperature, was not the same for each substrate investigated. Ravenelle et al. studied the stability of Pt/Al<sub>2</sub>O<sub>3</sub> during APR of glycerol and sorbitol at 225 °C [158]. They observed minor tendency of the support to be converted into boehmite when the organics were present in the solution, and in particular when the catalyst was treated with sorbitol solution. They proposed that polyols form a protective layer on the alumina surface preventing the hydrolytic attack that initiated the boehmite formation. Taking advantage of the extensive screening of compounds, we evaluated how the molecules investigated may affect this phenomenon. In fact, as suggested by Ravenelle, the stability of catalysts under real APR conditions, which means considering also the substrate, is of critical importance.

We performed ATR-IR analysis on the catalysts recovered after the screening of the seventeen compounds at 270 °C. In the Figure 55, some characteristic results are reported. Firstly, the absence of peaks characteristic of coke was observed. As reported by Karge et al., at 1610 cm<sup>-1</sup> there is the so-called coke band, due to a complex mixture of carbonaceous, hydrogen-deficient deposits, as polyethenes and/or aromatics, while at 1540 cm<sup>-1</sup> can be observed the presence of structures such as alkylnapthalenes and polyphenylene [159]. Neither of these nor other characteristic peaks were observed, suggesting its absence.

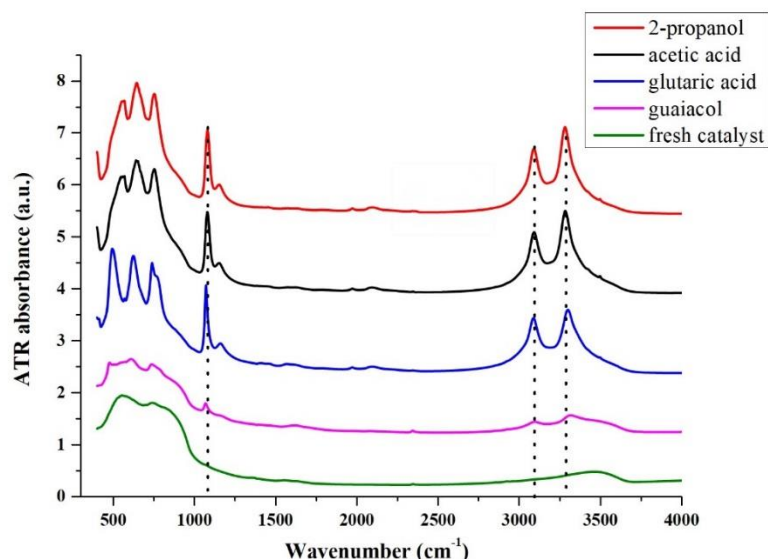


Figure 55. ATR-IR spectra of spent catalysts after APR; the spectra of the fresh catalyst is added for comparison.

The catalyst after APR of acetic acid, 2-propanol and glutaric acid presented a sharp peak at  $1064\text{ cm}^{-1}$  and shoulder bands close to  $3304$  and  $3124\text{ cm}^{-1}$  that are assigned to OH deformation and stretching vibrational modes of the boehmite phase, respectively [160]. Therefore, it seems that the transformation was insensitive to the fact that we dealt with a carboxylic acid, an alcohol or a dicarboxylic acid. Contrary to what suggested by Ravenelle, the increase in the carbon chain length moving from acetic to glutaric acid had no influence on the boehmite formation in this case. Anyway, some compounds did prevent this phenomenon to happen. It is reported that when APR of guaiacol was carried out, the recovered catalyst showed less evident boehmite peaks, and it is similar to the fresh catalyst sample, actually Pt/Al<sub>2</sub>O<sub>3</sub>. This is an interesting result because it showed clearly that not only the reaction conditions, but also the compound that is investigated must be considered to study the deactivation issues of the catalyst.

In order to determine which is the effect of the modification of the support on the performance of the reaction, two tests were performed reusing the catalyst after its recovery (Figure 56). The tests were performed with the ternary mixture glycolic-acetic-lactic acid, at 1.8 wt.% of carbon, in order to be close to the conditions observed by Panisko et al. in their work [144].

The results showed that the performances were maintained up to the third run (after that, an insufficient amount of catalyst was recovered to further investigate). This is an important observation as it points out that, despite the structural change, the catalyst was stable toward each indicator, and no deactivation was observed. Further experiments in a continuous system are planned to evaluate the stability at higher time on stream.

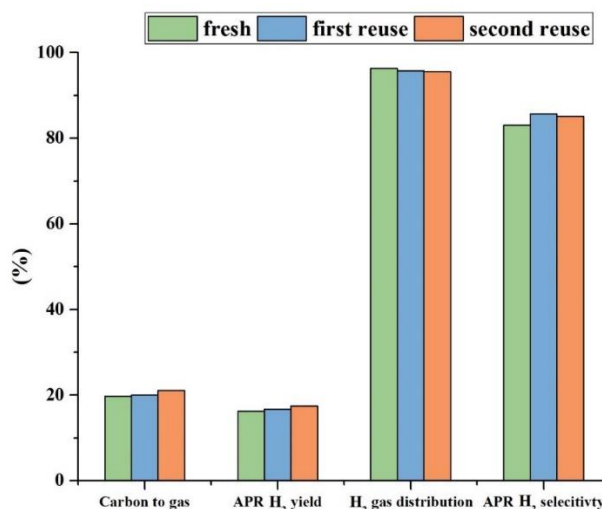


Figure 56. Influence of catalyst reuse on the performance of APR of a glycolic-acetic-lactic mixture. Reaction conditions: 0.133 M feed (0.044 M per acid), 270 °C, 0.375 g 5% Pt/Al<sub>2</sub>O<sub>3</sub>, reaction time 2 h.

### 5.3 Conclusions

The aqueous phase after a hydrothermal process contains organics that need to be disposed. In this work, the catalytic reforming of representative compounds present in these streams was investigated to give a path of valorization for these by-products. Some of the molecules present in the work (e.g. glycolic acid, guaiacol, 4 methyl 2 pentanone) were subjected to APR for the first time. We observed an increase of the hydrogen yield with temperature, mostly thanks to the increase of the conversion and the constant selectivity to hydrogen production. Some compounds, such as acetic acid, were recalcitrant toward reforming, therefore they require major efforts to increase the possibility of their valorization: this is because they are both present in the starting solution, but also common reaction intermediates. Decarboxylation mechanism appeared as main pathway in the case of carboxylic acids. Binary and ternary mixtures were tested to understand the behaviour of a possible synthetic biorefinery stream, and it was observed that adsorption kinetics on the catalyst may constitute an issue to overcome. Acetic acid decreased its conversion when present in a mixture compared to the test in which it was the only compound tested. The characterization of the catalyst showed that the degradation of the support depends also on the compound subjected to APR but leaching and coking were excluded in the present reaction conditions; despite of that, the catalyst showed stability at least for three consecutive runs. Thanks to this work, we tried to fill a gap in the field of the hydrothermal processes, where there is a lack of information in the study of the C-laden aqueous phases and their valorization.

# Chapter 6 Valorization of aqueous phase derived from lignin-rich hydrothermal liquefaction

## 6.1 Introduction

In the previous chapter, a screening of several representative model compounds based on the cited literature works was performed, evaluating their reactivity for the APR process at different temperatures (230-270 °C) [128].

In the present chapter, APR was deeply investigated in order to understand if it can be a viable option to valorize the water stream derived from a hydrothermal liquefaction process. Indeed, as an alternative to the above cited gasification and/or anaerobic digestion, APR can also contribute to the production of the hydrogen necessary for upgrading the HTL biocrude through hydrotreatments. In this context, the aqueous phase reforming would be perfectly integrated in a biorefinery concept, reducing the dependency from external sources of hydrogen, helping to generate a biofuel with an oxygen level compatible with the final specification downstream processing (Figure 57). We initially investigated the APR of model compounds, looking at the influence of the nature of the substrate, its concentration and the reaction time, increasing the knowledge on APR of HTL-derived compounds depicted in Chapter 5. The majority of the literature research has been devoted to the study of alcohols and poly-alcohols such as methanol and glycerol (for example [37,42,43,98,154,161,162]), but most of the remaining compounds have not been studied yet in detail for aqueous phase reforming (i.e. glycolic acid, propionic acid, cyclopentanone, guaiacol), despite their importance for the sustainability of the process. A ternary mixture was also tested to simulate a possible multi-component aqueous phase composition.

Finally, in order to be as close as possible to the actual application, we performed the APR of a water produced by the hydrothermal liquefaction of a biorefinery-derived lignin-rich stream. To the best of our knowledge, this is the first work that reports such investigation. A thorough study was performed in order to evaluate how the solvent, used during the extraction of the aqueous phase, affects the following APR step, referring in particular to the influence on the activity and stability of the catalyst.

This chapter (results, figures and tables) is based on the published work reported in [163].

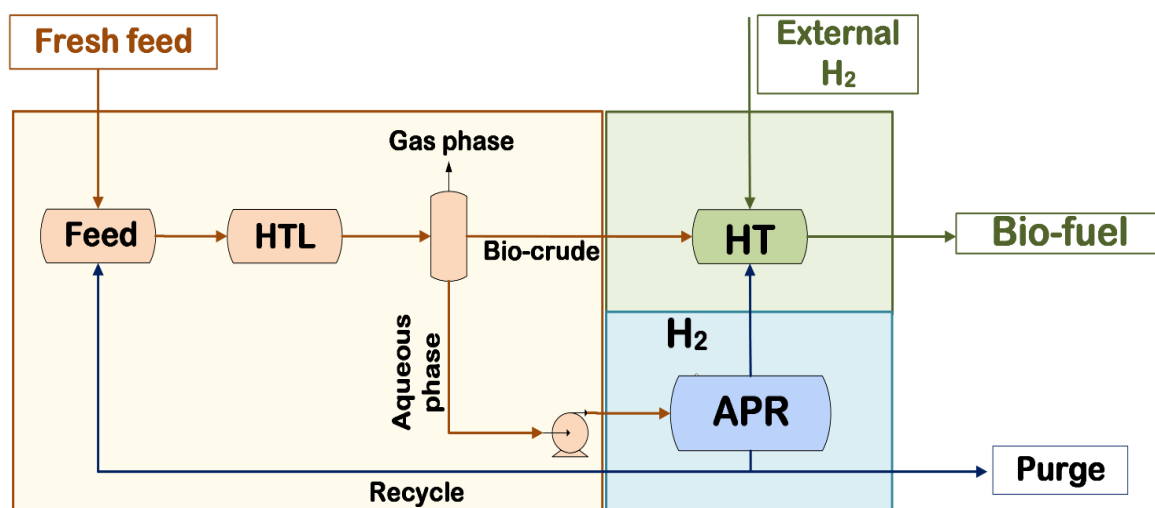


Figure 57: Block flow diagram of a HTL-APR integrated plant. HTL: hydrothermal liquefaction; HT: hydrotreatment (upgrade block).

## 6.2 Results and discussion

### 6.2.1 Model compounds

#### *Influence of carbon concentration*

Based on the analysis of the literature and authors' previous work, ten compounds were selected for the evaluation of the influence of the concentration on the APR process [128,144].

The main results are reported in Table 12 for each compound in the range 0.3 – 1.8 wt.% of carbon. This range was chosen in order to investigate the diluted conditions commonly observed in literature.

Acetic acid and propionic acid were chosen to represent the carboxylic acids class. Both compounds showed a drastic decrease of the carbon conversion to gas with the increase of the concentration in the solution, moving from 80% to 15% for acetic acid and from 75% to 5% for propionic acid. Even if the reaction conditions did not allow to extrapolate kinetics, we may assume that there was a strong inhibiting effect of the feed, as the levels of conversion are inversely proportional to the concentration [43]. On the other hand, the selectivity towards alkane formation (i.e. the hydrogen gas distribution) and the  $H_2/CO_2$  ratio remained constant on the whole range. It should indicate that new reaction pathways are not favoured.

As we reported in chapter 5 (and in [128]), in which a  $Pt/Al_2O_3$  catalyst was used, acetic acid and propionic acid mainly lead to the formation of a gas mixture composed by 50% carbon dioxide and 50% methane (or ethane in the case of propionic acid). This result was confirmed with the active carbon support used in this work, highlighting that the gas product distribution is neither influenced by

the concentration nor by the support used for the catalyst, the nature of the active sites being the main responsible of the catalytic decomposition to CO<sub>2</sub> and alkanes. Given the low H<sub>2</sub> selectivity, the APR-H<sub>2</sub> yield was low at each tested concentration.

Glycolic acid and lactic acid were chosen as the most representative hydroxyacids in the aqueous effluent of hydrothermal liquefaction. Indeed, glycolic acid was reported as the main compound in the aqueous phase coming from the HTL of corn stover [144]. Despite a decrease of the carbon conversion to gas, the influence of the concentration is less evident as compared to the case of the carboxylic acids. On the other hand, a strong difference between the two compounds can be observed looking at their hydrogen yield. Glycolic acid showed a decrease in the hydrogen production due to the lower conversion, but maintained at least 30% yield at 1.8 wt.% C. Instead, the lactic acid yield was always below 5%, despite similar levels of conversion. As reported in the following section 3.1.2, lactic acid produces carbon dioxide and ethane due to the formation of propionic acid as reaction intermediate, recalcitrant to hydrogen production. On the other hand, the glycolic acid led only to a slight production of acetic acid, while selectively produced carbon dioxide and hydrogen in a ratio close to the stoichiometric one. Please note that the APR H<sub>2</sub> selectivity higher than 100% are ascribed to further hydrogen-producing reactions, such as dehydrogenation (the same comment is valid for methanol).

Methanol and ethanol were investigated as they are likely present in the post-HTL aqueous phase [144]. The carbon conversion to gas of methanol decreased with the increase of the carbon concentration from 58% to 20%, while the APR-H<sub>2</sub> selectivity and H<sub>2</sub> gas distribution remained almost constant and close to 100%. Methanol was largely investigated as model compound for APR since it is the simplest alcohol to perform this kind of investigation [37,43,154,164–166]. These results can be explained by the structure of the alcohol that is readily dehydrogenated producing only hydrogen and carbon monoxide, reducing parallel and consecutive reactions (e.g. methanation or Fischer-Tropsch) involving different fragments of the molecule (such as alkyl groups); afterwards, the carbon monoxide is converted to carbon dioxide and hydrogen by reaction with activated water. Ethanol showed higher carbon to gas conversion than methanol thanks to the production of methane, together with carbon dioxide. Due to the production of the alkane, the hydrogen gas distribution was nearly 50%, constant in the whole range of concentration. It is interesting to observe that no difference in performance were reported between 0.3% and 0.9%. This fact should be due to the lower strength of adsorption of ethanol compared to methanol, that caused an apparently linear rate of consumption up to 0.9% of carbon.

Cyclopentanone was reported as one of the most present ketones in the post-HTL aqueous phase [144]. It is a valuable compound used, for example, in the preparation of specialty chemicals for the pharmaceutical or cosmetic sector [167]. Nevertheless, as it is present in very diluted concentrations, it is uneconomically envisaging a selective recovery. It was almost unreactive in the investigated reaction conditions (with about 20% of conversion of the feed in the

whole range of concentration), showing the lowest carbon conversion to gas among the ten screened compounds. It is interesting to observe that the hydrogen gas distribution and the APR-H<sub>2</sub> selectivity were strongly influenced by the carbon concentration. The latter increased strongly with the increase of the concentration, thanks to the fact that the hydrogen production linearly increased in the studied range, while the carbon dioxide production had a maximum at 0.9% wt.% carbon. Moreover, it was observed that the weight of the catalyst recovered was higher than the initial 375 mg (the accuracy of the recovery procedure should be in  $\pm 5\%$  range, assessed in organics-free blank tests). For this reason, it can be assumed that high-molecular weight compounds may be produced by aldol-condensation [168].

Glutaric acid was chosen as a typical example of bi-carboxylic acid. A strong decrease in the carbon conversion to gas was observed with the increase of the concentration, from 75% down to 25%. Interestingly, the analysis of the liquid phase showed an increase of the selectivity toward the formation of liquid products, mainly butanoic acid. In fact, while the conversion to gas phase decreased, the conversion of the feed remained approximately constant, favouring the formation of liquid by-products (propionic and acetic acid together with the butanoic acid). In analogy with the mono-carboxylic acid, the first reaction seems to be therefore the decarboxylation. Afterwards, as they are recalcitrant towards hydrogen production, the APR-H<sub>2</sub> yield remained low in all the investigated concentration range.

Guaiacol was studied as representative aromatic compound. As reported in the paragraph 6.2.3, aromatics can be present in the aqueous phase in the case of the hydrothermal liquefaction of lignin. As shown in the Table 12, the carbon conversion to gas decreased from 20% to 3%, while the hydrogen gas distribution and APR-H<sub>2</sub> selectivity increased. This is due to an increase of the hydrogen production, together with a decrease of the formation of methane and carbon dioxide. The analysis of the liquid phase can give a hint on the reason behind these results. The methane can be obtained by breaking the ether bond of the guaiacol, leading to catechol [169]. The HPLC chromatograms showed a decrease of the catechol production with the increase of the concentration, resulting in a greater hydrogen gas distribution. Phenol, the second most present by-product, can be obtained by consecutive deoxygenation from catechol itself.

Glycerol was also investigated in order to include in our study molecules not strictly related to the aqueous phase post lignin HTL, but still generally interesting for the valorization of organics dissolved in water. Glycerol can be found as soluble organic in the water phase, in particular from the hydrothermal liquefaction of aquatic biomass [170,171]. This is due to the hydrolysis of triglycerides, that lead to fatty acids (ending up in the biocrude) and glycerol (ending up in the aqueous phase). The carbon to gas conversion constantly decreased from 73% to 30%; contrarily to the other compounds screened in the present work, a clear influence of the carbon concentration was observed also in the case of the hydrogen gas distribution and APR-H<sub>2</sub> selectivity, due to the change of selectivity in the intermediate liquid products (i.e. hydroxyacetone).

Table 12. Influence of carbon concentration on APR of model compounds. Reaction conditions: 0.375 g 5% Pt/C, Liquid phase amount: 75 g, Temperature 270°C, Reaction time 120 min.

Concentration (wt. %C)	APR H <sub>2</sub> yield (%)	Carbon to gas (%)	APR selectivity (%)	H <sub>2</sub> gas distribution (%)
<b>Glycolic acid</b>				
0.3	65.1	65.9	99.8	98.8
0.9	55.3	53.2	104.4	99.4
1.8	31.1	33.9	92.4	99.1
<b>Acetic acid</b>				
0.3	1.2	79.2	3.3	2.9
0.9	0.6	33.5	4.1	3.4
1.8	0.5	16.0	7.0	6.0
<b>Lactic acid</b>				
0.3	2.3	66.8	8.1	7.0
0.9	1.0	32.7	5.6	7.4
1.8	0.8	19.9	5.8	11.5
<b>Propionic acid</b>				
0.3	2.2	75.1	8.8	6.3
0.9	0.8	28.2	7.7	5.9
1.8	0.2	4.4	8.5	8.0
<b>Glutaric acid</b>				
0.3	2.5	76.6	3.4	7.1
0.9	0.8	37.1	1.7	6.3
1.8	0.4	22.6	1.3	6.7
<b>Glycerol</b>				
0.3	58.9	74.4	102	80.6
0.9	37.8	53.4	96.4	76.0
1.8	19.9	31.9	85.7	73.6
<b>Methanol</b>				
0.3	58.8	54.7	109.9	98.4
0.9	32.1	29.2	113.5	98.2
1.8	19.9	19.4	105.4	98.0
<b>Guaiacol</b>				
0.3	0.3	18.6	2.8	4.2
0.9	0.2	12.5	3	2.9
1.8	0.2	2.2	20	14.5
<b>Ethanol</b>				
0.3	23.8	70.0	75.4	48.4
0.9	24.4	70.5	75.0	49.3
1.8	17.0	51.0	70.9	48.8
<b>Cyclopentanone</b>				
0.3	0.9	4.4	25.7	65.0
0.9	0.8	3.9	35.2	42.4
1.8	0.5	0.4	131	96.9

### *Influence of reaction time*

Based on results available in literature [144], three compounds were selected as the most representative ones of a post-HTL aqueous stream: glycolic acid, acetic acid and lactic acid. The APR of these compounds was performed at different reaction times to evaluate the presence of reaction intermediates and suggest a plausible reaction pathway. Since the sampling of the gas phase during the reaction is experimentally difficult, a series of tests was carried out at different time durations with the same initial conditions. For the sake of clarity, 0 h is



intended as the point in which the set temperature is reached (heating time approximately 60 minutes).

Acetic acid converted up to 35% before reaching the set temperature, producing with a high selectivity a gas mixture with a 1:1 carbon dioxide/methane ratio (Figure 58-A). It is clear that the consumption of acetic acid moles is almost entirely ascribed to the formation of methane and carbon dioxide. The relative production of the gas remained almost constant during the investigated reaction times. Hydrogen was present in small amount. This is due to the favourable cracking of the C-C bond, as confirmed in literature at different reaction conditions, and in our previous work with an alumina-supported Pt catalyst [128].

Glycolic acid reached a 28% conversion during the heating time and almost complete conversion after 2 hours. Hydrogen was the main product in the gas phase at each reaction time, reaching a plateau at about 2 hours, while carbon dioxide slightly increased up to 8 hours. According to the reaction mechanism suggested in our previous work, glycolic acid should produce 1.5 moles of hydrogen per mole of carbon dioxide [128]. This ratio is higher during the heating time, likely because the dehydrogenation (first step of APR) is predominant on the reaction mechanism compared to the reforming. In the following, it decreases also because of the formation of acetic acid, the only quantifiable liquid product. It may be obtained by the hydrogenation of the hydroxyl group of the glycolic acid, arising an issue of series-selectivity. As reported by Neira D'Angelo, the reactor configuration might be designed to allow the hydrogen to escape from the solution once formed, without being consumed in parasite reactions using a microchannel reactor, together with an inert gas stripping [64]. Acetic acid did not appreciably react because methane was barely detected in the gas phase.

Finally, lactic acid converted completely during the heating time. For this reason, it was decided to stop the heating period after 20 min (where reached temperature was about 165 °C) and 40 min (about 245 °C). While there was no conversion during the first step, at 245 °C a small conversion of the lactic acid was already observed. Two parallel but interacting pathways have been proposed for lactic acid (Figure 59). In analogy with acetic acid behaviour, lactic acid can be decarboxylated producing ethanol and carbon dioxide (light blue frame); subsequently, ethanol can readily react producing methane, carbon dioxide and hydrogen (red frame); for this reason, ethanol may not be observed by HPLC analysis. The second pathway involves the hydrogenation of lactic acid (using the hydrogen produced from ethanol APR) leading to propionic acid (green frame), that will subsequently lead to ethane and carbon dioxide, as reported in [128].

We tried to verify this hypothesis looking at the results of lactic acid conversion vs time evolution. At 0 h, 4.0 mmoles of methane have been produced; it follows that, according to the proposed reaction scheme, 8.0 mmoles of hydrogen and of carbon dioxide should be obtained as well (experimentally, 8.8 mmoles of CO<sub>2</sub> were quantified). The presumed amount of hydrogen was not detected as it almost completely reacted to produce propionic acid (9.4 mmoles detected at 0 h). From this point on, only propionic acid slowly reacted: from 0 to 8 h, 3.9 mmoles of propionic acid converted into carbon dioxide (3.7 mmoles measured increase from

0 h to 8 h) and ethane (3.4 mmoles measured increase over the same time), as the stoichiometry in the proposed scheme suggests.

The simplified scheme in Figure 59, although not fully comprehensive of the possible reaction pathways involved in lactic acid conversion, is in fair agreement with the experimental observations, notwithstanding the possible uncertainties in gas and liquid phase quantifications.

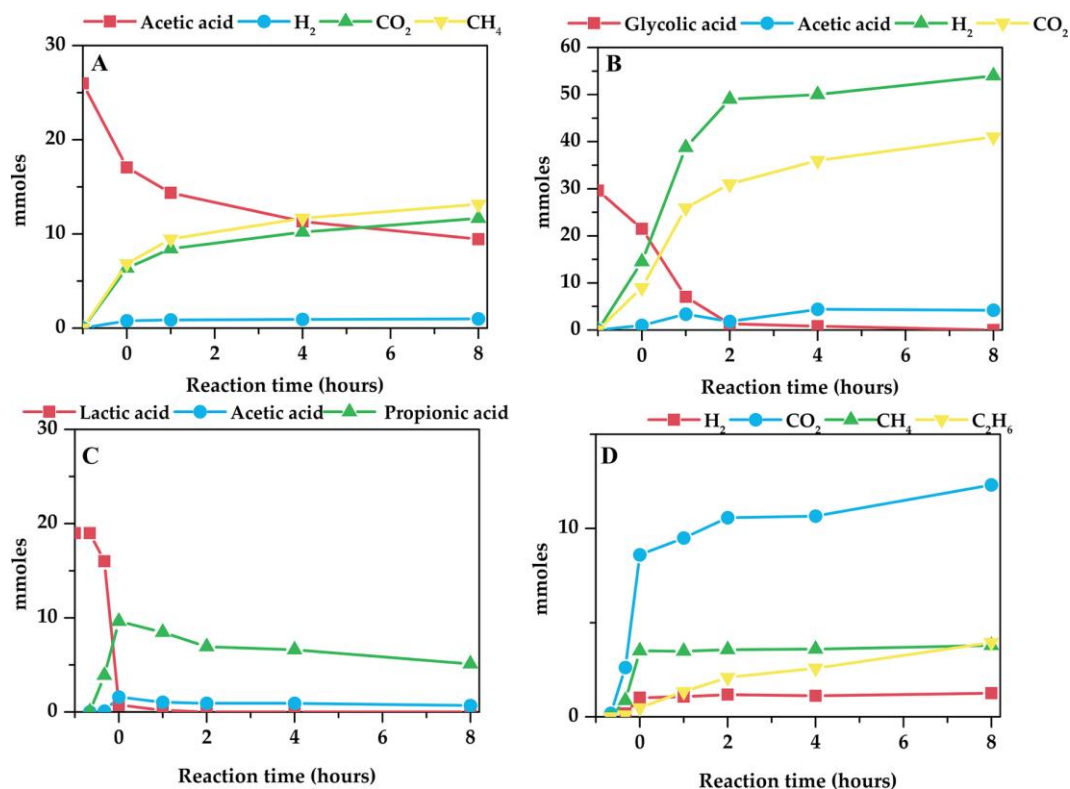


Figure 58. Amount-time profile for APR of acetic acid (A), glycolic acid (B), Lactic acid (C-D). Reaction conditions: 0.375 g 5% Pt/C, Liquid phase amount: 75 g, 0.9 wt.% C feed, Temperature 270°C.

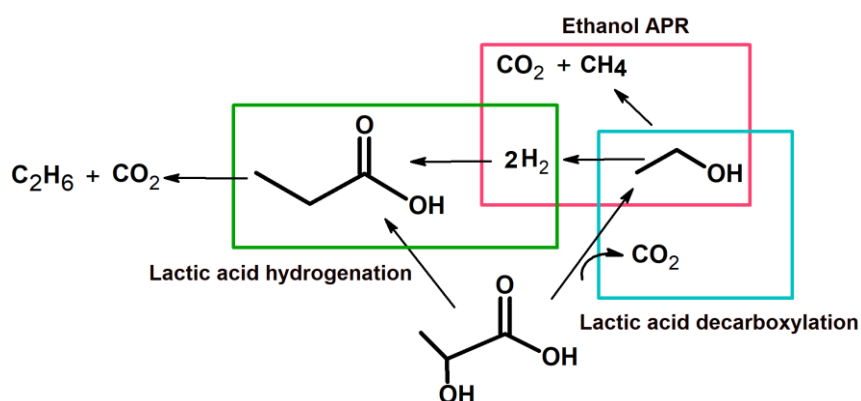


Figure 59. Proposed reaction scheme for lactic acid APR.

## 6.2.2 HTL aqueous phase synthetic mixture

Glycolic, acetic and lactic acid were tested in a ternary mixture with global 0.9 wt.% C concentration, equally divided in each component (Figure 60). It was previously observed that the molecules own different reactivity if they are tested alone or in mixture, likely because of competitive adsorption issues [128]. In the present study, we further investigated this aspect, looking at the influence of the reaction time.

Some characteristic outcomes can be highlighted. First of all, it was observed that glycolic acid was the compound with the highest initial rate of consumption, reaching 92% of conversion during the heating period. Hydrogen and carbon dioxide were produced from glycolic acid with the same selectivity reported in the single test, i.e. about 1:1.5 ratio hydrogen: carbon dioxide, and 1 mole of CO<sub>2</sub> per mole of glycolic acid converted. On the other hand, lactic acid, that almost disappeared in the test reported in the previous section, showed an initial low conversion. This result suggests a clear competition in the adsorption of the molecules on the active sites. In the case of the mixture, the adsorption of a reactant implicates also the displacement of the other adsorbed specie, leading to a more complex scenario compared to the test with a single compound [172]. It can be hypothesized that glycolic acid and lactic acid, co-adsorbing on the surface sites, limited the adsorption of acetic acid and, as a consequence, decreased strongly its reactivity [173]. The conversion of acetic acid from 2 h to 8 h led to the selective increase of carbon dioxide and methane in 1:1 ratio, with the same selectivity noted in the single test.

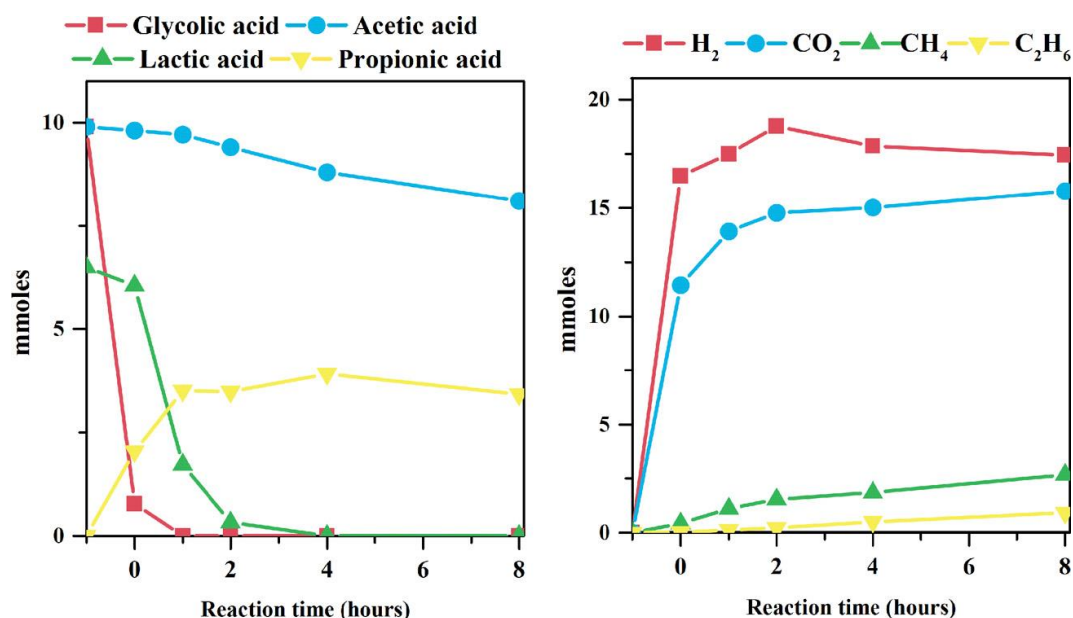


Figure 60. Amount-time profile for APR of a synthetic ternary mixture. Reaction conditions: 0.375 g 5% Pt/C, Liquid phase amount: 75 g, total 0.9 wt.% C glycolic, acetic and lactic acid (0.3 wt.% C per component), 270 °C reaction temperature.

In the following Figure 61-A the influence of the total carbon concentration on the APR parameters is reported. A decrease in the carbon conversion to gas

from 35 to 20% was observed, while the hydrogen gas distribution and the APR H<sub>2</sub> selectivity increased from 59% to 82% and from 47% to 68% respectively. The different trends between the conversion and the selectivity led to an almost constant hydrogen yield in the investigated range of carbon concentration. In order to understand this behaviour of the mixture, it is interesting to observe the conversion of each molecule (Figure 61-B). Moving from 0.3 to 0.9 wt.% of carbon, glycolic acid still fully converted and lactic acid up to 90%, while acetic acid remained almost unconverted. Due to this different reactivity, likely linked to the previously described influence of reaction time, the carbon conversion to gas decreased, but the selectivity increased (mainly thanks to the intrinsic high selectivity of glycolic acid). In an analogous way, the increase of the selectivity from 0.9 to 1.8 wt.% can be explained. Indeed, as the conversion of the lactic acid decreased to 20%, the produced gas phase was mainly ascribed to the conversion of glycolic acid.

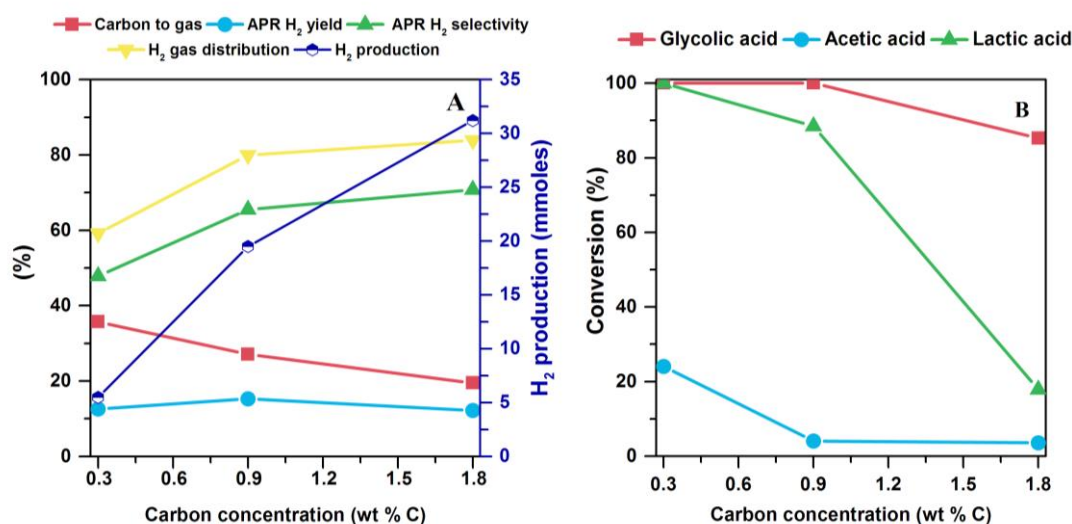


Figure 61. Influence of carbon concentration on the reaction parameters (A) and conversion (B) of APR of the synthetic mixture. Reaction conditions: 0.375 g 5% Pt/C, Liquid phase amount: 75 g, 270°C reaction temperature, 2 h reaction time.

Finally, the influence of the reaction temperature is reported in Figure 62. A constant increase of the carbon to gas conversion was observed, in accordance to literature, due to the more readily breakable C-C bond [39]. The APR-H<sub>2</sub> selectivity decreased slightly from 250 and 270 °C because of the higher carbon dioxide production due to the higher conversion of acetic acid. At the same time, the higher reactivity of acetic acid at higher temperature led to higher production of methane and, therefore, to a smaller hydrogen gas distribution.

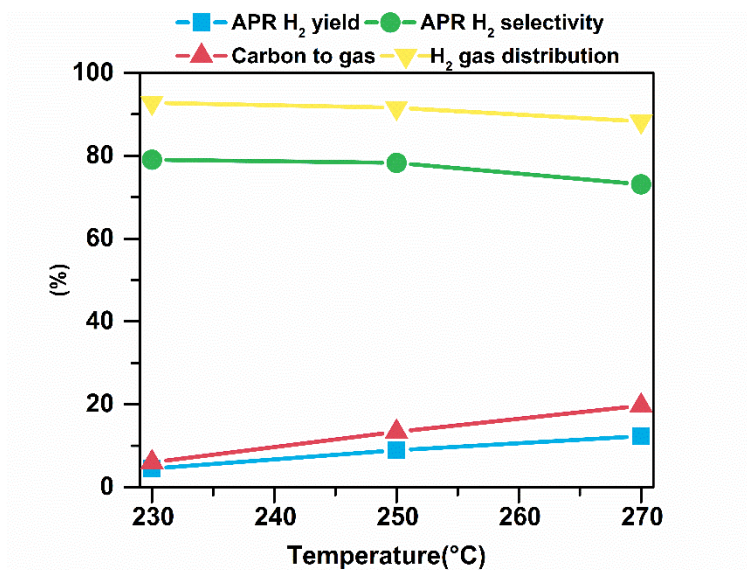


Figure 62. Influence of reaction temperature on the reaction parameters of APR of the synthetic mixture. Reaction conditions: 0.375 g 5% Pt/C, Liquid phase amount: 75 g, 1.8 wt. % C, 2 h reaction time.

### 6.2.3 Case study: APR of the water fraction from HTL of lignin

#### *Characterization of the aqueous phase*

In order to assess the possible valorization of the aqueous phase from biomass hydrothermal liquefaction via APR, an organics-laden aqueous stream originated from the HTL of lignin was investigated. Indeed, the available literature lacks on knowledge about the APR of real water streams, underestimating the complexity deriving from mixtures of compounds, inorganics etc.

Few works reported an extensive characterization of the products of lignin HTL [174]. In the following Table 13, the classification and quantification of the main compounds present in the water are reported. While the sample named simply “HTL-AP” was obtained with a separation by gravity filtration, the samples named “Treated HTL-AP x” were obtained washing with an excess diethyl ether in a 5:1 ratio to reduce the phenolic compounds concentration, whose motivation will be clearer in the following. From the HPLC and GC analysis, it was possible to identify most of the compounds in the water fraction (approximately 70% of the total organic content). Figure 63 shows the HPLC chromatograms of the HTL-AP sample. Several classes of compounds were identified, such as carboxylic acids (e.g. acetic acid, glycolic acid, lactic acid), alcohols (methanol, ethanol, 2-propanol), ketones (acetone), polyalcohols (glycerol), aromatics (phenol, catechol, guaiacol) and aldehydes. As it can be noticed, the screening of model compounds performed in the paragraph 6.2.1 reflects the species found in the actual aqueous phase.

Methanol is the most present compound, followed by lactic acid, phenolic compounds, glycolic acid, acetic acid and glycerol. Moreover, the quantification of inorganic species (sodium, calcium, potassium, sulphur and phosphorous) is given in the same table. As far as the total organic content is concerned, the tested samples have a carbon content of around 1 wt.% C. This value is lower than the typical ones reported in literature from the hydrothermal liquefaction of lignocellulosic biomass [144].

The storage of the sample was carried out at  $-5^{\circ}\text{C}$ : despite the low temperature, the formation of solid particles was observed during storage, likely due to oligomerization reactions involving the phenolic compounds [175]. In order to evaluate the influence of this solid phase, two tests were performed with and without a filtration of the aqueous phase. Both carbon conversion and hydrogen production were negatively affected by the presence of the particles: the former doubled and the latter became three times higher in the case of filtrated solution. For this reason, as they can contribute to affect the activity and the stability of the catalyst, a pre-filtration of the as-received liquid phase was performed in the following experimental campaign with a  $0.2\ \mu\text{m}$  nylon filter.

Table 13. HTL-AP quantification of main compounds and ICP analysis.

Sample	Carbon weight concentration (wt. % C)						Inorganic species (ppm)					Total organic carbon (mgC/L)
	Glycolic	Lactic	Acetic	Methanol	Glycerol	Phenolic compounds	Na	K	Ca	S	P	
HTL-AP	0.047	0.112	0.083	0.138	0.029	0.116	518	281	13	116	11	11558
Treated HTL-AP 1	0.049	0.102	0.078	0.124	0.022	0.056	190	140	15	19	1	10810*
Treated HTL-AP 2	0.051	0.109	0.051	0.099	0.020	0.017	n.a.	n.a.	n.a.	n.a.	n.a.	10540*
Treated HTL-AP 3	0.050	0.099	0.044	0.096	0.020	$\approx 0$	350	233	0	53	43	10358*

\*excluding DEE

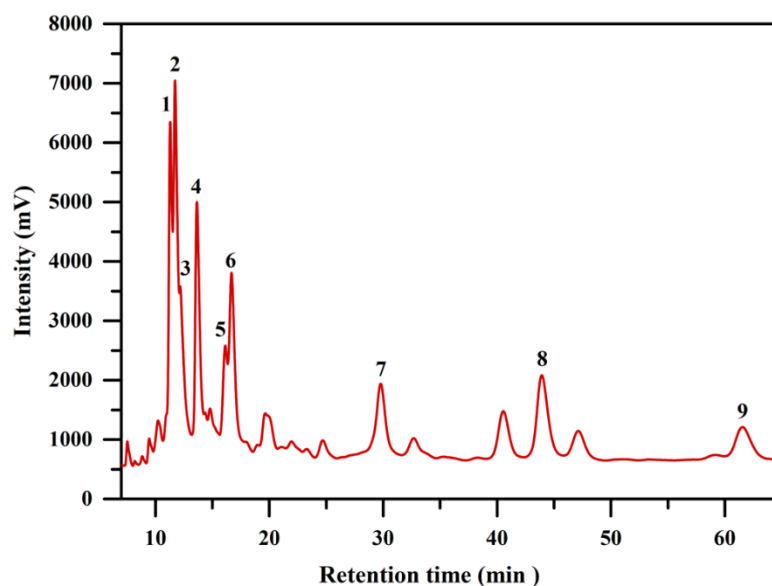


Figure 63. HPLC chromatograms of the HTL-AP (1: glycolic acid, 2: lactic acid, 3: glycerol, 4: acetic acid, 5: acetaldehyde, 6: methanol, 7: catechol, 8: phenol, 9: guaiacol).

### *HTL-AP catalytic tests*

The influence of the carbon concentration on the carbon to gas conversion and hydrogen production of the APR of the HTL-AP is shown in the Figure 64. It is important to highlight that the amount of hydrogen (reported in mmoles) obtained in the gas phase decreased strongly at increasing carbon concentration. This was a surprising result, as the increase of the concentration may surely negatively affect the hydrogen yield, but the amount of product should at least remain constant (unless of the rare case of kinetics with negative reaction orders).

In Figure 65 (right) the chromatogram of the feed and liquid product of the APR performed on 1 wt.% C HTL-AP is reported (named in the figure Product 1<sup>st</sup> test). It is possible to notice a similar peak intensity of most of the present molecules in the APR product (glycolic acid, lactic acid, glycerol, methanol) with respect to their original content in the feed, leading to a low carbon conversion to gas and a negligible hydrogen production. This outcome was not coherent with the previous results reported for the synthetic mixture (paragraph 6.2.2), where glycolic and lactic acid were highly reactive and converted completely before the end of the reaction.

In order to exclude an experimental error, the obtained solution after the filtration was subjected again to an APR test, using a fresh catalyst. The HPLC chromatogram of the liquid APR product obtained at the end of the 2<sup>nd</sup> test is reported in Figure 65 (left) and is compared to the one at the beginning of the test, which in fact is the liquid phase obtained after the 1<sup>st</sup> test.

As it can be noticed, thanks to the 2<sup>nd</sup> test, most of the initially present compounds were converted, being the peaks of glycolic acid, lactic acid, glycerol

and methanol almost disappeared. Please note that the higher conversion cannot be due to the global longer reaction time (as the HTL-AP was subjected in this way to two runs, each one at 2 hours) because a test performed on a HTL-AP for 4 h reaction time led to the same result obtained with the 2 h test.

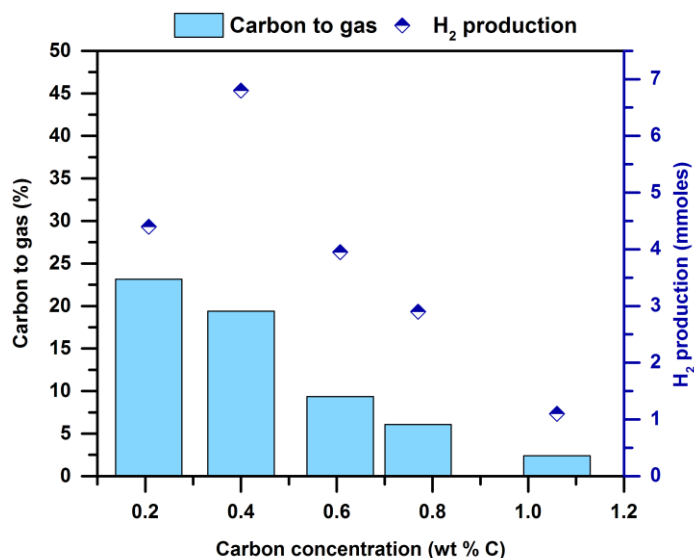


Figure 64. Influence of carbon concentration on reaction parameters of APR of the HTL-AP. Reaction conditions: 0.375 g 5% Pt/C, Liquid phase amount: 75 g, 270°C reaction temperature, 2 h reaction time.

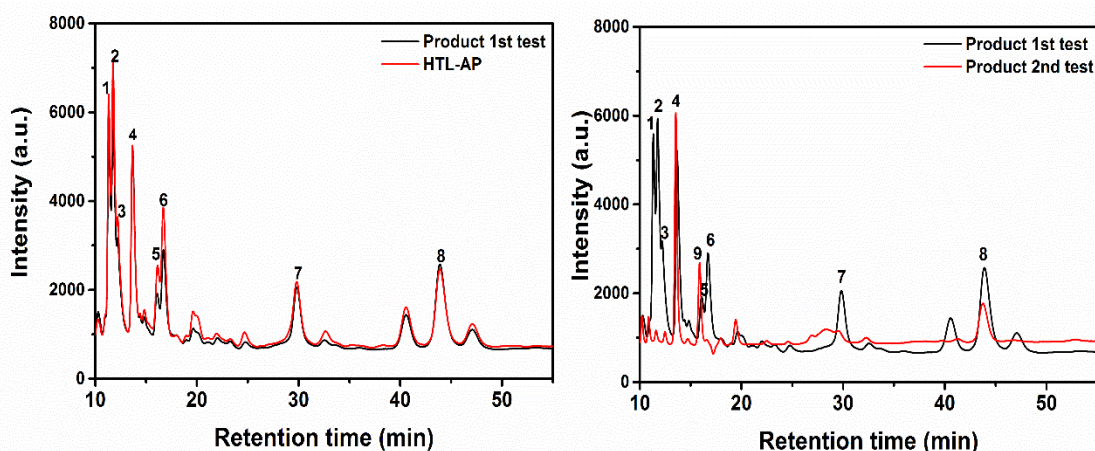


Figure 65. HPLC chromatograms of the feed and product for the first test (left) and second test (right) of the HTL-AP sample. Reaction conditions: 0.375 g 5% Pt/C, wt.% C feed, 270°C reaction temperature, 2 reaction time (1: glycolic acid 2: lactic acid 3: glycerol 4: acetic acid 5: acetaldehyde 6: methanol 7: catechol 8: phenol 9: propionic acid).

The higher conversion in the 2<sup>nd</sup> test led to a higher hydrogen production, as showed in Figure 66-A, where the hydrogen productivity (i.e. the hydrogen production normalized by the moles of carbon in the feed) is reported for the 1<sup>st</sup> and 2<sup>nd</sup> tests. It can be observed that the 2<sup>nd</sup> test reported a higher and almost constant hydrogen productivity, contrarily to the trend obtained by the 1<sup>st</sup> runs, that was decreasing in the entire range of carbon concentrations investigated. It is



highlighted here how the 2<sup>nd</sup> test had a lower starting carbon concentration compared to the corresponding 1<sup>st</sup> test. This is due to the impossibility to recover the entire liquid phase after the first reaction and, secondarily, to the low but not negligible conversion obtained during the 1<sup>st</sup> test.

The sum of the hydrogen mmoles produced during 1<sup>st</sup> test (black) and 2<sup>nd</sup> test (red) are showed in Figure 66-B. It can be observed that the decreasing trend observed in the 1<sup>st</sup> runs, was substituted by an almost constant hydrogen production (about 10 mmoles) if the 2<sup>nd</sup> tests are added to the 1<sup>st</sup> ones.

The dramatic difference in the performance between 1<sup>st</sup> and 2<sup>nd</sup> test denoted the probable deactivation of the catalyst because of species (organic or inorganic) present during the first test. For this reason, the next paragraph is devoted to the investigation of this important issue, hardly reported in literature because of the lack of study on HTL-derived actual streams.

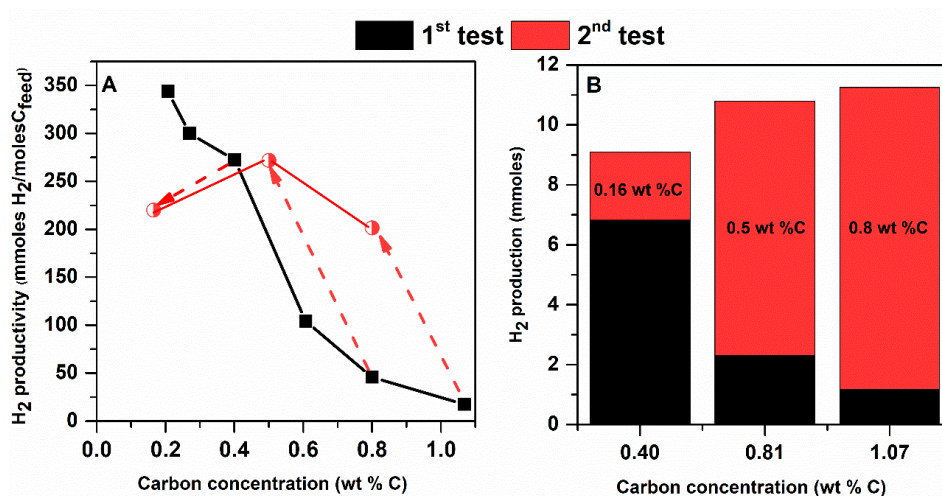


Figure 66. H<sub>2</sub> productivity (A) and H<sub>2</sub> production (B) for the APR of HTL-AP. Reaction conditions: 0.375 g 5% Pt/C, Liquid phase amount: 75 g, 270°C reaction temperature, 2 h reaction time.

### *Deactivation of the catalyst*

In order to assess the hypothesis of catalyst deactivation, further experiments were performed, and the spent catalysts characterized.

As it was assumed an endogenous deactivation, the stability of the catalyst could not be evaluated with the common procedure of re-using the catalyst with a fresh solution. In fact, we would have observed still a negligible conversion, and no other conclusion could have been drawn. For this reason, it was decided to test the stability of the catalyst versus a reactive reference compound. The catalyst used during the 1<sup>st</sup> APR run on HTL-AP was recovered, dried overnight (105°C) and used for the APR of glycolic acid (formerly proven to provide high H<sub>2</sub> yields).

The carbon to gas conversion and hydrogen production of the reference test (obtained with a fresh catalyst) and of the runs with two used catalysts are

compared in the following Figure 67. We previously assessed that the stability of the catalyst was maintained after an APR run with glycolic acid, therefore the differences cannot be ascribed to the hydroxyacid itself.

The catalyst used with the HTL-AP showed a serious deactivation: the conversion of the glycolic acid in the liquid phase decreased from 91% to 20%. On the other hand, the test named “Treated HTL-AP 3” is the APR of glycolic performed with the catalyst that had previously undergone an APR test with the treated HTL-AP 3 aqueous phase reforming. It is important to observe that the deactivation was still present, but at a lower extent than the previous one referred to the APR of an untreated feed (HTL-AP). Indeed, the conversion of glycolic acid raised to 42%, with the carbon to gas and the hydrogen production more than doubled.

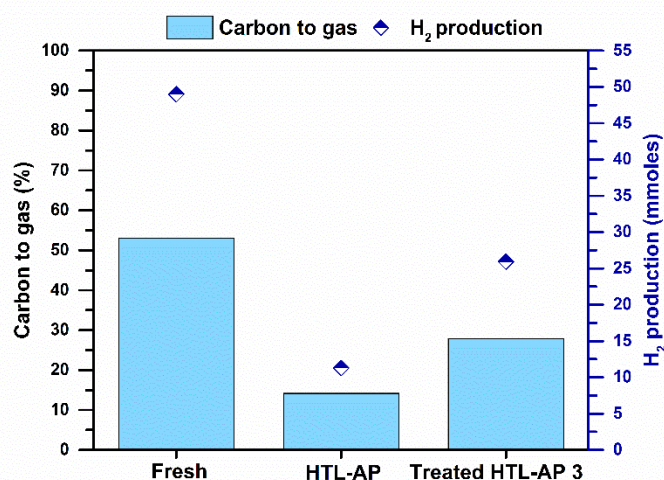


Figure 67. APR of glycolic acid with different catalysts. Reaction conditions: 0.375 g 5% Pt/C, Liquid phase amount: 75 g, 0.9 wt.% C glycolic acid, reaction temperature 270°C, reaction time 2 h.

Two main reasons were investigated to explain the deactivation of the catalyst, i.e. the presence of phenolic oligomers and sulphur-containing molecules.

HTL-AP solution washed with diethyl-ether had the effect of selectively removing the phenolic compounds from the water, while keeping the other organic compounds nearly unchanged in terms of concentration in the water (Table 13). Afterwards, they were tested to assess if the phenolics can be associated to the catalyst deactivation. Few works studied the deactivation of noble metal catalyst in the presence of phenolics, and no works were found in the currently investigated APR conditions with Pt/C as a catalyst. APR of glycerol with the purpose of hydrogenating phenol in-situ was studied with Raney Ni<sup>®</sup> [176]: the investigation showed an improvement of glycerol conversion due to the shift of the equilibrium. On the other hand, other researchers reported catalyst deactivation due to deposits formation on the catalyst surface, in different reaction conditions. Hydrodeoxygenation (HDO) of guaiacol with noble metal catalysts (Pt, Pd, Rh, Ru) supported on activated carbon led to catalyst deactivation due to polyaromatic deposits in different extents for each catalyst [177]. The catalytic

wet air oxidation of phenol was studied on Pt/Al<sub>2</sub>O<sub>3</sub> and Pt/CeO<sub>2</sub> during the reaction deposit of carbonaceous material were deposited on the catalyst leading to a catalyst deactivation [178]. De Souza et al. studied the HDO of phenol over Pd catalyst with different supports; they assessed a deactivation of the catalyst supported on Al<sub>2</sub>O<sub>3</sub>, SiO<sub>2</sub>, TiO<sub>2</sub> and ZrO<sub>2</sub> [179].

From a preliminary glance, it is not possible to infer in our case that the deactivation is due to the presence of phenolic monomers (phenol, guaiacol, catechol). As reported in Figure 65 (left), there is no apparent difference between the feed and the 1<sup>st</sup> test product in terms of the phenolics amount. However, there was an improvement of the performance in 2<sup>nd</sup> test: it is more likely that phenolic oligomers, not visible in the HPLC analysis, underwent polymerization during the 1<sup>st</sup> reaction, blocking the pores of the catalyst (as suggested by the textural analysis in the following), which therefore acted as a sacrificial adsorbent that removed them from the product of the 1<sup>st</sup> test. Consequently, these compounds were likely absent in the 1<sup>st</sup> test product and consequently did not affect the catalyst in the 2<sup>nd</sup> test.

For this reason, the phenolic compounds were removed via an HTL-AP treatment with DEE, whose effect was is showed in Figure 68. As observed in the chromatogram, the main consequence of washing the aqueous phase with the organic solvent is the elimination of phenolics (monomers and presumably also oligomers), without affecting the concentration of the remaining compounds. This is an important result, because it allows an easier interpretation of the results as only the different concentration of aromatics can be considered. Each treatment was able to extract different amount of phenolics, depending on *a-posteriori* evaluated effectiveness of the procedure. In the side-table, the phenolic content (guaiacol peak number 10, phenol peak number 9 and catechol peak number 8) of these batches are reported.

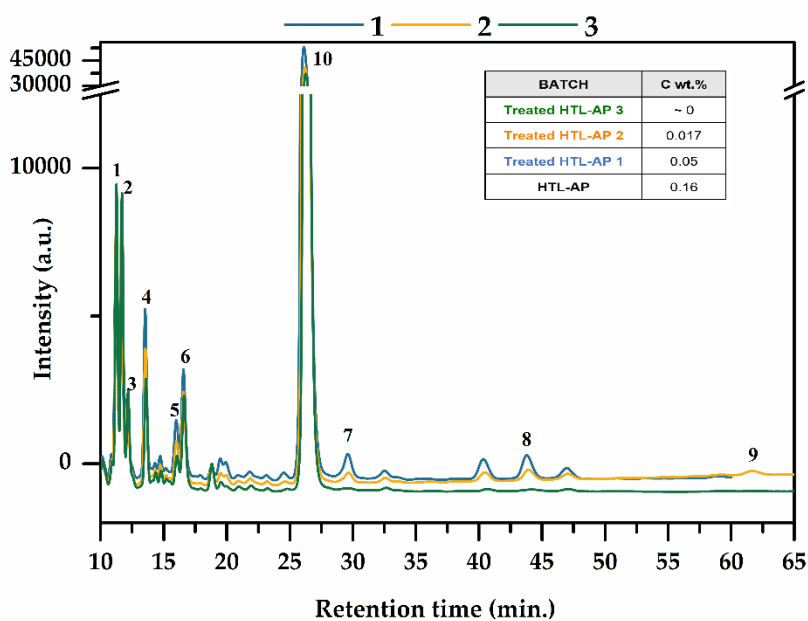


Figure 68. HPLC chromatograms of HTL-AP and treated HTL-AP feeds (1: glycolic acid 2: lactic acid 3: glycerol 4: acetic acid 5: acetaldehyde 6: methanol 7: catechol 8: phenol 9: guaiacol 10: DEE).

The hydrogen production as a function of carbon concentration (excluding diethyl-ether) is reported in the following Figure 69; when the phenolics content increased, the hydrogen production decreased to reach almost zero at the highest phenolics content. Moreover, it is clearly highlighted the difference in the hydrogen production between 1<sup>st</sup> and 2<sup>nd</sup> test on the HTL-AP, but in comparison to the treated HTL-AP 1. Finally, it can be observed that the treated HTL-AP 3 (with no detected phenolics) led to a trend analogous to the synthetic mixture, with a hydrogen productivity almost constant on the investigated carbon concentration range, equal to 300 mmol H<sub>2</sub>/mol C.

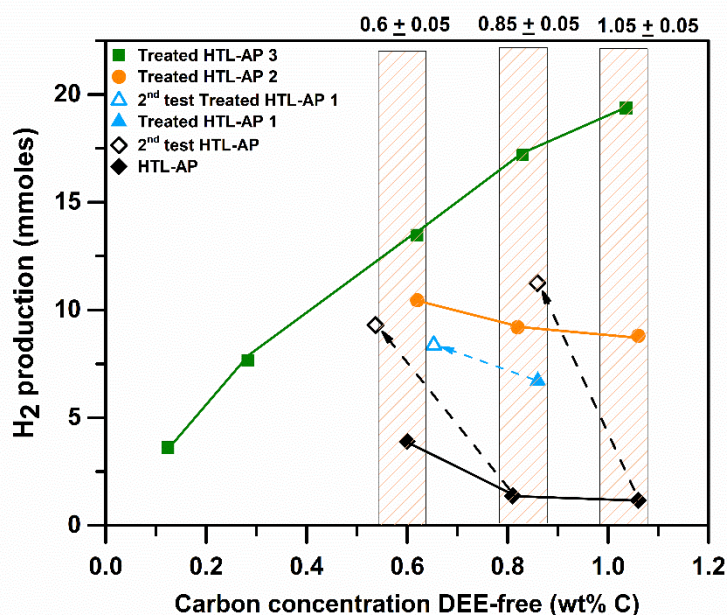


Figure 69. Influence of carbon concentration and DEE pretreatment on the H<sub>2</sub> production for APR of different batches. Reaction conditions: 0.375 g 5% Pt/C, Liquid phase amount: 75 g, 270 °C reaction temperature, 2 h reaction time.

In order to assess the contribution of DEE to the hydrogen production, we performed the APR of DEE alone and together with the synthetic mixture glycolic/acetic/lactic acid. As reported in the Table 14, the amount of the main produced gas during the aqueous phase reforming of the synthetic mixture with and without DEE is almost identical. This means that the addition of the solvent for the removal of the phenolics did not change the product distribution and the hydrogen yield. It is highlighted that, despite the APR of DEE (0.9 wt.% C) produced considerable amount of hydrogen, the different selectivity in terms of methane/hydrogen ratio in the synthetic mixture + DEE test and in the DEE-alone test suggests that its conversion is negligible in the mix test, therefore negligible in terms of hydrogen production. The reason may be ascribed to the competitive

adsorption of DEE against, for example, glycolic and lactic acid, which are readily converted.

Table 14. Aqueous phase reforming of synthetic mixtures with and without DEE. Reaction conditions: 0.375 g 5% Pt/C, Liquid phase amount: 75 g, 0.9 wt.% C acids + 0.9 wt.% C DEE, 270 °C reaction temperature, 2 h reaction time.

Test	Hydrogen (mmoles)	Carbon dioxide (mmoles)	Methane (mmoles)
Synthetic mixture	19.5	16.1	2.0
Synthetic mixture + DEE	20.6	16.5	2.2
DEE	4.9	3.6	4.0

The textural analysis of some selected catalysts, together with the characterization of the fresh one, is reported in the Table 15 . The catalyst used for the APR of the HTL-AP (i.e. with the highest content of phenolics) showed the highest decrease of the surface area and pore volume, indicating that high molecular weight compounds blocked the pore of the catalysts, reducing the availability of active sites for the reaction. Coherently with the reported results, both the pore volume and surface area of the catalyst used for the 2<sup>nd</sup> test of the HTL-AP sample were higher than the former. Analogously, the catalyst used for the APR of the treated HTL-AP 3 (i.e. with negligible content of phenolics) showed a minor loss of textural properties compared to the untreated feed. It can be noticed anyway a strong difference compared to the fresh catalyst, that is in line with the results reported with the glycolic acid, where a worsening of the performance was noticed anyway.

Table 15. Textural characteristic of the fresh and spent catalysts.

Sample	BET surface area (m <sup>2</sup> /g)	Pore Volume (cm <sup>3</sup> /g)	Average pore size (nm)
Fresh	923	0.632	5.1
HTL-AP 0.8% C	195	0.344	5.7
HTL-AP 1.1% C	216	0.361	5.6
HTL-AP 1.1% 2 <sup>nd</sup> test	430	0.480	5.2
Treated HTL-AP 3 0.8% C	410	0.471	5.3

The spent catalysts were also characterized thanks to thermogravimetric analysis coupled with infrared spectroscopy.

The fresh catalyst showed a total weight loss equal to 15 wt.% when exposed to a heating treatment up to 1000 °C under inert flow, divided into three different steps: the first one, with a maximum at 80°C, due to the loss of adsorbed water; the second step, between 200°C and 600°C, was due to the decomposition of the carbon support, which is composed from a certain percentage of oxygen, with formation of carbon dioxide; the third step is a further decomposition of the carbon substrate with formation of carbon monoxide [180]. In fact, the infrared analysis of the curves of developed gasses showed a maximum for water at

around 100°C, a maximum at 600°C for CO<sub>2</sub> and an increase in CO concentration over the 600°C.

The TGA analyses of the spent catalysts showed that the weight loss is quite similar for all the catalysts, ranging from 15 to 20 wt.%. Please note that this information cannot be directly linked to the amount of deposits on the catalyst as the tests were not performed in an oxidative environment to allow the IR analysis of the evolved species. However, the degradation products were quite different whether the catalyst was used for a 1<sup>st</sup> or 2<sup>nd</sup> test (Figure 70 and Figure 71, respectively).

On one hand, the spent catalysts used for the 1<sup>st</sup> tests showed the presence of degradation products such as CO<sub>2</sub>, CO, H<sub>2</sub>O, aliphatic fragments and the presence of primary alcohols; for the sake of representativeness, the TGA-IR of the sample HTL-AP is reported in the Figure 71 (analogous results were obtained for the samples treated HTL-AP 1 and treated HTL-AP 2).

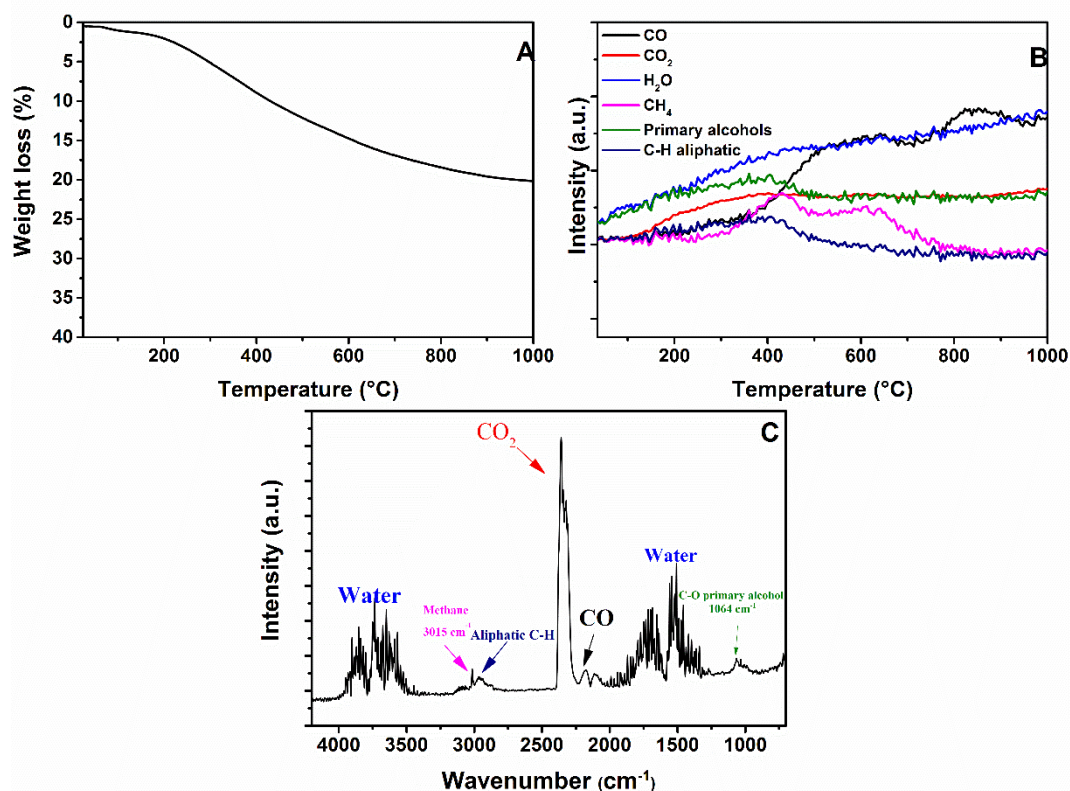


Figure 70. TGA-IR of spent catalyst after APR 1<sup>st</sup> test of HTL-AP. Reaction conditions: 0.375 g 5% Pt/C, 0.8 wt.% C, reaction temperature 270 °C, reaction time 2 h. Analysis conditions: heat from 30 °C to 1000 °C @ 20 °C/min in nitrogen atmosphere with a purge rate of 20 mL/min under nitrogen. A: TG results; B: IR-Absorption peak during TGA of water, CO<sub>2</sub>, CH<sub>4</sub>, aliphatic fragments and primary alcohols; C: Infrared spectra at 408°C.

The degradation of the catalyst occurred in a single step with a maximum of degradation speed at about 383 °C (from the slope of the weight loss curve in Figure 70-A). The main volatile products of this degradation were visible in the infrared spectra at 408 °C (Figure 70-C). The infrared spectra showed the presence of water, carbon dioxide, carbon monoxide, and methane derived from the degradation of the organic substrate adsorbed on the catalyst. The spectra

showed also more complex degradation products: between 2800 and 3000  $\text{cm}^{-1}$  the stretching of  $\text{CH}_2$  and  $\text{CH}_3$  from aliphatic fragments were easily recognized, while the band at 1064  $\text{cm}^{-1}$  is typical of primary alcohols. From the figure it was possible to consider that the first part degradation is mainly due to the evaporation of aliphatic compounds containing alcohols, while at higher temperatures the organic compounds (presumably of higher molecular weight and non-volatile at these temperatures) decomposed to form carbon monoxide, carbon dioxide, methane and water. The presence of alcoholic species can be considered as an indication of the low reactivity of these catalysts. Indeed, it was showed throughout the present work as the alcohols are characterized by high reactivity: for this reason, their presence on the surface of the catalyst states the sites are not available for activating the breaking of the molecules. The characteristic band of phenolics in the gaseous phase are located at about 3650  $\text{cm}^{-1}$ , 3100-3000  $\text{cm}^{-1}$  and 1600-1500  $\text{cm}^{-1}$ . However, these bands are covered from water and methane, therefore it was not possible to recognize the presence of phenol, guaiacol, catechol or other molecules containing phenolic groups.

On the other hand, different phenomena were observed for the catalysts used for the 2<sup>nd</sup> tests investigation and similarly for the treated HTL-AP 3 (that is the batch without phenolic content and with the best performance). In these cases, the main degradation step of the catalyst used for the second test of the feed HTL-AP, had a maximum at 322 °C (Figure 71-A). The degradation products in the first part of this step, namely below 200 °C, were mainly  $\text{CO}_2$  and volatile organic molecules with anhydride functionalities as underlined from the CO asymmetric and symmetric stretching at 1792 and 1773  $\text{cm}^{-1}$  and from the COC stretching at 1174  $\text{cm}^{-1}$  in Figure 71-B and from the IR adsorption peak during TGA (Figure 71-D). Above 300 °C, more complex organic fragments are produced with an increase of the stretching of  $\text{CH}_2$  and  $\text{CH}_3$  from aliphatic fragments between 2800 and 3000  $\text{cm}^{-1}$  and the appearance of a small quantity of water (Figure 71 C-D). At temperatures higher than 500 °C the degradation products are mainly water,  $\text{CO}_2$  and CO (Figure 71-B). This behaviour was similar for all the spent catalysts with high conversion in APR experiments (i.e. used in the 2<sup>nd</sup> tests or in the absence of detectable phenolic content). In these cases, the alcohols were not identified, giving an indication of the higher reactivity of these catalysts; at the same time, anhydride peaks were present. It can be supposed that the anhydrides derived from the reaction of the carboxylic acids formed during dehydrogenation reaction that underwent dehydration during the TGA. The presence of carboxylic acids can be a further proof of the better performance of the catalysts as they are by-products of alcohols reforming [128].

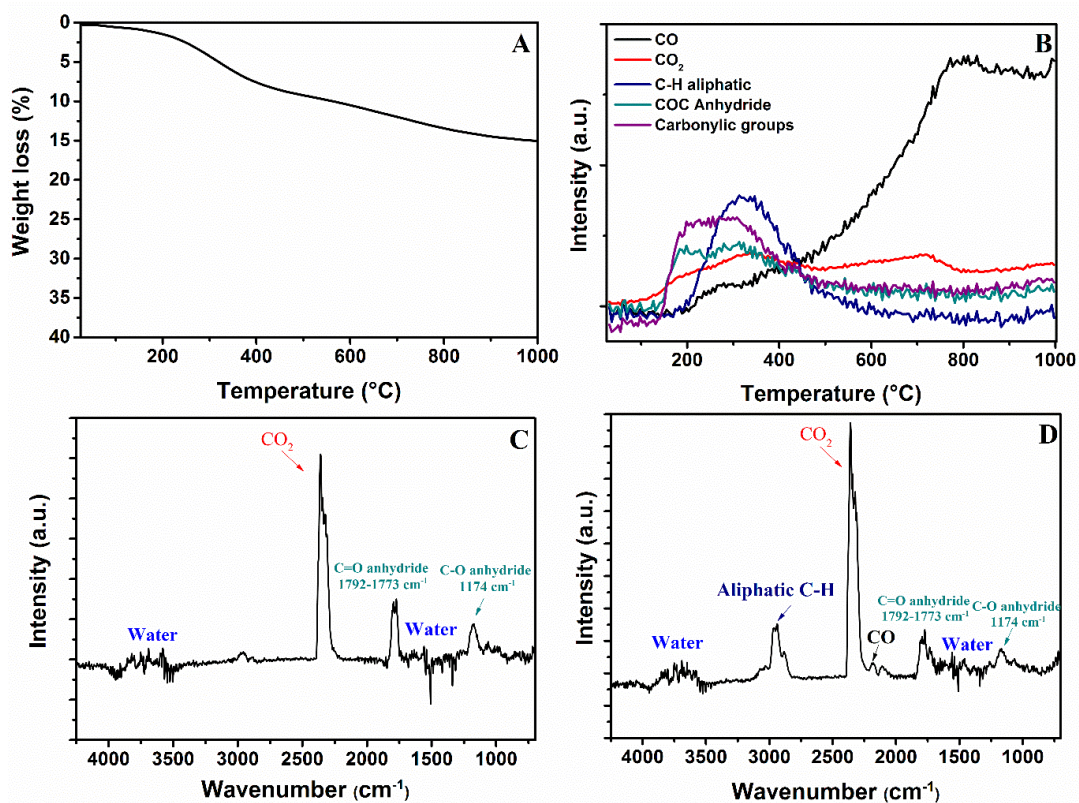


Figure 71. TGA-IR of spent catalyst after APR 2<sup>nd</sup> test of HTL-AP. Reaction conditions: 0.375 g 5% Pt/C, 0.8 wt.% C, reaction temperature 270 °C, reaction time 2 h. Analysis conditions: heat from 30 °C to 1000 °C @ 20 °C/min in nitrogen atmosphere with a purge rate of 20 mL/min under nitrogen. A: TG results; B: IR-Absorption peak during TGA; C: Infrared spectra at 198°C; D: Infrared spectra at 298 °C.

The second possible cause of deactivation is related to the presence of organosulfur compounds, derived from lignin. As it is known, sulphur can chemisorb irreversibly on the Pt sites, leading to their deactivation.

ICP-MS analysis was performed on the spent catalyst to assess the presence of sulphur. The catalysts used for APR of HTL-AP and treated HTL-AP 3 showed the existence of sulphur on the catalyst, in the 0.08-0.2 wt.% range. This amount may be enough to explain the worsening of the performance; on the other hand, only the ICP-MS does not allow to understand the degree of interaction of the sulphur with the catalyst.

For this reason, potential chemical bonds between platinum and sulphur have been investigated by XPS. In Figure 16, the XPS spectra of Pt<sub>4f</sub> of fresh and spent catalysts after APR of HTL-AP and treated HTL-AP 3 are reported. First of all, it is observed that the binding energies of the doublet in the fresh catalyst agree with the literature data regarding Pt metal, with the typical 3.33 eV splitting. Moreover, none of the spent catalysts showed an increase in the binding energies, being an indication of the lack of strong (chemical) interactions between the platinum and sulphur [181]. Therefore, based on this result, the sulphur poisoning can be reasonably excluded as cause for the catalyst deactivation and its presence may be ascribed to the physical adsorption of S-containing species compounds on the



high surface-area carbon support and to a negligible extent to the chemisorption on the active sites.

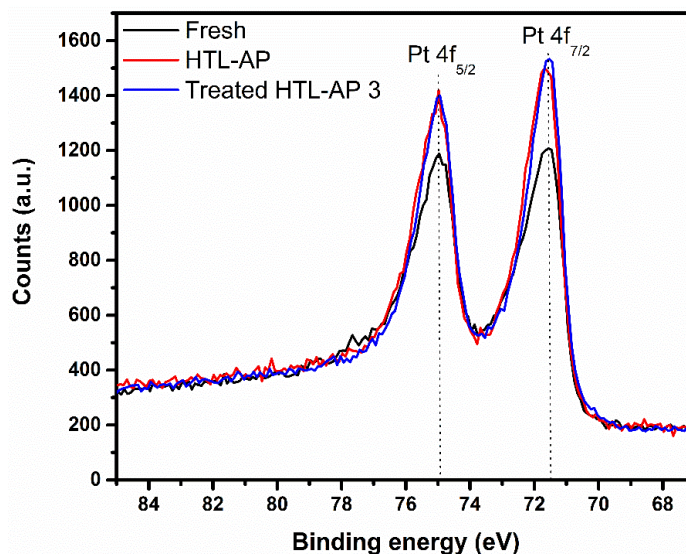


Figure 72. XPS spectra of fresh and spent catalysts after aqueous phase reforming. Reaction conditions: 0.375 g 5% Pt/C, 0.8 wt.% C feed (HTL-AP or treated HTL-AP 3), 270 °C reaction temperature, 2 h reaction time.

### 6.3 Conclusion

The water fraction from the hydrothermal liquefaction of lignin was subjected to aqueous phase reforming for the production of hydrogen. A screening performed with representative model compounds allowed to identify the molecules prone to reforming, while the study of a synthetic mixture highlighted competitiveness issues on the active sites. This outcome is particularly crucial for the valorization of secondary streams as they are complex mixtures constituted by several different classes of compounds. The study of the real water fraction showed a dramatic dependence of the performance on the phenolics content, highlighting the necessity of pretreatment of the water phase to increase the stability of the catalyst. Indeed, the lower was the concentration of phenolics (i.e. phenol, guaiacol, catechol) in the feed, the higher was the hydrogen production. The textural characterization showed that the worsening of the performance may be associated to a decrease of the surface area and pore volume, likely due to the fouling mechanism caused by phenolic oligomers. At the same time, sulphur-related poisoning mechanisms were excluded. Despite the coupling of hydrothermal liquefaction and aqueous phase reforming needs further investigation, it gives promising results in the direction of decreasing the need of hydrogen for a biorefinery, helping to reduce both the economic and environmental impact.

# Conclusions

The valorization of aqueous side-streams of biorefineries is a key challenge for the development of sustainable and renewable processes. In the present work, the aqueous phase reforming has been investigated as a possible catalytic process being able of treating a waste stream and leading to a valuable product at the same time, i.e. hydrogen.

The experimental campaign focused on three kind of secondary streams: one generated from the processing of an aquatic biomass; one derived from the bioethanol production; one obtained as by-product from lignocellulosic biomass hydrothermal liquefaction. One of the scopes of the work was going closer to the possible industrial application of APR, looking at single compounds and mixtures readily available in biorefineries.

Alginate, an oligosaccharide, was used to mimic the carbohydrate fraction of aquatic biomass. Several reaction conditions were analysed (effect of alginate, catalyst loading, temperature, time reaction, pH, hydrogen partial pressure). Among the others, the variation of pH showed a strong effect on the APR performance, increasing by one order of magnitude the hydrogen selectivity when it was carried out in basic conditions.

Sugars and sugar alcohols were investigated as representatives of the bioethanol production chain. Moreover, a stream derived from the hydrolysis step of a bioethanol plant was subjected to APR to produce hydrogen. The influence of the reaction temperature and carbon concentration were systematically investigated, even for synthetic binary mixtures. The pre-hydrogenation carried out on the sugar mixture showed a higher hydrogen production, even taking into consideration the amount consumed for the hydrogenation itself. The catalyst characterization showed the presence of humins blocking the pores of the support in the case of the sugar-rich feedstock, while the hydrogenated mixture increased the stability of the catalyst.

Finally, the carbon-laden aqueous phase from hydrothermal liquefaction was modelled looking at seventeen representative compounds. Decarboxylation mechanism appeared as the main pathway for carboxylic acids. Binary and ternary mixtures were tested to understand the behaviour of a possible synthetic biorefinery stream, and it was observed that adsorption kinetics on the catalyst may constitute an issue to overcome (especially for acetic acid). Investigating a real water fraction showed a strong dependence of the performance on the phenolics content, highlighting the necessity of a liquid-liquid extraction pretreatment to increase the activity and stability of the catalyst.

In conclusion, this work allowed to extend the knowledge on APR looking at new classes of molecules, mixtures and real biorefinery side-streams. New reaction pathways were suggested for key molecules (acetic acid, glycolic acid, lactic acid), together with process alternatives (such as the pre-hydrogenation in

the case of sugar streams). The screening of several compounds consented the identification of similarities and differences in the behaviour per classes of molecules. For example, different chemisorption phenomena associated with the sugar mixtures and acids mixtures have been observed; on the other hand, analogies among a complex molecule such as alginate and the corresponding building blocks have been deduced in terms of negative influence of increasing carbon concentration. Moreover, the plateau in the hydrogen production in the study of alginate was linked to the formation of recalcitrant by-products, i.e. carboxylic acids, as confirmed in the study of the HTL-derived water fraction.

Further research on this field is suggested, regarding the transfer of knowledge on continuous set-ups, the identification of new adapt waste streams and the design of more effective and cheap catalysts.

# References

- [1] S. Arrhenius, *Philos. Mag. Journal Sci.* 41 (1896) 237–276.
- [2] C. Wei-Yin, T. Suzuki, L. Maximillian, *Handbook of Climate Change Mitigation and Adaptation*, 2017.
- [3] D. Lüthi, M. Le Floch, B. Bereiter, T. Blunier, J.M. Barnola, U. Siegenthaler, D. Raynaud, J. Jouzel, H. Fischer, K. Kawamura, T.F. Stocker, *Nature*. 453 (2008) 379–382.
- [4] A.J. McMichael, J.W. Powles, C.D. Butler, R. Uauy, *Lancet*. 370 (2007) 1253–1263.
- [5] V. Strezov, *Renewable Energy Systems from Biomass*, 2018.
- [6] REN21, *Renewables 2019 global status report*, 2019.
- [7] International Energy Agency (IEA), (2018) 1–8.
- [8] D.K. Okot, *Renew. Sustain. Energy Rev.* 26 (2013) 515–520.
- [9] G.M. Joselin Herbert, S. Iniyar, E. Sreevalsan, S. Rajapandian, *Renew. Sustain. Energy Rev.* 11 (2007) 1117–1145.
- [10] A. Tummala, R.K. Velamati, D.K. Sinha, V. Indrajaya, V.H. Krishna, *Renew. Sustain. Energy Rev.* 56 (2016) 1351–1371.
- [11] M. Thirugnanasambandam, S. Iniyar, R. Goic, *Renew. Sustain. Energy Rev.* 14 (2010) 312–322.
- [12] N. Kannan, D. Vakeesan, *Renew. Sustain. Energy Rev.* 62 (2016) 1092–1105.
- [13] N.L. Panwar, S.C. Kaushik, S. Kothari, *Renew. Sustain. Energy Rev.* 15 (2011) 1513–1524.
- [14] (n.d.). <https://ourworldindata.org/renewable-energy>.
- [15] F. Cherubini, N.D. Bird, A. Cowie, G. Jungmeier, B. Schlamadinger, S. Woess-gallasch, *Biomass Bioenergy*. 53 (2009) 434–447.
- [16] S.S. Hassan, G.A. Williams, A.K. Jaiswal, *Renew. Sustain. Energy Rev.* 101 (2019) 590–599.
- [17] International Energy Agency (IEA), *Technology Roadmap Delivering Sustainable Bioenergy*, 2017.
- [18] M. Rabaçal, A.F. Ferreira, C.A.M. Silva, M.C. Editors, *Biorefineries Targeting Energy, High Value Products and Waste Valorisation*, 2017.
- [19] E. de Jong, H. Langeveld, R. van Ree, *IEA Bioenergy*. (2013) 28. [http://www.biorefinery.nl/fileadmin/biorefinery/docs/Brochure\\_Totaal\\_definitief\\_HR\\_opt.pdf](http://www.biorefinery.nl/fileadmin/biorefinery/docs/Brochure_Totaal_definitief_HR_opt.pdf).
- [20] F. Cherubini, *Energy Convers. Manag.* 51 (2010) 1412–1421.
- [21] L.J. Konwar, J.-P. Mikkola, N. Bordoloi, R. Saikia, R.S. Chutia, R. Katak, *Sidestreams From Bioenergy and Biorefinery Complexes as a Resource for Circular Bioeconomy*, Elsevier B.V., 2018.
- [22] K. Robak, M. Balcerek, *Food Technol. Biotechnol.* 56 (2018) 174–187.
- [23] V.N. Gunaseelan, *Biomass and Bioenergy*. 13 (1997) 83–114.
- [24] L. Zhang, C. (Charles) Xu, P. Champagne, *Energy Convers. Manag.* 51 (2010) 969–982.
- [25] A. Kumar, D.D. Jones, M.A. Hanna, *Energies*. 2 (2009) 556–581.
- [26] T. Kan, V. Strezov, T.J. Evans, *Renew. Sustain. Energy Rev.* 57 (2016) 1126–1140.
- [27] A. Kruse, A. Funke, M.M. Titirici, *Curr. Opin. Chem. Biol.* 17 (2013) 515–521.

- [28] T. Wang, Y. Zhai, Y. Zhu, C. Li, G. Zeng, *Renew. Sustain. Energy Rev.* 90 (2018) 223–247.
- [29] J. Akhtar, N.A.S. Amin, *Renew. Sustain. Energy Rev.* 15 (2011) 1615–1624.
- [30] A. Kruse, *J. Supercrit. Fluids.* 47 (2009) 391–399.
- [31] M. Usman, H. Chen, K. Chen, S. Ren, J.H. Clark, J. Fan, G. Luo, S. Zhang, *Green Chem.* 21 (2019) 1553–1572.
- [32] Y. Zhu, M.J. Bidy, S.B. Jones, D.C. Elliott, A.J. Schmidt, *Appl. Energy.* 129 (2014) 384–394.
- [33] Y. Chen, J.J. Cheng, K.S. Creamer, *Bioresour. Technol.* 99 (2008) 4044–4064.
- [34] O.K. Dalrymple, T. Halfhide, I. Udom, B. Gilles, J. Wolan, Q. Zhang, S. Ergas, *Aquat. Biosyst.* 9 (2013) 1.
- [35] A. Lavrinovičs, T. Juhna, *Constr. Sci.* 20 (2018) 17–25.
- [36] M.H. Waldner, F. Vogel, *Ind. Eng. Chem. Res.* 44 (2005) 4543–4551.
- [37] R.D. Cortright, R.R. Davda, J.A. Dumesic, *Nature.* 418 (2002) 964–967.
- [38] J.J. Baschuk, X. Li, *Int. J. Energy Res.* 25 (2001) 695–713.
- [39] R.R. Davda, J.W. Shabaker, G.W. Huber, R.D. Cortright, J.A. Dumesic, *Appl. Catal. B Environ.* 56 (2005) 171–186.
- [40] R. Alcalá, M. Mavrikakis, J.A. Dumesic, *J. Catal.* 218 (2003) 178–190.
- [41] G.H. Gu, G.R. Wittreich, D.G. Vlachos, *Chem. Eng. Sci.* 197 (2019) 415–418.
- [42] I. Coronado, M. Stekrova, M. Reinikainen, P. Simell, L. Lefferts, J. Lehtonen, *Int. J. Hydrogen Energy.* 41 (2016) 11003–11032.
- [43] J.W. Shabaker, R.R. Davda, G.W. Huber, R.D. Cortright, J.A. Dumesic, *J. Catal.* 215 (2003) 344–352.
- [44] B.M. Kabyemela, T. Adschiri, R.M. Malaluan, K. Arai, *Ind. Eng. Chem. Res.* 38 (1999) 2888–2895.
- [45] J. Remón, J.R. Giménez, A. Valiente, L. García, J. Arauzo, *Energy Convers. Manag.* 110 (2016) 90–112.
- [46] A. Seretis, P. Tsiakaras, *Renew. Energy.* 85 (2016) 1116–1126.
- [47] B. Roy, H. Sullivan, C.A. Leclerc, *J. Power Sources.* 267 (2014) 280–287.
- [48] R.R. Davda, J.W. Shabaker, G.W. Huber, R.D. Cortright, J.A. Dumesic, *Appl. Catal. B Environ.* 43 (2003) 13–26.
- [49] J.W. Shabaker, G.W. Huber, R.R. Davda, R.D. Cortright, J.A. Dumesic, *Catal. Letters.* (2003).
- [50] G. Wen, Y. Xu, H. Ma, Z. Xu, Z. Tian, *Int. J. Hydrogen Energy.* 33 (2008) 6657–6666.
- [51] Y. Xu, Z. Tian, G. Wen, Z. Xu, W. Qu, L. Lin, *Chem. Lett.* 35 (2006) 216–217.
- [52] A. Wawrzetz, B. Peng, A. Hrabar, A. Jentys, A.A. Lemonidou, J.A. Lercher, *J. Catal.* 269 (2010) 411–420.
- [53] J. So, Y. Chung, D.S. Sholl, C. Sievers, *Mol. Catal.* 475 (2019) 110423.
- [54] G.W. Huber, J.W. Shabaker, S.T. Evans, J.A. Dumesic, 62 (2006) 226–235.
- [55] H.D. Kim, H.J. Park, T.W. Kim, K.E. Jeong, H.J. Chae, S.Y. Jeong, C.H. Lee, C.U. Kim, *Int. J. Hydrogen Energy.* 37 (2012) 8310–8317.
- [56] D.L. King, L. Zhang, G. Xia, A.M. Karim, D.J. Heldebrant, X. Wang, T. Peterson, Y. Wang, *Appl. Catal. B Environ.* 99 (2010) 206–213.
- [57] A. Ciftci, D.A.J.M. Ligthart, A.O. Sen, A.J.F. Van Hoof, H. Friedrich, E.J.M. Hensen, *J. Catal.* 311 (2014) 88–101.

- [58] D.L. King, L. Zhang, G. Xia, A.M. Karim, D.J. Heldebrant, X. Wang, T. Peterson, Y. Wang, *Appl. Catal. B Environ.* 99 (2010) 206–213.
- [59] A. Tanksale, C.H. Zhou, J.N. Beltramini, G.Q. Lu, *J. Incl. Phenom. Macrocycl. Chem.* 65 (2009) 83–88.
- [60] A. Tanksale, J.N. Beltramini, J.A. Dumesic, G.Q. Lu, *J. Catal.* 258 (2008) 366–377.
- [61] J. Liu, B. Sun, J. Hu, Y. Pei, H. Li, M. Qiao, *J. Catal.* 274 (2010) 287–295.
- [62] J.W. Shabaker, G.W. Huber, J.A. Dumesic, *J. Catal.* 222 (2004) 180–191.
- [63] G. Wen, Y. Xu, Q. Liu, C. Wang, H. Liu, Z. Tian, *Catal. Letters.* 141 (2011) 1851–1858.
- [64] M.F. Neira D'Angelo, V. Ordonsky, J. Van Der Schaaf, J.C. Schouten, T.A. Nijhuis, *Catal. Sci. Technol.* 3 (2013) 2834–2842.
- [65] M.F. Neira D'Angelo, V. Ordonsky, J. Van Der Schaaf, J.C. Schouten, T.A. Nijhuis, *Int. J. Hydrogen Energy.* 39 (2014) 18069–18076.
- [66] M.F.N. D'Angelo, V. Ordonsky, J.C. Schouten, J. Van Der Schaaf, T.A. Nijhuis, *ChemSusChem.* 7 (2014) 2007–2015.
- [67] B. Entezary, M. Kazemeini, *Int. J. Hydrogen Energy.* (2018) 1–14.
- [68] R.M. Ripken, J.A. Wood, J.G.E. Gardeniers, S. Le Gac, *Chem. Eng. Technol.* (2019) 1–9.
- [69] M.B. Valenzuela, C.W. Jones, P.K. Agrawal, *Energy and Fuels.* 20 (2006) 1744–1752.
- [70] X. Li, L. Kong, Y. Xiang, Y. Ju, X. Wu, F. Feng, J. Yuan, L. Ma, C. Lu, Q. Zhang, *Sci. China, Ser. B Chem.* 51 (2008) 1118–1126.
- [71] T.P. Vispute, G.W. Huber, *Green Chem.* 11 (2009) 1433–1445.
- [72] G. Wen, Y. Xu, Z. Xu, Z. Tian, *Catal. Commun.* 11 (2010) 522–526.
- [73] S. Irmak, L. Öztürk, *Int. J. Hydrogen Energy.* 35 (2010) 5312–5317.
- [74] A.S. Oliveira, J.A. Baeza, L. Calvo, N. Alonso-Morales, F. Heras, J. Lemus, J.J. Rodriguez, M.A. Gilarranz, *Environ. Sci. Water Res. Technol.* 4 (2018) 1979–1987.
- [75] A.S. Oliveira, J.A. Baeza, L. Calvo, N. Alonso-Morales, F. Heras, J.J. Rodriguez, M.A. Gilarranz, *Appl. Catal. B Environ.* 245 (2019) 367–375.
- [76] P.D. Vaidya, J.A. Lopez-Sanchez, *ChemistrySelect.* 2 (2017) 6563–6576.
- [77] S.M. Swami, V. Chaudhari, D.S. Kim, S.J. Sim, M.A. Abraham, *Ind. Eng. Chem. Res.* 47 (2008) 3645–3651.
- [78] D.A. Sladkovskiy, L.I. Godina, K. V. Semikin, E. V. Sladkovskaya, D.A. Smirnova, D.Y. Murzin, *Chem. Eng. Res. Des.* 134 (2018) 104–116.
- [79] N. Dave, R. Selvaraj, T. Varadavenkatesan, R. Vinayagam, *Algal Res.* 42 (2019) 101606.
- [80] J. McLachlan, *Plant Soil.* 89 (1985) 137–157.
- [81] T.M. Aida, T. Yamagata, C. Abe, H. Kawanami, M. Watanabe, R.L. Smith, A.T. Michael, Y. Takuji, A.B.E. Chihiro, K. Hajime, W. Masaru, S.R. L., S.R. L., *J. Supercrit. Fluids.* 65 (2012) 39–44.
- [82] W. Jeon, C. Ban, G. Park, T. Yu, J. Suh, H. Chul, D. Heui, *J. Mol. Catal. A. Chem.* 399 (2015) 106–113.
- [83] C. Ban, W. Jeon, G. Park, C. Woo, D. Heui, *ChemCatChem.* 9 (2017) 329–337.
- [84] B. Bharathiraja, M. Chakravarthy, R.R. Kumar, D. Yogendran, D. Yuvaraj, J. Jayamuthunagai, R.P. Kumar, S. Palani, *Renew. Sustain. Energy Rev.* 47 (2015) 634–653.
- [85] G. Pipitone, D. Tosches, S. Bensaid, A. Galia, R. Pirone, *Catal. Today.* 304 (2018) 153–164.

- [86] B. Meryemoglu, B. Kaya, S. Irmak, A. Hesenov, O. Erbatur, *Fuel*. 97 (2012) 241–244.
- [87] T.M. Aida, T. Yamagata, M. Watanabe, R.L. Smith, *Carbohydr. Polym.* 80 (2010) 296–302.
- [88] G.D. Yadav, P.A. Chandan, D.P. Tekale, *Ind. Eng. Chem. Res.* 51 (2012) 1549–1562.
- [89] R.R. Davda, J.A. Dumesic, *E. Drive, Chem. Commun.* (2004) 36–37.
- [90] A. V. Kirilin, A. V. Tokarev, E. V. Murzina, L.M. Kustov, J.P. Mikkola, D.Y. Murzin, *ChemSusChem*. 3 (2010) 708–718.
- [91] D.E. Mears, *Ind. Eng. Chem. Process Des. Dev.* 10 (1971) 541–547.
- [92] D.Ö. Özgür, B.Z. Uysal, *Biomass and Bioenergy*. 35 (2011) 822–826.
- [93] S.N. Delgado, D. Yap, L. Vivier, C. Especel, *J. Mol. Catal. A Chem.* 367 (2013) 89–98.
- [94] J.W. Shabaker, J.A. Dumesic, *Ind. Eng. Chem. Res.* 43 (2004) 3105–3112.
- [95] T. Nozawa, Y. Mizukoshi, A. Yoshida, S. Naito, *Appl. Catal. B Environ.* 146 (2014) 221–226.
- [96] K. Niemela, E. Sjoström, *Carbohydr. Res.* 144 (1985) 241–249.
- [97] G.W. Huber, R.D. Cortright, J.A. Dumesic, *Angew. Chemie - Int. Ed.* 43 (2004) 1549–1551.
- [98] K. Lehnert, P. Claus, *Catal. Commun.* 9 (2008) 2543–2546.
- [99] H. Xiong, H.N. Pham, A.K. Datye, *Green Chem.* 16 (2014) 4627–4643.
- [100] N. Luo, X. Fu, F. Cao, T. Xiao, P.P. Edwards, *Fuel*. 87 (2008) 3483–3489.
- [101] F.H. Isikgor, C.R. Becer, *Polym. Chem.* 6 (2015) 4497–4559.
- [102] H. Zabed, J.N. Sahu, A.N. Boyce, G. Faruq, *Renew. Sustain. Energy Rev.* 66 (2016) 751–774.
- [103] H.B. Aditiya, T.M.I. Mahlia, W.T. Chong, H. Nur, A.H. Sebayang, *Renew. Sustain. Energy Rev.* 66 (2016) 631–653.
- [104] R.A. Sheldon, *J. Mol. Catal. A Chem.* 422 (2016) 3–12.
- [105] P. Kaparaju, M. Serrano, A.B. Thomsen, P. Kongjan, I. Angelidaki, *Bioresour. Technol.* 100 (2009) 2562–2568.
- [106] B.C.H. Chu, H. Lee, *Biotechnol. Adv.* 25 (2007) 425–441.
- [107] K. Eisenhuber, K. Krennhuber, V. Steinmüller, A. Jäger, *Energy Procedia*. 40 (2013) 172–181.
- [108] J. Lessard, J.F. Morin, J.F. Wehrung, D. Magnin, E. Chornet, *Top. Catal.* 53 (2010) 1231–1234.
- [109] A.B. Díaz, C. Marzo, I. Caro, I. de Ory, A. Blandino, *Bioresour. Technol.* 225 (2017) 225–233.
- [110] X. Li, P. Jia, T. Wang, *ACS Catal.* 6 (2016) 7621–7640.
- [111] S.Y. Wu, C.Y. Lin, K.S. Lee, C.H. Hung, J.S. Chang, P.J. Lin, F.Y. Chang, *Energy and Fuels*. 22 (2008) 113–119.
- [112] F. Aiouache, L. McAleer, Q. Gan, A.H. Al-Muhtaseb, M.N. Ahmad, *Appl. Catal. A Gen.* 466 (2013) 240–255.
- [113] A. V. Kirilin, A. V. Tokarev, L.M. Kustov, T. Salmi, J.P. Mikkola, D.Y. Murzin, *Appl. Catal. A Gen.* 435–436 (2012) 172–180.
- [114] H.A. Duarte, M.E. Sad, C.R. Apesteguía, *Int. J. Hydrogen Energy*. 41 (2016) 17290–17296.
- [115] A. Kirilin, J. Wärnå, A. Tokarev, D.Y. Murzin, *Ind. Eng. Chem. Res.* 53 (2014) 4580–4588.
- [116] Y. Guo, X. Liu, M.U. Azmat, W. Xu, J. Ren, Y. Wang, G. Lu, *Int. J. Hydrogen Energy*. 37 (2012) 227–234.
- [117] T.W. Kim, M.C. Kim, Y.C. Yang, J.R. Kim, S.Y. Jeong, C.U. Kim, *Int. J.*

- Hydrogen Energy. 40 (2015) 15236–15243.
- [118] A. V. Tokarev, A. V. Kirilin, E. V. Murzina, K. Eränen, L.M. Kustov, D.Y. Murzin, J.P. Mikkola, *Int. J. Hydrogen Energy*. 35 (2010) 12642–12649.
- [119] T. Jiang, Q. Zhang, T.J. Wang, Q. Zhang, L.L. Ma, *Energy Convers. Manag.* 59 (2012) 58–65.
- [120] A. V. Kirilin, A. V. Tokarev, H. Manyar, C. Hardacre, T. Salmi, J.P. Mikkola, D.Y. Murzin, *Catal. Today*. 223 (2014) 97–107.
- [121] D.Y. Murzin, S. Garcia, V. Russo, T. Kilpiö, L.I. Godina, A. V. Tokarev, A. V. Kirilin, I.L. Simakova, S. Poulston, D.A. Sladkovskiy, J. Wärnä, *Ind. Eng. Chem. Res.* 56 (2017) 13240–13253.
- [122] L.I. Godina, A. V. Kirilin, A. V. Tokarev, I.L. Simakova, D.Y. Murzin, *Ind. Eng. Chem. Res.* 57 (2018) 2050–2067.
- [123] B. Meryemoglu, S. Irmak, A. Hasanoglu, O. Erbatur, B. Kaya, *Fuel*. 134 (2014) 354–357.
- [124] G. Wen, Y. Xu, Z. Xu, Z. Tian, *Catal. Letters*. 129 (2009) 250–257.
- [125] B. Meryemoglu, A. Hesenov, S. Irmak, O. Malik, O. Erbatur, *Int. J. Hydrogen Energy*. 35 (2010) 12580–12587.
- [126] G. Pipitone, G. Zoppi, A. Frattini, S. Bocchini, R. Pirone, S. Bensaid, *Catal. Today*. (2019).
- [127] A. V. Kondratyuk, V. V. Lunin, A.E. Koklin, V.I. Bogdan, T.A. Klimenko, *Kinet. Catal.* 56 (2015) 84–88.
- [128] G. Pipitone, G. Zoppi, S. Ansaloni, S. Bocchini, F.A. Deorsola, R. Pirone, S. Bensaid, *Chem. Eng. J.* 377 (2019).
- [129] D.A. Boga, F. Liu, P.C.A. Bruijninx, B.M. Weckhuysen, *Catal. Sci. Technol.* 6 (2016) 134–143.
- [130] S. Irmak, B. Meryemoglu, A. Hasanoglu, O. Erbatur, *Fuel*. 139 (2015) 160–163.
- [131] L.I. Godina, H. Heeres, S. Garcia, S. Bennett, S. Poulston, D. Yu, *Int. J. Hydrogen Energy*. 44 (2019) 14605–14623.
- [132] L. Negahdar, P.J. Peter, S. Sibirtsev, S. Palkovits, R. Palkovits, *Int. J. Chem. Kinet.* 50 (2018) 325–334.
- [133] I. Van Zandvoort, Y. Wang, C.B. Rasrendra, E.R.H. Van Eck, P.C.A. Bruijninx, H.J. Heeres, B.M. Weckhuysen, *ChemSusChem*. 6 (2013) 1745–1758.
- [134] B. Girisuta, L.P.B.M. Janssen, H.J. Heeres, *Green Chem.* 8 (2006) 701–709.
- [135] A. Tanksale, Y. Wong, J.N. Beltramini, G.Q. Lu, *Int. J. Hydrogen Energy*. 32 (2007) 717–724.
- [136] Z. Fang, R.L. Smith, J.A. Kozinski, T. Minowa, K. Arai, *J. Supercrit. Fluids*. 56 (2011) 41–47.
- [137] K. Tekin, S. Karagöz, S. Bektaş, *Renew. Sustain. Energy Rev.* 40 (2014) 673–687.
- [138] G. Brunner, *J. Supercrit. Fluids*. 47 (2009) 373–381.
- [139] J. Akhtar, N.A.S. Amin, *Renew. Sustain. Energy Rev.* 15 (2011) 1615–1624.
- [140] D.C. Elliott, P. Biller, A.B. Ross, A.J. Schmidt, S.B. Jones, *Bioresour. Technol.* 178 (2015) 147–156.
- [141] S.S. Toor, L. Rosendahl, A. Rudolf, *Energy*. 36 (2011) 2328–2342.
- [142] S. Bensaid, R. Conti, D. Fino, *Fuel*. 94 (2012) 324–332.
- [143] S.R. Villadsen, L. Dithmer, R. Forsberg, J. Becker, A. Rudolf, S.B. Iversen, B.B. Iversen, M. Glasius, *Energy & Fuels*. 26 (2012) 6988–6998.



- [144] E. Panisko, T. Wietsma, T. Lemmon, K. Albrecht, D. Howe, *Biomass and Bioenergy*. 74 (2015) 162–171.
- [145] B. Maddi, E. Panisko, T. Wietsma, T. Lemmon, M. Swita, K. Albrecht, D. Howe, *Biomass and Bioenergy*. 93 (2016) 122–130.
- [146] B. Maddi, E. Panisko, T. Wietsma, T. Lemmon, M. Swita, K. Albrecht, D. Howe, *ACS Sustain. Chem. Eng.* 5 (2017) 2205–2214.
- [147] S. Ghosh, J.P. Ombregt, P. Pipyn, *Water Res.* 19 (1985) 1083–1088.
- [148] D.C. Elliott, T.R. Hart, A.J. Schmidt, G.G. Neuenschwander, L.J. Rotness, M. V. Olarte, A.H. Zacher, K.O. Albrecht, R.T. Hallen, J.E. Holladay, *Algal Res.* 2 (2013) 445–454.
- [149] Y. Yasaka, K. Yoshida, C. Wakai, N. Matubayasi, M. Nakahara, *J. Phys. Chem. A*. 110 (2006) 11082–11090.
- [150] B. Matas Güell, I. Babich, K. Seshan, L. Lefferts, *J. Catal.* 257 (2008) 229–231.
- [151] J. Carlos Serrano-Ruiz, J.A. Dumesic, *Green Chem.* 11 (2009) 1101.
- [152] P. Mäki-Arvela, I.L. Simakova, T. Salmi, D.Y. Murzin, *Chem. Rev.* 114 (2014) 1909–1971.
- [153] K.I. Gursahani, R. Alcalá, R.D. Cortright, J.A. Dumesic, *Appl. Catal. A Gen.* 222 (2001) 369–392.
- [154] I. Coronado, M. Pitinová, R. Karinen, M. Reinikainen, R.L. Puurunen, J. Lehtonen, *Appl. Catal. A Gen.* 567 (2018) 112–121.
- [155] Y. Ukisu, T. Miyadera, *React. Kinet. Catal. Lett.* 81 (2004) 305–311.
- [156] J.P. Breen, R. Burch, K. Griffin, C. Hardacre, M. Hayes, X. Huang, S.D. O'Brien, *J. Catal.* 236 (2005) 270–281.
- [157] X. Carrier, E. Marceau, J.F. Lambert, M. Che, *J. Colloid Interface Sci.* 308 (2007) 429–437.
- [158] R.M. Ravenelle, J.R. Copeland, A.H. Van Pelt, J.C. Crittenden, C. Sievers, *Top. Catal.* 55 (2012) 162–174.
- [159] H.G. Karge, W. Nießen, H. Bludau, *Appl. Catal. A Gen.* 146 (1996) 339–349.
- [160] K. Koichumanova, K.B. Sai Sankar Gupta, L. Lefferts, B.L. Mojet, K. Seshan, *Phys. Chem. Chem. Phys.* 17 (2015) 23795–23804.
- [161] R.M. Ravenelle, J.R. Copeland, A.H. Van Pelt, J.C. Crittenden, C. Sievers, *Top. Catal.* 55 (2012) 162–174.
- [162] T.W. Kim, H.J. Park, Y.C. Yang, S.Y. Jeong, C.U. Kim, *Int. J. Hydrogen Energy*. 39 (2014) 11509–11516.
- [163] G. Pipitone, G. Zoppi, S. Bocchini, A.M. Rizzo, D. Chiaramonti, R. Pirone, S. Bensaid, *Catal. Today*. (2019).
- [164] J. Shabaker, J. Dumesic, *Ind. Eng. Chem.* (2004) 3105–3112. <http://pubs.acs.org/doi/abs/10.1021/ie049852o>.
- [165] Z. Tang, J. Monroe, J. Dong, T. Nenoff, D. Weinkauf, *Ind. Eng. Chem. Res.* 48 (2009) 2728–2733.
- [166] T. Sakamoto, H. Kikuchi, T. Miyao, A. Yoshida, S. Naito, *Appl. Catal. A Gen.* 375 (2010) 156–162.
- [167] Y. Liu, Z. Chen, X. Wang, Y. Liang, X. Yang, Z. Wang, *ACS Sustain. Chem. Eng.* 5 (2017) 744–751.
- [168] J. Cueto, L. Faba, E. Díaz, S. Ordóñez, *ChemCatChem*. 9 (2017) 1765–1770.
- [169] R. Ma, K. Cui, L. Yang, X. Ma, Y. Li, *Chem. Commun.* 51 (2015) 10299–10301.
- [170] W. Yang, X. Li, S. Liu, L. Feng, *Energy Convers. Manag.* 87 (2014) 938–

945.

- [171] D. Zhou, L. Zhang, S. Zhang, H. Fu, J. Chen, *Energy and Fuels*. 24 (2010) 4054–4061.
- [172] C. Sievers, S.L. Scott, Y. Noda, L. Qi, E.M. Albuquerque, R.M. Rioux, *ACS Catal.* 6 (2016).
- [173] J. Struijk, Scholten J. J. F, *Appl. Catal.* 82 (1992) 277–287.
- [174] R.B. Madsen, P. Biller, M.M. Jensen, J. Becker, B.B. Iversen, M. Glasius, *Energy and Fuels*. 30 (2016) 10470–10483.
- [175] X. Bai, K.H. Kim, R.C. Brown, E. Dalluge, C. Hutchinson, Y.J. Lee, D. Dalluge, *Fuel*. 128 (2014) 170–179.
- [176] R. Ni, R. Dhimas, D. Putra, H.L. Trajano, S. Liu, H. Lee, K. Smith, C. Soo, *Chem. Eng. J.* 350 (2018) 181–191.
- [177] D. Gao, C. Schweitzer, H.T. Hwang, A. Varma, *Ind. Eng. Chem. Res.* 53 (2014) 18658–18667.
- [178] D.K. Lee, D.S. Kim, T.H. Kim, Y.K. Lee, S.E. Jeong, N.T. Le, M.J. Cho, S.D. Henam, *Catal. Today*. 154 (2010) 244–249.
- [179] P.M. De Souza, R.C. Rabelo-Neto, L.E.P. Borges, G. Jacobs, B.H. Davis, D.E. Resasco, F.B. Noronha, *ACS Catal.* 7 (2017) 2058–2073.
- [180] C. Contescu, S. Adhikari, N. Gallego, N. Evans, B. Biss, *C.* 4 (2018) 51.
- [181] W.M.H.S. P. Biloen, J. N. Helle, H. Verbeek, F. M. Dautzenberg, *J. Catal.* 18 (1980) 112–118.